2020

Investigation Of Molecular Mechanisms Of Liver Preservation Injury: A Complication Preceding Organ Transplantation

Ria C. Fyffe-Freil
Virginia Commonwealth University

Follow this and additional works at: https://scholarscompass.vcu.edu/etd

Part of the Cellular and Molecular Physiology Commons, Critical Care Commons, and the Surgery Commons

Downloaded from
https://scholarscompass.vcu.edu/etd/6480

INVESTIGATION OF MOLECULAR MECHANISMS OF LIVER

PRESERVATION INJURY: A COMPLICATION PRECEDING ORGAN

TRANSPLANTATION

A dissertation submitted in a partial fulfillment of the requirements for the degree Doctor of

Philosophy at Virginia Commonwealth University.

By

Ria Christian Fyffe-Freil

BA Chemistry, 2011

MS Addiction Science, 2015

Director: Dr. Martin Mangino

Professor

Department of Surgery

Virginia Commonwealth University

Richmond, Virginia

Virginia Commonwealth University

Richmond, Virginia

November 2020

Table of Contents

Acknowledgements

Tackling a PhD is unlike any challenge I have experienced. Some days, I didn't know whether to laugh or cry (or a combination of the two) when my experiments went awry. It takes a village of support to make it through this journey, and without the support of the following folks, I wouldn't be here today. First, I want to thank Nina Wickramaratne, for moving into the office at the perfect time and handling the nuclear bomb I tossed over the friendship wall with grace and humor. I couldn't have finished this journey without you, truly. Heather Reichstetter was paramount to acclimating me to the laboratory, showing me how to survive animal surgery, procuring brains when I needed them for RNA and protein lysate (despite almost amputating her thumb), and cheering me on during the first half of my graduate training. Loren Liebrecht introduced me to cell culture, which would become my life for five years. She is the best troubleshooter I know, and our impromptu lunch discussions mean the world to me and helped push me through to the end. We will conquer the world together, friend. To other members of the lab who supported me along the way, I couldn't have completed this work without your help: Caitlin, Ru, Tao, Will, Courtney, Renee, Jad, Hae Sung, Anna, Dr. Dixon, Nancy, Melissa, and Chuck. To my PhD partner-in-crime, Jenny: we did it, COVID pandemic and all! I am so proud of you. My graduate advisory committee gave me critical feedback, gentle nudging, and supported me through graduate school journey. Therefore, I want to thank Phil Hylemon, Murthy Karnam, Fadi Salloum, and Shanaka Wijesinghe for getting me to the finish line. My program directors, Gail Christie and Mike McVoy, were paramount to my success in the MBG program, while Roland Pittman supported me on the physiology portion of my training. Finally, I want to thank Martin Mangino, who never gave up on my stubbornness, sarcasm, and all-around shenanigans. He challenged me to become an independent thinker and allowed me to learn from my own mistakes

(even when I was ready to throw in the towel). Dr. Mangino taught me technical, troubleshooting, and creative thinking skills during my 5 years in his laboratory. He supported me every single step of the way, from submitting two (ultimately unfunded) F31 grant proposals to learning how to teach and even joining a clinical field at the end of my training. When my personal life threatened my success, he jumped in to help and guide me through getting back on track. There aren't enough words in the English language to show my gratitude for his mentorship and friendship.

Dedication

Graduate school is a challenge, in the best of times. I have been working on various higher education degrees since I met my patient husband in 2010. From finishing my Sweet Briar education, to a post-baccalaureate program, two MCATs, two GREs, medical and graduate school applications, a master's degree, a PhD, and finally clinical chemistry fellowship applications and interviews (all in the times of the COVID-19 pandemic) his support never wavered. Sure, he gave me a list of chores to do "when my brain could handle it", like cleaning up my living room corner and putting away the clothes that have laid in the basket for a month. He helped take care of "my" cats, and "his" dogs while I was in the lab. He kept me entertained, fed, wined, happy, laughing, and loved during what was the most challenging chapter of our lives, professionally and personally. Matt, I promise it is your turn next, to pursue whatever career makes your heart happy. Thank you for saving lives in the meantime.

I want to also dedicate this dissertation to my parents for giving me the best start in life and unconditional support throughout this process. To my dad, who constantly answers my calls for statistics and experimental logistics assistance, and my mom who raises me up when I need support and a kind word: this success is yours as well. Thank you for loving me with reckless abandon and teaching me to be a kind human with a decent head on my shoulders. My in-laws were also

paramount to my degree, first for raising Matt to be able to support me throughout, and second for supporting me. Candi believed in me and knew that I could make it across the finish line. Michael, despite losing his beloved wife Candi in May 2020, has become a friend and fierce advocate for my education. Finally, I want to dedicate this dissertation to my friends (and their families) who have been there for me as early as middle school. Without additional guidance in my formative years, I may not have made it this far. Thank you Victoria, Dylan, Dan, Dede, Cabel, Zach, Chelsea, Greg, Astrid, Jim, Ellie, Melaina, and everyone else who impacted my life leading to this point. It certainly takes a village, and my village is unparalleled.

I have been dedicating each seminar presentation for the duration of my PhD journey to my (and my husband's) friend/coworker Meredith Haga Fox. After an autoimmune disease, called *crescentic IgA nephropathy*, destroyed her kidneys at age 17, she received a living kidney donation from her stepfather, Bruce. This bought her 7 more years of life, which she spent advocating for organ donation and eventually working clinically as an organ recovery coordinator, marrying her love Tanner, adopting a golden Goose, and buying a house.

>*"When I went into renal failure in 2011, I remember feeling like my world stopped turning. I guess selfishly, I thought everyone else's should've too."*

Meredith Haga Fox lost her battle against AMR-induced pneumocystis pneumonia on July 20, 2018 and our lives stopped turning too, sweet friend. #signupsavelives #donatelife

Table of Figures

Table of Tables

Abstract

Of the over 108,000 Americans awaiting a life-saving organ transplant today, over 12,000 (11%) of those need a new liver (OPTN, 2020). Last year, only 35% of patients on the waiting list for an organ were transplanted. Improving the quality of marginal organs by preventing preservation injury could vastly increase the number of transplants performed. Preservation injury refers to the injury that occurs in an organ graft during cold storage (hypothermic ischemia), and it is proportional to graft dysfunction in the recipient. Many of the intracellular molecular mechanisms of this injury remain elusive and are not mitigated by current preservation methods. During procurement, liver grafts are flushed with cold preservation solution *in situ*, which washes away blood and any circulating, endogenous molecules that may promote survival. Circulating lysophospholipids (LPLs), such as lysophosphatidic acid (LPA) and sphingosine-1-phosphate (S1P) are attractive targets due to their terminal downstream effectors (primarily cytoskeletal structure and mitochondrial activity). Using an *in vitro* model of organ preservation, we found that biologically relevant concentrations of LPA did not prevent preservation injury in hepatocytes (though higher concentrations did show a protective effect). Inhibiting RhoA and Rho kinase (which are downstream of LPL surface receptors) during cold storage worsens the preservation injury phenotype. Albumin, which carries and sequesters lipids in aqueous solution, is dose-dependently cytotoxic during cold storage; this supports the idea that growth and survival factors are important in dampening preservation injury. The ratio of intracellular S1P:ceramide, a barometer for cell health, was shifted in favor of cell death following cold storage, implicating that sphingolipid signaling is disrupted. Pharmacologically inhibiting sphingosine kinase-2 (SK2), the enzyme responsible for producing most of the intracellularly acting S1P, proved devastating in

rodent liver transplant, *ex vivo* perfusion, and *in vitro* models. Upon further investigation, the mechanism of ABC294640 (the selective SK2 inhibitor) toxicity is, in fact, two-fold: ABC294640 directly inhibits complex I of the electron transport chain (ETC) in the mitochondria, independent of its effects on SK2 (clarifying its vastly devastating effects on liver grafts following transplantation in rodents). These results indicate that LPLs, such as LPA and S1P, may be relevant signaling pathways to target for improved liver graft function following cold storage. Determining how to modulate these pathways in favor of maintaining hepatocyte survival, and thus liver graft viability, is on the horizon, with the ultimate goal of improving liver preservation methods.

Chapter 1: Organ preservation and the pathophysiology of preservation injury

1.1 The history of organ preservation

1.1.1 It all began in the 1800s…

More than two centuries ago, a French scientist named César Julien Jean La Gallois described his theory that extracorporeal perfusion could preserve the heart indefinitely; James Phillips Kay and Eduard Brown-Séquard demonstrated the benefits of perfusion in practice (though not to the extent we think of today) (Jing et al. 2018; Fye 1995). The first isolated organ perfusion is thought to be that of Carl Eduard Loebell on a porcine model while investigating urine secretion in the mid-1800s (Boettcher, Merkle, and Weitkemper 2003). The late 1800s gave way to the first isolated artificial perfusion system and a double circulator that paved the way to the development of extracorporeal membrane oxygenation (ECMO) as we know it today. Early perfusion apparatuses used blood to perfuse the biological sample; however, trouble arose when

scientists realized that the available blood volume in the animal was not adequate, and hemodilution with lactated ringer's (LR) led to irreversible edema (Jing et al. 2018). Perfusion was initially performed at room temperature, then physiologic temperatures in the late 1870s, and finally at hypothermic temperatures in the 1960s (Boettcher, Merkle, and Weitkemper 2003).

1.1.2 The first preservation solution

After it was determined that blood was not a good perfusate, researchers began concocting their own preservation solutions in order to keep grafts viable without histological and functional changes. The first commercially available solution for organ preservation was marketed in 1969 by Geoffrey Collins (Jing et al. 2018). Aptly named, Collins solution contained a low concentration of sodium, high potassium, glucose, and a phosphate buffer. The next generation, Euro-Collins, included more glucose and excluded magnesium sulfate (Collins, Bravo-Shugarman, and Terasaki 1969). While Euro-Collins solution is still used in Europe, it was quickly replaced in the US by more advanced preservation solutions, such as University of Wisconsin (UW) and histidine-tryptophan-ketoglutarate (HTK) solutions, which contained cellular impermeants and amino acids, respectively (Petrowsky and Clavien 2015).

1.1.3 "Firsts" in transplantation and the role of organ preservation

While the main barrier to successful organ transplantations early was the lack of immunosuppressant therapy, undeveloped organ preservation methods also proved a significant challenge. This limited the radius of acceptable donors, and essentially made the procedure an emergency since there wasn't a good way to preserve organs longer than a few hours. A timeline of successful "firsts" in the transplantation field is shown in Figure 1.1. The first successful kidney transplant, performed in 1954 by Joseph Murray at Brigham and Women's Hospital in Boston, MA, did not advance the field in terms of knowledge. The technical skills associated with kidney

3

transplant had been worked out previously in animal models, and it was known that skin graft

transplants between identical twins avoided rejection (Barker and Markmann 2013).
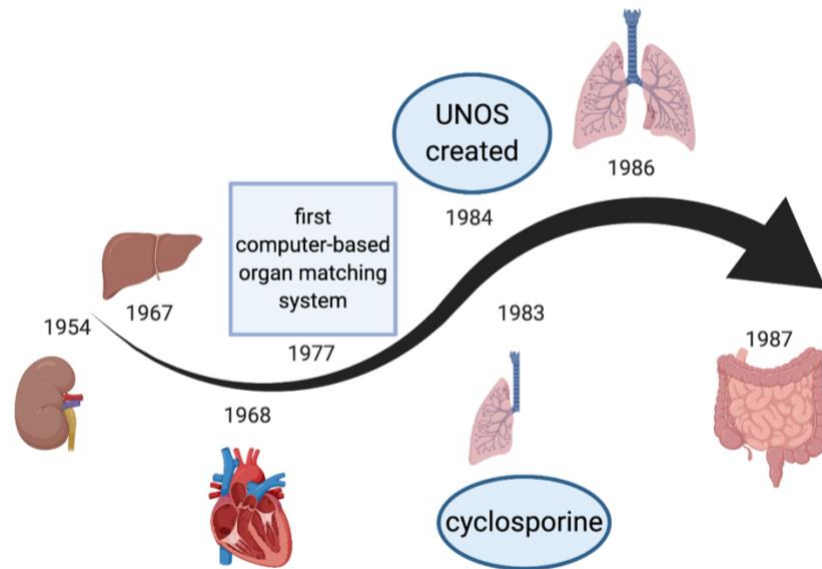
Figure 1.1 The timeline of human clinical transplantation "firsts"
Adapted from UNOS History of Transplant.

Thomas Starzl, a transplant surgeon first with the University of Colorado and subsequently

with the University of Pittsburgh, is credited with not only performing the first successful liver

transplant in 1967, but also with introducing the idea of hypothermia to preserve donor organs

prior to transplant (Starzl et al. 1963). Until the clinical introduction of cyclosporin, preservation

of the organs wasn't as high a priority since immunosuppression wasn't on the table and rejection

was a more immediate threat (Barker and Markmann 2013). Despite the existing trouble with

rejection, Christiaan Barnard completed the first heart transplant in South Africa in 1968 (for a

riveting take on the competition that led to the first heart transplant, read *Every Second Counts:*

The Race to Transplant the First Human Heart, by Donald McRae) (Barker and Markmann 2013;

Alivizatos 2017). In order to promote fair and equal organ allocation processes across the US, the

United Network for Organ Sharing (UNOS) was established in 1977 to implement a national waiting list. Cyclosporin, the first clinically relevant immunosuppressant for organ transplantation, was utilized beginning in 1983 to prevent rejection (Barker and Markmann 2013). That same year, the first isolated single lung transplant was completed by the Toronto Lung Transplant Group (Venuta and Van Raemdonck 2017; Toronto Lung Transplant 1986). In 1986, the Toronto group successfully transplanted double lungs into a terminal emphysema patient (Patterson et al. 1988). Finally, the last organ graft to be transplanted was the intestines in 1987 (Margreiter 1997). Cyclosporin exhibited a very narrow therapeutic window and nephrotoxicity and was replaced by Tacrolimus in the late 1980s, moving the field of organ transplantation lightyears into the future (Starzl et al. 1989). Now, patients were living long enough post-transplant to assess organ graft viability as a function of ischemic injury during procurement.

1.2 The cellular basis for organ preservation

1.2.1 Principles of organ preservation

Developed by Drs. Belzer and Southard, the principles of organ preservation were published in the 1980s and provided a basis for the invention of the standard organ preservation solution (see Section 1.3.1). They contended that good surgical technique and adequate donor selection were not enough to support success of an organ transplantation: good preservation was also required to maintain the cadaveric organ between donor procurement and recipient transplantation. These principles (hypothermia, metabolic energy synthesis, cellular housekeeping, and protection against ischemia-reperfusion injury, or IRI) are meant to mitigate the deleterious effects of ischemia (Belzer and Southard 1988; Southard and Belzer 1993). Collectively, the damages sustained by organ tissue before, during, and after organ preservation are referred to as preservation injury.

1.2.2 Hypothermia

The primary objective of hypothermia is to decrease cellular metabolism to a level that is manageable during organ preservation. Van't Hoff's rule (Figure 1.2) states that for every 10°C drop in temperature, there is an approximately 50% reduction in oxygen consumption (measure of enzyme reaction rate, or metabolism) (Belzer and Southard 1988; Taylor 2007; Petrowsky and Clavien 2015). This results in fewer active enzymes requiring significantly less oxygen to satisfy cellular metabolic needs.

The graph shows Enzymatic activity (%) on the y-axis (0 to 100) versus Temperature (°C) on the x-axis (0 to 37), with curves for LDH and NA⁺, K⁺-ATPase.

$$Q_{10} = \left(\frac{k_2}{k_1}\right)^{\frac{10}{T_2 - T_1}}$$
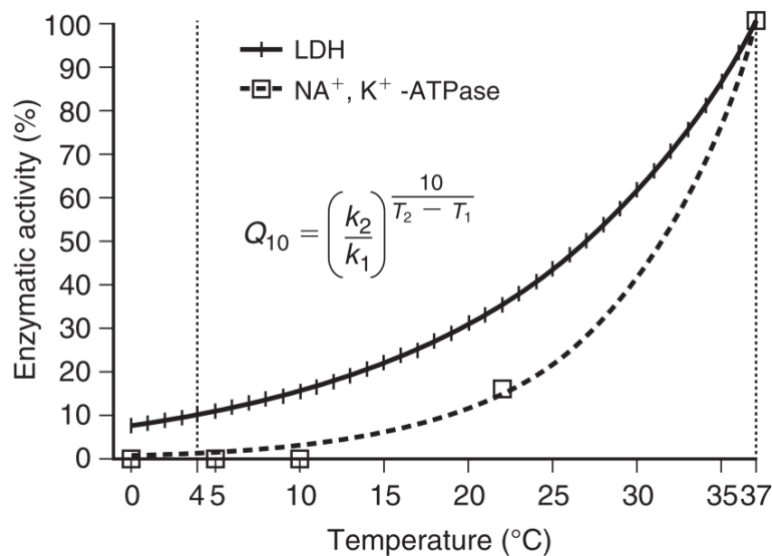
Figure 1.2 Van't Hoff's rule for metabolic changes as a function of temperature

As shown in <u>Principles of Liver Transplantation</u> *(2015) by Petrowsky and Clavien. For every 10°C decrease in temperature, there is a two-fold reduction in enzymatic activity. k_1 and k_2 represent the reaction rates at temperatures T_1 and T_2; Q_{10} is the van't Hoff's coefficient for a temperature change of 10° C and has been determined to be 2 for lactate dehydrogenase (LDH).*

Arguably the most detrimental target of this decrease in enzymatic activity are the membrane-associated pumps that help maintain ion balance across the plasma membrane. One such pump, the Na-K ATPase (sodium-potassium ATPase, or Na+ pump) located in the basolateral epithelial cell membrane, maintains osmotic balance for the cell by pumping three (3) Na+ ions

out for every two (2) K+ ions pumped in. Hypothermia knocks out this Na+ pump by depleting all available ATP, and where Na+ ions travel, water follows down its osmotic gradient. Catastrophic cellular edema results and can lead to cell lysis if left uncorrected (Figure 1.3a).
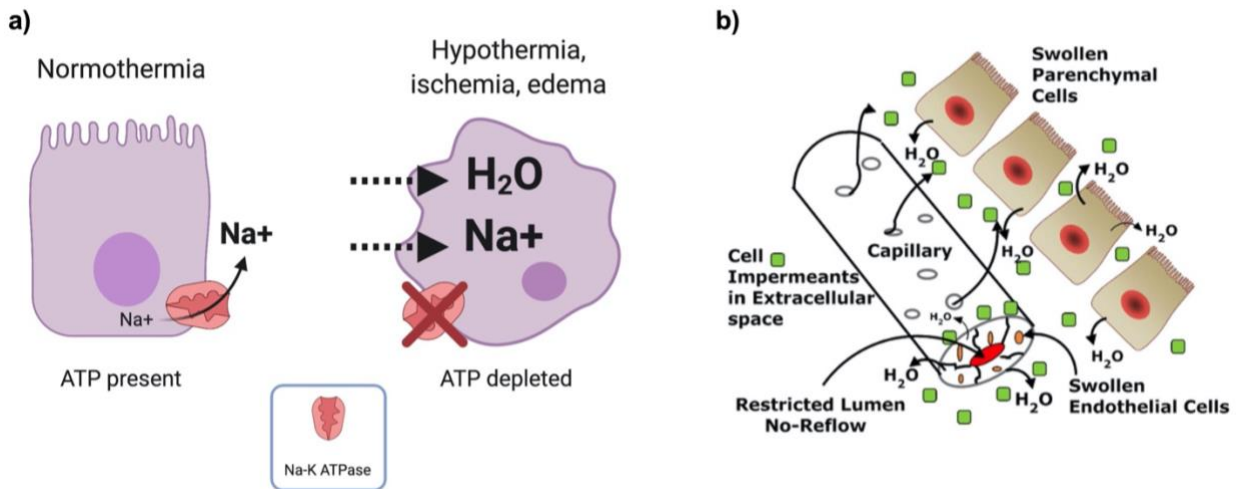
Figure 1.3 Prevention of hypothermia-induced cell swelling with cellular impermeants

a) Hypothermia prevents membrane-associated ion pumps from functioning, leading to rapid influx of Na+ and water, and edema/lysis. b) Organ preservation solutions contain cell impermeants, which balance the osmotic driving forces in the interstitial space and prevent cell swelling.

Preservation solutions contain cellular impermeants that are small enough to leave the capillaries, but too large to enter cells to restore the osmotic driving forces in the extracellular space to prevent cell swelling during hypothermia (Figure 1.3b). Edema is not only present at the cellular level, but also in the parenchyma (Fig 1.4). This leads to compression of the capillaries, resulting in end-organ hypoperfusion (Petrowsky and Clavien 2015).
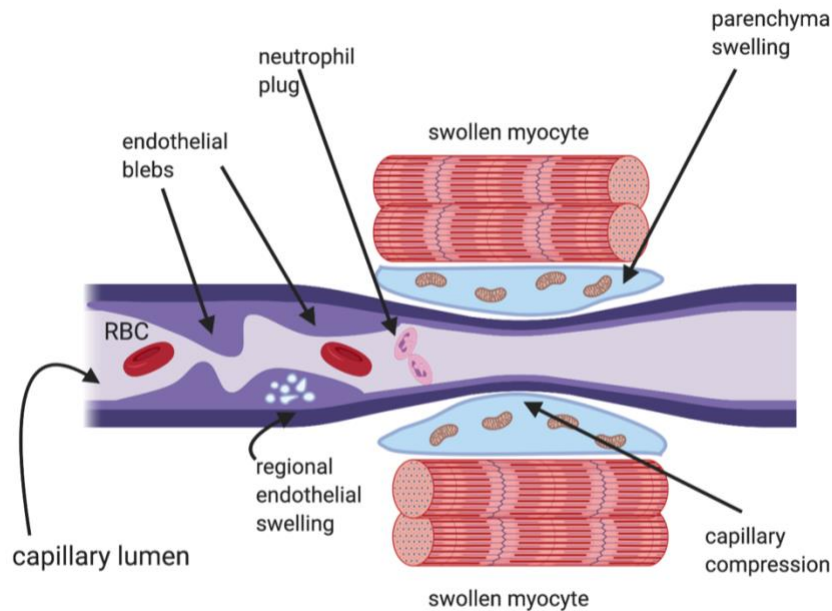
Figure 1.4 Swollen parenchyma stops blood flow to small vessels

Adapted from (Reffelmann and Kloner 2002). *Edema is not limited to cells during organ preservation. The parenchyma retains water as well, leading to compression of the vasculature and decreased perfusion to those tissues.*

1.2.3 Metabolic energy synthesis

On the one hand, hypothermic temperatures experienced during organ preservation decrease cellular metabolism by nearly 97% and as a result, energy consumption and oxygen demand is *vastly* reduced. On the other hand, this reduction in enzyme activity impacts ATP synthesis, leading to a deficit in available intracellular ATP (and a rapid depletion of any stored ATP). Not only is ATP hydrolyzed quickly during hypothermia, but the resulting degradation products (such as adenosine) are permeable and cross the plasma membrane freely. There is therefore a lack of available ATP synthesis precursors in the hypothermic cell (Belzer and Southard 1988).

Many downstream processes, such as membrane-associated ion pumps, have a hefty ATP requirement that cannot be satisfied during hypothermia. The aforementioned Na-K ATPase is a

prime example. As such, jump-starting ATP production upon reperfusion is absolutely paramount to organ preservation success. Including the precursor molecules required for ATP synthesis (such as adenine, ribose, and adenosine) during preservation ensure that the mitochondria will be well-supplied upon reperfusion to begin rapidly making ATP (Belzer and Southard 1988; Southard and Belzer 1993; Taylor 2007).

1.2.4 Cellular housekeeping

In addition to ion dysregulation, hypothermic ischemia is deleterious to other intracellular processes. Increase in intracellular pH is the result of several processes, including increased glycolysis and glycogenolysis, as well as lactic acid production and other processes that lead to the presence of more hydrogen ions in the intracellular space. This ultimate decrease in pH is detrimental to both lysosomes and mitochondrial stability and must be mitigated through the preservate. Though a minor contributor to preservation injury, hypothermic ischemia generates increased reactive oxygen species (ROS). In the liver and kidney, the impact of increased ROS is not as significant as in the lungs, due to the balance of enzymes that create and scavenge these oxygen free radicals (i.e., xanthine oxidase and superoxide dismutase, respectively). Finally, increased intracellular calcium as a result of an open mitochondrial permeability transition pore (mPTP) leads to hyperosmolarity, so the inclusion of calcium chelators in the preservation solution is important (Wu et al. 2018; Belzer and Southard 1988; Southard and Belzer 1995; Taylor 2007).

1.2.5 Protection against preservation injury

Ultimately the best protection against this hypothermic ischemia-induced reperfusion injury is prevention. Organ grafts procured from brain-dead donors (DBD) experience four (4) sources of damage (pre-preservation, cold preservation, rewarming, and reperfusion injuries), and those grafts from donation after cardiac death (CDC) experience an additional injury during the

time following cardiac arrest and *in situ* flushing prior to procurement. Protecting against all of these sources of damage, in an ideal world, would be accomplished by the preservation method/solution. However, in order for this to occur, preservation would need to repair damages that occur prior to and after the actual contact between the organ graft and the preservation system (static cold storage, machine perfusion, etc.). Many advances are needed to attain this ambitious goal.

1.3 The process of organ procurement

In order to understand why improved organ preservation is so important, one must first understand the logistics around organ placement and the process of actually recovering the organ grafts from the donor (summarized in Figure 1.5). It all starts in the hospital, in the intensive care unit (ICU) where a potential organ donor is in declining health. Via either first-person consent (i.e., the potential donor is registered through the Department of Motor Vehicle, or through donatelife.org) or family consent, a potential donor is identified by the ICU staff and the local organ procurement organization (OPO) is called onsite to manage the patient and begin the process of allocating organ grafts to prospective recipients. In Virginia, LifeNet Health is the OPO and the multidisciplinary organ procurement team is made up of nurses, paramedics, scrub technicians, respiratory therapists, and surgical assistants.

1. Donor registers online or through the DMV

2. Illness or accident renders the donor hospitalized with poor prognosis

3. Transplant coordinator assessed donor stability and allocates organs

4. Donor taken to the operating room for organ procurement

5. Organs flushed *in situ* with preservate, and prepared for transport to recipient

Transplantation and reanastomosis

6. Graft flushed of preservate, reanastomosed in the recipient who is monitored for regain of graft function

Figure 1.5 The organ allocation, donation, and transplantation process

Once all of the viable, healthy organs are allocated to recipients and accepted by the surgeon, then the operating room (OR) can be scheduled. The donor is moved to the OR, and the teams begin working to isolate each viable organ graft prior to cross-clamp, which is when the ischemia clock starts ticking. Organ grafts are removed in order of preservation window, starting with the heart, then lungs, then abdominal organs (liver, kidneys, intestines and pancreas). Grafts are placed on ice in cold preservate and prepared for transport to their final destination (by car, ambulance, or air transport depending on the distance). Upon arrival at the recipients' hospitals, the grafts are flushed with saline and the vasculature is connected with that of the recipient, leading to reperfusion of the organ with warm, oxygenated blood. It is only after reperfusion that any preservation injury that occurred during cold storage manifests in the recipient. There are many

opportunities to intervene throughout the procurement process, from donor management (a therapeutic provided directly to the donor while they are still in the ICU), to *in situ* flush solution and SCS/MP preservation solution, finally to the rehabilitation of the organ on the recipient end prior to transplantation. It is important to remember that even with the best logistical preparation, unexpected delays and complications arise often and may prolong ischemic time; all the more reason to have an expanded toolbelt to deal with the consequences of hypothermic ischemia-induced preservation injury.

1.4 Expansion of the donor pool and the use of extended criteria donors

Signing up to be an organ donor is not a guarantee that upon your death, your wish will be fulfilled. In fact, the vast majority of deaths (up to 97%) occur in a manner that is not *currently* conducive to organ donation (Figure 1.6). Under the current guidelines and limits of organ preservation, a donor must be in the hospital and relatively hemodynamically stable at the time of death. There are two types of organ donors, those who donate after brain death (DBD) or after cardiac death (DCD). Most organ donors are declared brain dead after a devastating injury or illness results in cessation of blood flow to the brain (caused by brainstem herniation), while a portion have no chance for a meaningful recovery (though have not yet met the criteria for brain death). The latter pool of donors, at the request of the family, have their life-support withdrawn in a controlled setting and are allowed to pass away naturally (i.e., cardiac death). The warm ischemia clock starts, not after cardiac death, but when the donor enters a state of hypoperfusion: an oxygen saturation of less than 80% or a systolic blood pressure of less than 80. These vital signs are not conducive to adequate perfusion of organs (Petrowsky and Clavien 2015). After cardiac activity ceases, and a short waiting period has passed (at least 5 minutes), the organ procurement team gets to work in the operating room.
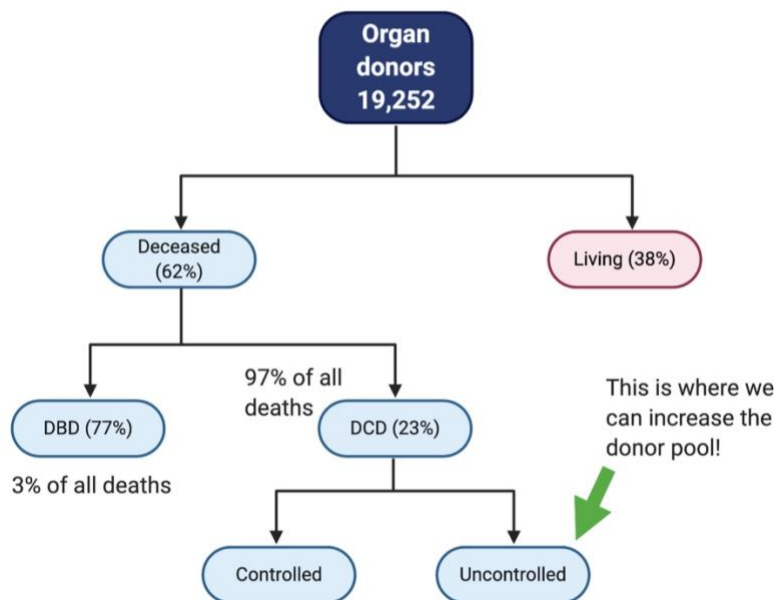
Figure 1.6 Types of organ donors from 2019

Of the 19,252 organ donors from 2019, 62% of those were deceased donors. 23% of those deceased donated after cardiac death (DCD). However, up to 97% of deaths are cardiac in nature, and those which are uncontrolled are the target for increasing the donor pool. Data from OPTN (2019).

Typically, the organs procured from DBD donors do not experience an appreciable amount of warm ischemia (cardiac function is intact in these donors, so blood continues to circulate until cross-clamp and removal of the organ grafts). However, DCD donors experience hypoperfusion during the withdrawal of care, followed by a period of warm ischemia before the organ grafts are procured. At present, only the liver and kidneys are suitable for transplant from DCD donors, and while work is being completed on how to rehabilitate the heart and lungs from these donors, it is not yet clinically useful. And yet, up to 97% of deaths are of the cardiac variety and only a small portion of these occur in a hospital (that is, they are "controlled"). The remainder of cardiac deaths

occur in an uncontrolled setting (and are thus considered "extended criteria donors"): at home, in the field, in the emergency department, and often rather unexpectedly. <u>This is where we can expand the pool of organ donors!</u> The primary concern with organs from uncontrolled DCD donors is extensive warm ischemia, and currently there is no way to reverse the associated cellular damage. The organ grafts from uncontrolled DCD donors would then necessitate cold storage, introducing yet another blow in the form of hypothermic ischemia. The combination of extensive warm and hypothermic ischemia damages these grafts beyond repair under the current preservation paradigm. In order to move preservation forward and introduce organ rehabilitation, we must understand the molecular mechanisms of preservation injury. New preservation solutions and strategies that can mitigate and even reverse a portion of this injury will move the field forward into new and exciting territory.

1.5 Advances in organ preservation

Kidney transplantation began in the 1950s, followed by liver transplantation, heart transplantation in 1968, and finally lung transplants in the 1980s. Transplant operations took place directly after procurement from the organ donor, necessitated by the lack of preservation methods and extensive cellular damage observed in early organ grafts (Starzl et al. 1963). As the transplantation field progressed, so too did the preservation field to keep up with the influx of available organs. Donors were arising faster than the surgeons could complete transplants and extending the viability of procured organs beyond immediate removal from the donor was critical to the success of the field. This shifted the transplant procedure from an emergent to a selective surgery, reducing organ waste and provider fatigue (Belzer and Southard 1988). As mentioned previously, the logistics of organ placement, procurement, and transplantation play a larger role in preservation than appreciated.

1.5.1 University of Wisconsin solution – the golden standard

Drs. Belzer and Southard recognized in the mid-1980s that they could create a solution to the problems associated with organ preservation, and University of Wisconsin (or UW) solution was born (Southard et al. 1990; Belzer and Southard 1988). Prior to the development of UW solution, a review on the cellular control of internal volume was published by MacKnight and Leaf (1977). It surmised that cell swelling as a result of ischemia was a) due to the lack of ATPase activity as cellular energy is depleted and sodium ions rush into the cell, and b) may not be recognized immediately, but only upon reperfusion when there is more interstitial fluid and potential organelle rupture to flood the cell leading to edema (Macknight and Leaf 1977).

Belzer and Southard realized these mechanisms, and how they contribute to the imbalance of ions across the plasma membrane, decreasing the membrane potential and increasing the osmotic driving forces that force sodium ions into the cell. Their solution was to add cellular impermeants to restore the osmotic gradient, keeping water in the interstitium and preventing cell swelling. Intracellular acidosis, the result of increased glycolysis combined with lactic acid production and increased hydrogen ion presence, necessitates preservation solution contain buffers to balance the pH. There is also the possibility of mesenchymal edema leading to compression of the microvasculature (see Figure 1.4), so UW solution contains solutes capable of creating oncotic pressure. Free-radical scavengers and ATP precursors (as previously described in section 1.2.3) round out the composition of UW solution, and it has hardly changed since its inception (Belzer and Southard 1988). Table 1.1 shows the composition of UW as it exists today.

Pentafraction	50	g/L
Lactobionic acid	35.83	g/L
Potassium phosphate monobasic	3.4	g/L
Magnesium sulfate heptahydrate	1.23	g/L
Raffinose pentahydrate	17.83	g/L
Adenosine	1.34	g/L
Allopurinol	0.136	g/L
Total glutathione	0.922	g/L
Potassium hydroxide	5.61	g/L
Sodium hydroxide/hydrochloric acid	Adjust to pH of 7.4	

Table 1.1 The components of UW solution

From https://bridgetolife.com/belzer-uw-cold-storage-solution-instructions.

1.5.2 Static cold storage

The earliest form of organ preservation was static cold storage (SCS): no perfusion, in a modified solution to prevent the known mechanisms of the associated hypothermic ischemic injury. There are many benefits of SCS, which is why it continues to be popular today. It is cost effective, technology-free, and universally implemented. However, there is still preservation injury associated with SCS. There is an inherent lack of oxygen, and for this reason the temperature must remain between 2-4°C in order to keep the basal metabolic rate low. The preservate mitigates the known causes of preservation injury but does not mitigate them all as we still see injury with SCS. As additional mechanisms are identified, it may be necessary for the preservate to circulate through the organ to deliver the components to the vasculature.

1.5.3 Alternatives to static cold storage

Conceptually, static cold storage lacks a fundamental aspect that may mitigate some of its own detrimental effects: perfusion. If the preservation solution were circulated through the organ during transit, there could be constant delivery of preservate constituents to the vasculature and subsequently the interstitial space for signaling through cell surface receptors.

Intuitively, since the hypothermia associated with traditional organ preservation methods is inherently destructive to the tissues and cells, many scientists have investigated the role of increasing the temperatures during preservation to midthermia (15-20°C) or even normothermia (37°C, physiologic temperatures). As a general rule, raising the temperature during preservation increases the metabolism, and thus the oxygen requirement of the organ. These mid- and normothermic preservation methods, therefore, must be perfused and oxygenated to pacify the increased cellular metabolism. Raising the temperature avoids the problems associated with hypothermia, but also increases the basal metabolic rate beyond the limits of the preservation method. Some machine perfusion (normothermic and hypothermic) trials have been successful, while others result in graft failure and cholangiopathy (Nasralla et al. 2018; Ceresa et al. 2018; Watson et al. 2017; Schlegel, Kron, and Dutkowski 2016). Unfortunately, a degree of ischemia-reperfusion injury is still observed, pointing to an underlying mechanism outside of those targeted by increasing the temperature of preservation.

1.7 Hepatic physiology and preservation injury phenotype

Since this research focuses on the liver specifically, it is prudent to review general liver physiology and how the preservation injury phenotype manifests in the liver – both at the cellular level and in terms of graft survival in the recipient.

The cellular majority in the liver is composed of two types: hepatocytes (around 85% of the biomass) and cholangiocytes (which line the bile ducts). Hepatocytes perform many of the core functions of liver, including drug and macromolecular (i.e. carbohydrates, lipids, and amino acids) metabolism, bile and serum production, and bilirubin detoxification (Tanimizu and Mitaka 2016). Cholangiocytes are also injured during organ preservation, which leads ischemic cholangiopathy and can be fatal to the recipient. Sinusoidal endothelial cells and Kupffer cells are also affected by preservation injury. (Petrowsky and Clavien 2015; Serracino-Inglott, Habib, and Mathie 2001).

The degree of preservation injury is directly proportional to graft function and recipient survival post-transplant. Preservation injury in the liver during cold storage manifests in the recipient as primary graft nonfunction, elevated liver enzymes, hemodialysis, prolonged postoperative ventilation, and other advanced intensive care measures (Glanemann et al. 2003). By the time preservation injury is realized in the recipient, it is too late to reverse the damage. Therefore, prevention is key to improving graft function post-liver transplant.

1.8 The problem

Despite all of the advances made in organ preservation over the past several decades, ischemia-reperfusion injury is still a major problem that manifests as acute and delayed graft rejection in the recipient (which can certainly be fatal). Even when the known cellular propagators of preservation injury are targeted with improved preservation solutions, a degree of this injury remains. This leads to the belief that there are underlying cellular mechanisms that contribute to the preservation injury phenotype that remain elusive. Uncovering these and providing a solution to the problem can vastly increase the pool of available donor livers by improving the quality of marginal liver grafts (which are currently unsuited for transplantation). As Kahn and Schemmer discuss in their recent review on liver transplantation, the processes that contribute to the

pathophysiology of preservation injury in the liver are complex and multifaceted. There is no *one* therapeutic strategy to prevent this injury, but rather a compilation of adjustments to existing methods and preservates that can tackle the complex mechanisms, improving graft viability and reducing preservation injury.

The overarching theme of these research projects over the past five (5) years has been solving the aforementioned problem of mystery cellular mechanisms of preservation injury that are independent of those mitigated by current preservation methods (i.e., UW solution, cold storage). This research, like many dissertations before, has taken unexpected twists and turns that are culminating in a pharmacology manuscript that is a bit divergent from the overall theme of organ transplantation and preservation. Nevertheless, we are proud of this journey and hope this work advances the fields of both organ preservation and cancer treatment (for reasons that will become apparent in Chapter 7).

Chapter 2: Pleiotropic lipid signaling molecules & their downstream effectors

2.1 Overview of lysophospholipids

One of the inherent features of the organ procurement and preservation process is what is known as the "washout effect"; pro-survival signaling molecules, ATP precursors, and other essential cellular mediators are washed out when the organ is flushed *in situ*. These include compounds that are circulating in the blood stream, and those that are found in the interstitial space (over time, the extracellular milieu mixes with the preservate in the interstitial space). Lysophospholipids (LPLs) are the focus of this work, due to their extracellular receptors, autocrine signaling mechanisms, and growth/survival pathway targets. Specifically, lysophosphatidic acid

(LPA) and sphingosine-1-phosphate (S1P) were investigated. These two LPLs are increasingly well-studied for their role in cancer among other disease processes (Anliker and Chun 2004). While there is overlap in cellular responses, LPA and S1P are structurally distinct and do not share synthetic or metabolic pathways. They each possess their own unique G-protein coupled receptors (GPCRs), with a diverging network of intracellular downstream effectors that modulate processes such as transcription, cytoskeletal architecture, and mitochondrial activity (Fig 2.1) (Kihara et al. 2014). Of interest to this research, LPL signaling pathways have been shown to modulate cell survival, proliferation, and migration (Gardell, Dubin, and Chun 2006).
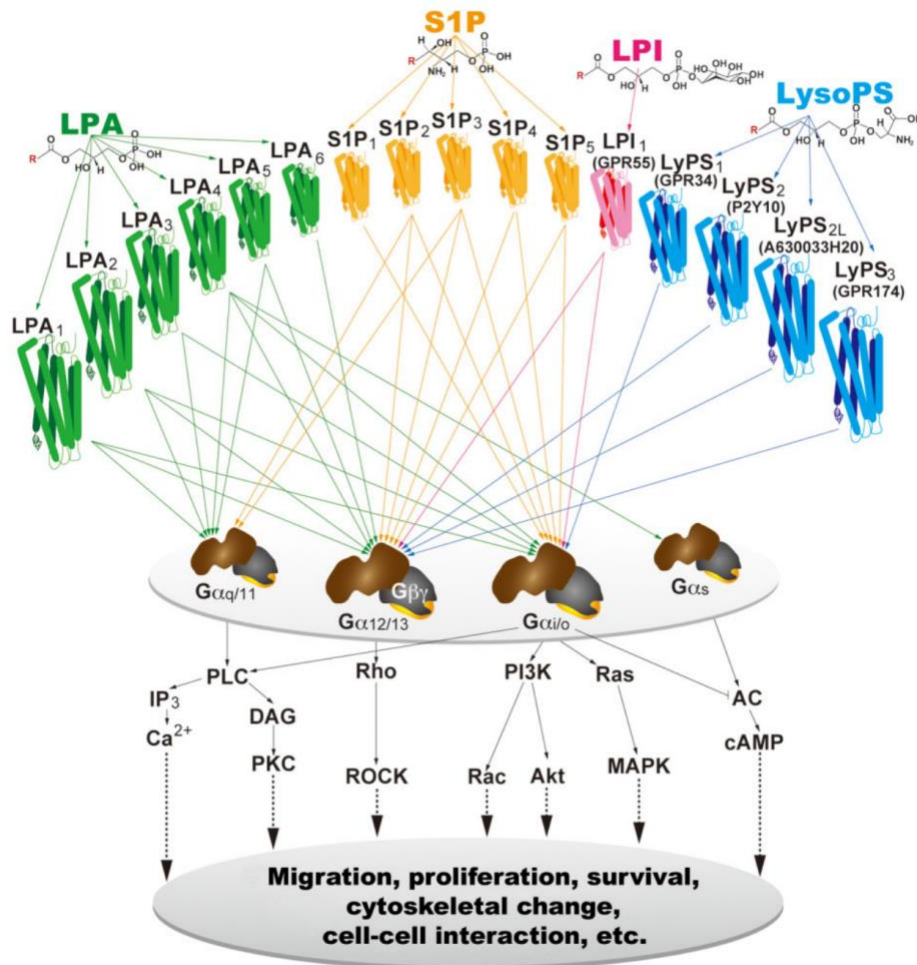
Figure 2.1 Summary of LPL surface receptors and downstream effectors of interest

Pathophysiologically, LPLs have many diverse actions in basic physiology as well as implications in development of disease. LPLs signal primarily through cell surface receptors, with intracellular actions such as transcriptional regulation, cell motility, differentiation, and apoptosis. However, some of these normal physiological actions of LPLs can be dysregulated and promote disease progression. For example, LPA plays a role in vascular and skeletal development, but also influences vessel and bone remodeling post-development (Binder et al. 2015). LPL signaling is upregulated in many cancers, and is implicated in inflammatory disease processes as well (Lewis, Voelkel-Johnson, and Smith 2018; Nielsen et al. 2017; Y. Zhao and Natarajan 2013).

2.2 Lysophosphatidic acid

Plasma [LPA] ranges from undetectable to 2nM, while serum [LPA] is 1-10uM (Panetti 2002). The concentration of LPA in the extracellular microenvironment remains unknown and is quite difficult to measure. Circulating LPA in the bloodstream is produced primarily by autotaxin (ATX) from precursor molecules secreted by platelets (Binder et al. 2015). LPA describes a collection of molecules with a fatty acid chain of varying length and varying degrees of saturation connected to a glycerol backbone. While there are a variety of biologically active LPA species, most studies use the 18:1 LPA molecule (Cerutis et al. 2014; Lin, Herr, and Chun 2010). LPA is produced primarily by two synthetic pathways: ATX and phospholipase A$_{1/2}$. *In vivo*, LPA is produced by platelets and hair follicles (as well as cancer cells, but these are not part of normal physiology) (Binder et al. 2015).

2.3 Sphingolipids

Plasma [S1P] is around 200nM, and serum [S1P] is 500nM (Panetti 2002). In contrast to LPA synthesis, there exists only one pathway for S1P synthesis: phosphorylation of sphingosine by one of two enzymes, sphingosine kinase-1 (SK1) or sphingosine kinase-2 (SK2) (Fig. 2.2). *In vivo*, S1P is produced by several cell types, including platelets, mast cells, and endothelial cells (Binder et al. 2015). However, unique to S1P is the known plethora of intracellular targets independent of cell surface GPCRs. S1P is important in complex IV assembly in the mitochondrial electron transport chain as well as gene regulation (binds to HDAC, altering transcription) (Strub et al. 2011; 2010).
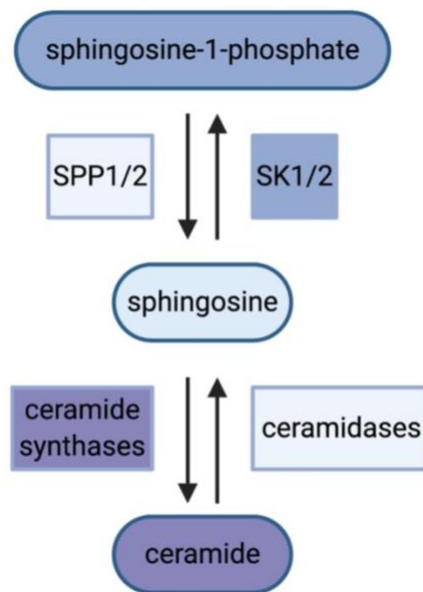
Figure 2.2 Overview of sphingolipid synthesis and metabolism

Sphingosine is interconverted between ceramide and S1P, depending upon many factors in the cellular micro- and macroenvironment. SK1, localized to the plasma membrane, is thought to produce most of the extracellularly acting S1P that is pumped through membrane transporters. SK2, localized to the nuclear and mitochondrial membranes, is thought to produce most of the intracellularly acting S1P (mitochondrial electron transport chain assembly and transcription factors). SPP1/2 (S1P phosphatases 1/2), figure adapted from (Takabe et al. 2008).

2.4 Downstream effectors of lysophospholipid receptors

LPA and S1P signaling cascades share several downstream effectors, including Erk/Akt, Rho/Rho kinase, Rac, and Ca^{2+} signaling to name a few. As seen above in Figure 2.1, there is a high degree of overlap between LPA and S1P receptors. These effectors control aspects of cell survival such as migration, morphology, proliferation (all of which may be involved in mediating the response of the cell to preservation injury) (Kihara et al. 2014). It is important to note the possibility that all or none of these downstream effectors play a causative role in hepatocyte preservation injury. This process is excessively complex, due to the myriad of catalysts involved in the injury cascade: hypothermia, ischemia, warm ischemia, and reperfusion. Once the immune system response to preservation injury is factored into the equation, the theoretical complexity increases substantially (Serracino-Inglott, Habib, and Mathie 2001). Instead of starting at the surface of the cell (at the LPL GPCR) and moving inward, we began our investigation at the level of cytoskeletal protein regulation.

2.5 The cytoskeleton: effects of preservation injury on actin and associated proteins

2.5.1 The intracellular actin network

The cytoskeleton has long been implicated as a contributing factor to preservation injury, starting in the kidney (Molitoris and Finn 2001). The intracellular actin network is dynamic, responsive to changes in intracellular calcium (among other stimuli) and accompanied by actin-associated proteins that serve to bundle, sever, and control interactions with the plasma membrane (Molitoris, Leiser, and Wagner 1997). After 24 hours of cold storage, biopsies from canine proximal tubules were found to have highly deformed microvilli compared to fresh controls (Fig 2.3).
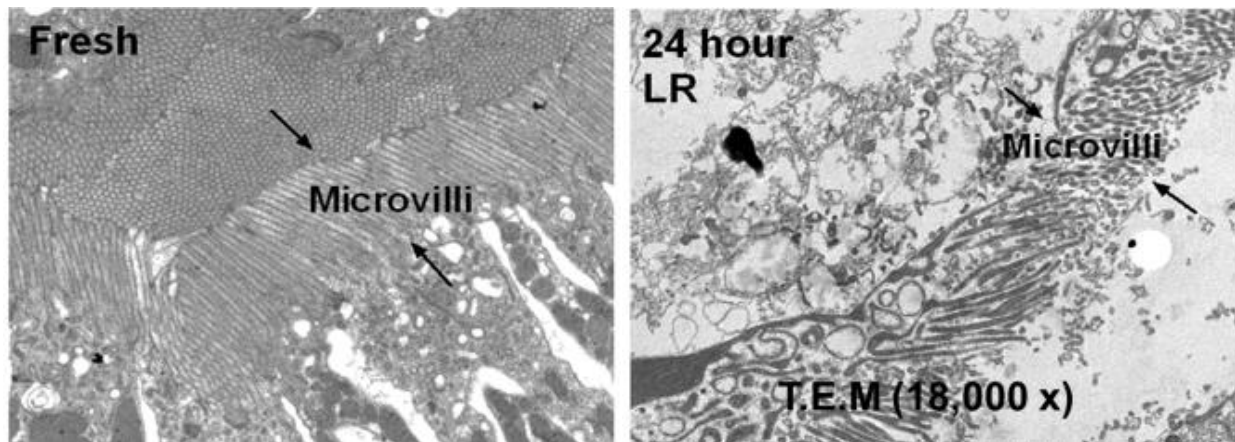
Figure 2.3 Proximal renal tubules are destroyed during cold storage

Canine kidneys were removed and stored in cold lactated ringer's (LR) solution for 24 hours. Biopsies were obtained and compared to those from fresh control canine kidneys. The structure of the microvilli in the fresh sample (left) are organized, homogeneous, and oriented appropriately. However, in the 24hr LR sample, the microvilli are collapsed, disorganized, and heterogeneous. Transmission electron micrograph at 18,000x magnification. Images from Mangino and Southard, 2004 (unpublished).

A key feature of epithelial cells, which make up the majority of the liver (hepatocytes), is their polarity. In biology, polarity refers to the organized and differential distribution of cell components, both intracellularly and along the plasma membrane, to confer specific functions. Organelles, cytoskeletal components, and cell surface proteins are not simply randomly located in epithelial cells, but rather strategically located to allow for geographically-selective membrane transport (Raman, Pinto, and Sonawane 2018). Epithelial cells in particular rely heavily on the cytoskeleton to maintain their organization and architecture, which is paramount to their function. For example, in the kidney, proximal renal tubule cells have increased surface area (microvilli) on the apical surface to selectively reabsorb molecules to concentrate urine; these microvilli are held together by actin filaments. Epithelial cells can also form a water-tight barrier using tight junctions, which are stabilized by actin and intermediate filaments. In the liver, hepatocytes are organized

into cord-like structures, usually two cells deep, that lie parallel to the liver sinusoids (allowing for nutrient exchange between the blood stream and hepatocytes).

2.5.2 Ezrin/radixin/moesin (ERM) proteins

The actin cytoskeleton requires linker elements to keep it anchored to the plasma membrane, such as ERM proteins. These sublamellar proteins bind to actin and anchors in the plasma membrane to stabilize the intracellular actin network. ERMs are important factors in maintaining microvillus structure during apoptosis, which supports the data shown in Figure 2.3 (breakdown of renal proximal tubule epithelial microvilli) (Kondo et al. 1997). ERMs also bind to microtubules, primarily during cell division, but this may have pathophysiological implications as more is uncovered about how these proteins behave (Solinet et al. 2013). ERM proteins are part of a larger family known as the band 4.1 superfamily and contain two functional domains connected by a coiled-coil linker. The FERM domain components form a clover-leaf shaped structure that is binds to plasma membrane linkers and Rho-associated proteins (Kawaguchi et al. 2017). At the other end, the C-terminal domain binds to either the FERM domain (deactivated protein) or actin (activated, phosphorylated protein) (Fehon, McClatchey, and Bretscher 2010). In addition to binding to Rho-related proteins directly, ERM proteins are activated by C-terminal phosphorylation by Rho kinase (ROK), opening the configuration of the linker protein and exposing its actin binding site (Matsui et al. 1998). The mechanism of ERM protein activation contains two simultaneous stages: first, the FERM domain binds to phosphatidyl-inositol-4,5-biphosphate (PIP_2) and then the actin binding domain at the C-terminus is phosphorylated by one of several kinases (Arpin et al. 2011; Ponuwei 2016; McClatchey 2014) (Fig 2.4). ERM protein inactivation occurs via dephosphorylation (either by protein phosphatases or via PIP_2 hydrolysis) (Ponuwei 2016).
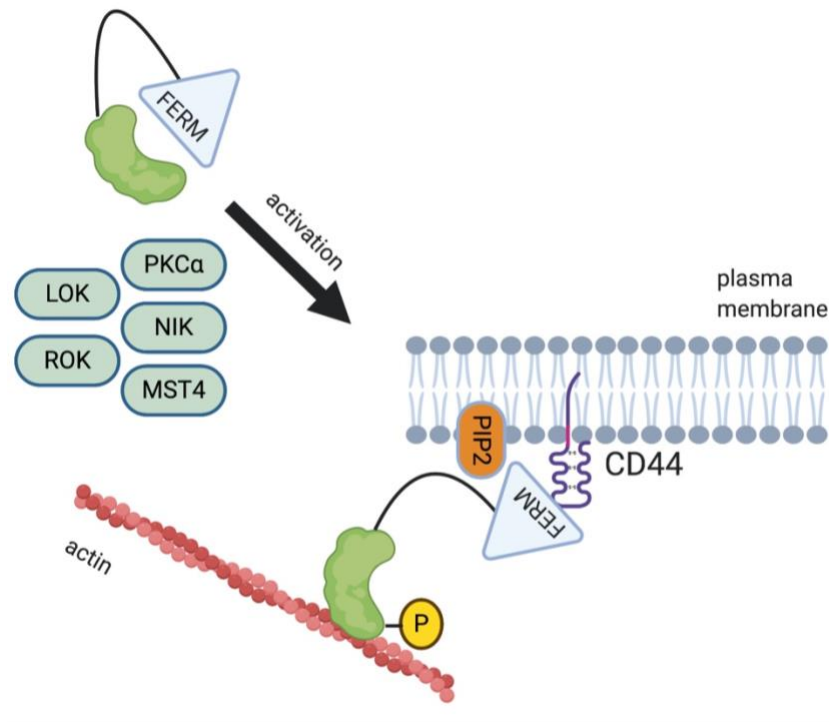
Figure 2.4 ERM protein regulation

*Protein kinase Cα (PKCα), NIK (NFκB-inducing kinase), LOK (Lymphocyte-Oriented Kinase),
ROK (Rho kinase) and MST4 are all known to phosphorylate the ERM C-terminal domain.
Binding to membrane-associated PIP₂ releases the FERM domain from the C-terminus. Adapted
from Pearson et al., 2000 and Ponuwei, 2016.*

Our laboratory found that moesin is important in maintaining hepatocyte viability during hypothermic ischemia in a cell model of organ preservation. Transfection of HepG2 cells with mutant moesin (T558D or T558A) resulted in cells with either constitutively ON or OFF moesin, respectively. HepG2 cells with ON moesin were significantly more resistant to preservation injury than those expressing OFF moesin (Tian et al. 2014). Similar results were obtained with mutant ezrin in LLC-PK1 cells, a porcine renal epithelial cell line (Tian et al. 2012). Lysophosphatidic acid treatment has been shown to result in ERM protein phosphorylation, and thus activation in fibroblasts (Shaw et al. 1998). S1P signaling through its surface receptor, S1P receptor 2, also

results in ERM protein activation (Gandy et al. 2012). However, no connection has been made between dysregulated ERM proteins in hypothermic ischemia and LPL receptor activation.

2.6 Mitochondria: more than a powerhouse

One of the major limiting factors for increasing organ preservation time is mitochondrial health following cold storage. After 24 hours of cold storage, mitochondria were significantly less active compared with fresh controls, and this effect was reversed when the mitochondria were stored in a mitochondria-specific preservate. It seems that providing ATP precursors in UW solution during preservation is not enough to protect the mitochondria against injury (Gnaiger et al. 2000). Determining which regulatory pathways are responsible for controlling mitochondrial activity during hypothermic ischemia will provide researchers with druggable targets to prevent this aspect of preservation injury.

2.6.1 Overview of mitochondrial biology

Traced to a prokaryotic origin, the mitochondria perform a plethora of valuable functions in the cell (Oliveira 2018). This quote from Milane et al. exemplifies the diverse importance of mitochondria:

"If the cell was a city, mitochondria would be the electric company (ATP production and metabolic center), the HVAC company (thermal regulation), the waste management company (ROS containment), the grim reaper (apoptotic regulation), the moving company (assists with intracellular and extracellular trafficking as well as cell movement), the department of defense (central to immunity, inflammation, the stress response, and the cell danger response), the historical society (evolutionary tracking through mtDNA), and if the Nucleic DNA is considered the Mayor of the city Cell, then mitochondria would assuredly be the

City Council as the only organelle with its own DNA, actively engaging with other organelles, performing diverse functions, profusely distributed, and maintaining cellular homeostasis (Milane et al. 2015)*."*

The tissue-variable mitochondrion is dynamic and promiscuous, constantly changing its shape/configuration and interacting with various organelles within the cell to accomplish a wide array of tasks. Mitochondrion number and intracellular localization are not static, but constantly changing to meet the needs dictated by the environment (Oliveira 2018). The only organelle to house their own non-nuclear DNA, the mitochondrion contains 37 genes encoding proteins that form the basic functional units of the electron transport chain. Each cell contains between one hundred (100) and several thousand mitochondria, and these organelles work together to form a network of signaling partners (Sharma, Lu, and Bai 2009). Because they are so diverse and interwoven with cellular function, it is no surprise that mitochondrial dysfunction is connected to many disease processes (including diabetes, obesity, cancer, neurodegenerative conditions, and rare mitochondrial diseases) (Milane et al. 2015). In addition to the synthesis of ATP (giving the organelle its designation as the "powerhouse" of the cell, the mitochondria produce sterols, fatty acids, purines, amino acids, and pyrimidines from the various metabolic pathways housed in this organelle (Oliveira 2018).

2.6.2 The electron transport chain (ETC)

What is of the most interest to organ preservationists is the mitochondria's central role in cellular energy production; the synthesis of ATP through oxidative phosphorylation (OXPHOS). The transfer of electrons down a chain of complexes in the inner mitochondrial membrane (electron transport chain, ETC), ending with an ATPase are the components of OXPHOS. Table

2.1 summarizes the five (5) ETC complexes. Complex I is the focus of the mitochondrial respiratory research presented in this dissertation.

Complex	Name	Main Function
I	NADH: ubiquinone oxidoreductase	transfer electrons from NADH in matrix to ubiquinone
II	Succinate: ubiquinone oxidoreductase	links Krebs to OXPHOS, oxidizes succinate into fumarate
III	Ubiquinol: cytochrome c oxidoreductase	transfers electrons from QH_2 to cytochrome c
IV	Cytochrome c oxidase	transfers electrons from cytochrome c to the final electron acceptor, O_2
V	H+ translocating ATP synthase	ATP synthesis via phosphorylation of ADP

Table 2.1 Summary of complexes I – V of the ETC (R. Z. Zhao et al. 2019)

NADH from the Krebs cycle files into complex I, leading to the transfer of electrons into the ETC. Complex I, the largest multiunit of the ETC, shuffles electrons through iron centers in the enzyme complex, ending in an iron-sulfur (Fe-S) center that transfers electrons to the next complex. The reduction of succinate at complex II results in transfer of electrons to QH_2 via another Fe-S center. Complex III is responsible for moving electrons to cytochrome c, and finally complex IV oxidizes cytochrome c, transferring the electrons to O_2 creating H_2O. A proton gradient is established as electrons move through the complexes, and this drives the ATP synthase to combine ADP and phosphate into ATP, the energy currency of the cell (R. Z. Zhao et al. 2019).

2.6.3 Structure of NADH: ubiquinone oxidoreductase: complex I of the ETC

Complex I of the ETC is composed of an enzyme (NADH dehydrogenase), a co-factor (flavin mononucleotide), and six (6) iron-sulfur (Fe-S) centers. The most crucial functions of complex I are carried out by fourteen (14) central subunits. Electron microscopy (EM) unveiled the structure L-shaped structure of complex I, with a membrane-bound arm and a peripheral arm which was further defined to 6.3Å by x-ray crystallography and more recently to 5.0Å by cryo-

EM. The peripheral arm is where NADH is oxidized and electrons are transferred to FMN and the Fe-S centers extend into the membrane-associated arm of the complex (Wirth et al. 2016).

Chapter 3: Materials & methods

3.1 Materials

3.1.1 Reagents

All reagents were purchased from Sigma-Aldrich (St. Louis, MO), unless otherwise specified. Western blotting supplies were from Invitrogen™, with the electrophoresis box, transfer chamber, and power supplies from Bio-Rad. All cell culture medium was manufactured by Gibco, and ordered through Thermo Fisher Scientific, Inc. Fetal bovine serum (FBS) and GlutaMAX™ supplement were purchased from Sigma-Aldrich. Antibiotic Antimycotic (AA) solution (100X) was supplied by Thermo Fisher Scientific, Inc.

3.1.2 Cell lines

The following cell lines were purchased from ATCC: HepG2 cells, derived from hepatocellular carcinoma in a 15-year-old male; SK Hep-1 cells, derived from adenocarcinoma in a 52-year-old male; and MDCK cells, derived from normal canine kidney epithelium.

3.2 *In vitro* model of organ preservation

3.2.1 Model development

Our lab developed an *in vitro* model of organ preservation, first published in 2008, involving the induction of hypothermic ischemia in canine renal proximal tubules primary cells stored in UW solution for five (5) days (Mangino et al. 2008). Briefly, primary cells plated in 96-well plates were grown to confluency in cell culture medium (DMEM). The DMEM was aspirated

and replaced with cold UW solution, and the plates were placed in airtight containers then purged with nitrogen to create ischemic conditions. The ischemic containers were then placed in cold storage at 4°C for the duration of the experiment. After five (5) days, the cells were washed and incubated in fresh DMEM at 37°C, 5% CO_2 in the incubator to simulate reperfusion for one (1) hour. During this time, each well was also incubated with a tetrazolium dye as an indicator of mitochondrial health and after the hour, plates were read at 450nm in a plate reader. The intensity of the signal of WST-1 conversion was a correlate for mitochondrial redox activity, and thus cell viability.

This *in vitro* model of cold storage provided a valuable tool to assess how cells responded to hypothermia ischemia, and the endpoints measured were typically cell viability (WST-1 or WST-8 formazan-based dye conversion and LDH release assays) or protein assays (such as western blots and ELISAs) (Fig 3.1). The cell viability data gave an overview of how the cells were handling the stress of hypothermic ischemia, and the protein assays told researchers exactly *how* those cells were responding. This model was expanded to immortalized cell lines, and then plasmid-transfected cells (both primary and immortalized), all with the goal of expanding our intracellular mechanistic knowledge of the preservation injury phenotype.
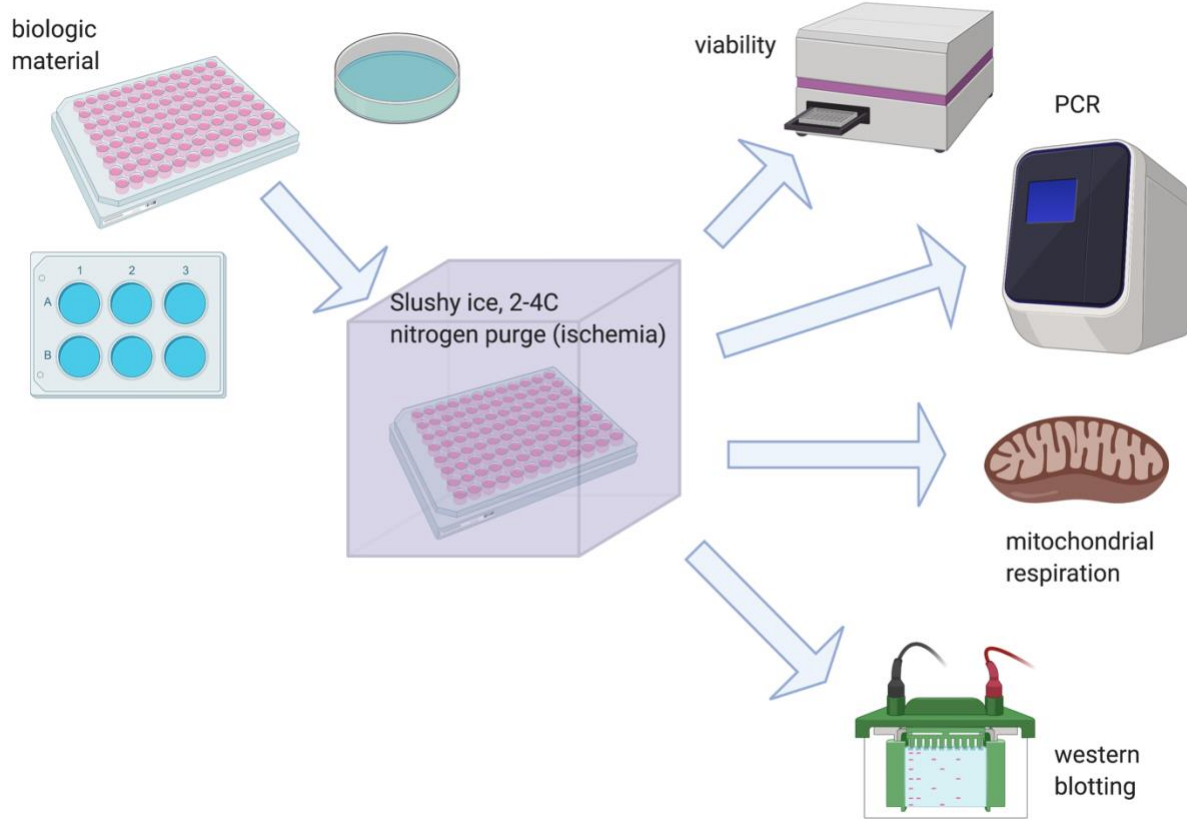
Figure 3.1 In vitro model of organ preservation

Biologic material, such as immortalized cell lines or primary hepatocytes, were plated on 96-well (viability), 6-well (PCR and western blotting), and 150mm dishes (mitochondrial respiration). Plates were sealed in an airtight container and ischemia induced via 95% N_2/5% CO_2 purge for 10 minutes. Following a 12-24 hour cold storage, plates were reperfused for one (1) hour and the desired endpoint was evaluated.

In terms of translatability, organs for transplantation (even kidneys) are typically not cold-stored for five (5) days. Figure 3.2 shows the standard limits of cold storage time for each organ before viability and functional decline become too problematic. Why, then, does the *in vitro* model for organ preservation expose the samples to double or triple the amount of hypothermic ischemia? The goal of the model is to induce a specific amount of preservation injury in the cells being studied that is *experimentally* useful. While there is no specific clinical correlate to the amount of

preservation injury required for a "successful" cold storage experiment, the model was developed such that an appropriate amount of cell death was observed but not too much that a treatment effect wouldn't be evident. The model aims for about 50-60% cell viability in vehicle controls following cold storage compared to physiologic incubator baseline cultures. This allows room for an increase in or decline of cell viability as a result of the applied treatment.
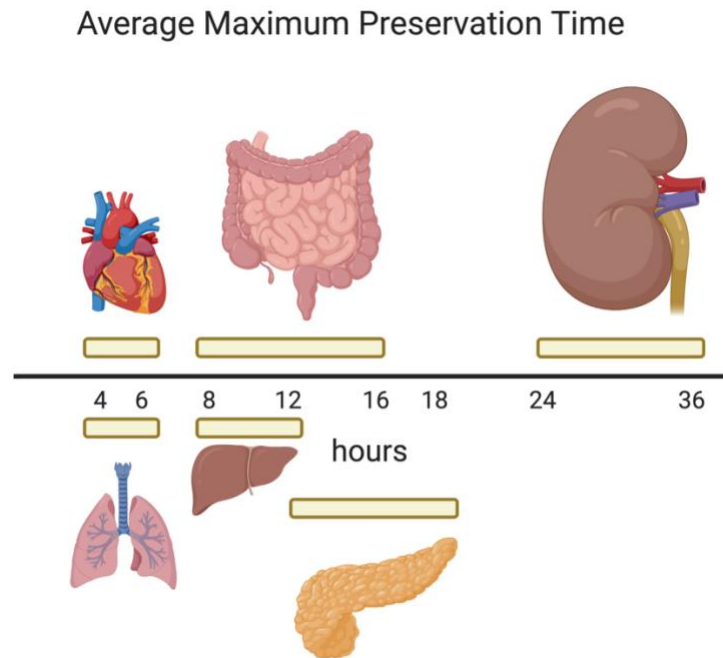
Figure 3.2 Windows of storage of all organs for transplantation

The heart and lungs have the shortest window, between 4-6 hours, followed by the liver (8-12 hours), intestines (8-16 hours), the pancreas (12-18 hours), and finally the kidneys with a longer viability window (24-36 hours).

3.2.2 Optimization of cold storage model

This model was developed in primary renal tubule cells and the parameters for that cell type do not translate into other types of biological material. Each time a new vial of cells is received and expanded for experimental use, a new "kill curve" must be generated to determine the tolerance of those particular cells to hypothermic ischemia. Examples of this include primary cells

isolated using a new collagenase vendor/type, a new aliquot of immortalized cells (such as HepG2 or MDCK cells), or a new primary cell isolation method/surgeon.

When the degree of desired preservation injury is defined (see section 3.1.1), then a dose-response curve is obtained for the new cell type. Cells are dispensed into a 96-well plate, grown to about 70% confluence, and then exposed to increasing amounts of hypothermic ischemia (i.e., 12, 24, 36, and 48 hours). At each time point, a plate is kept in the incubator for the same period of time to control for any cell proliferation during that time. After the allotted time, cold-stored plates are rewarmed (simulating reperfusion) in the incubator for one (1) hour ($37\,^\circ$C, 5% CO_2) with 10μL WST-8 to assess mitochondrial redox activity (which correlates to cell viability).

Other parameters that may vary include cell passage (the more times a cell line is passaged, the more resistant to preservation injury; see Fig 3.3), medium type, endpoint measures, and plating conditions (i.e., collagen-coated plates for primary hepatocytes).
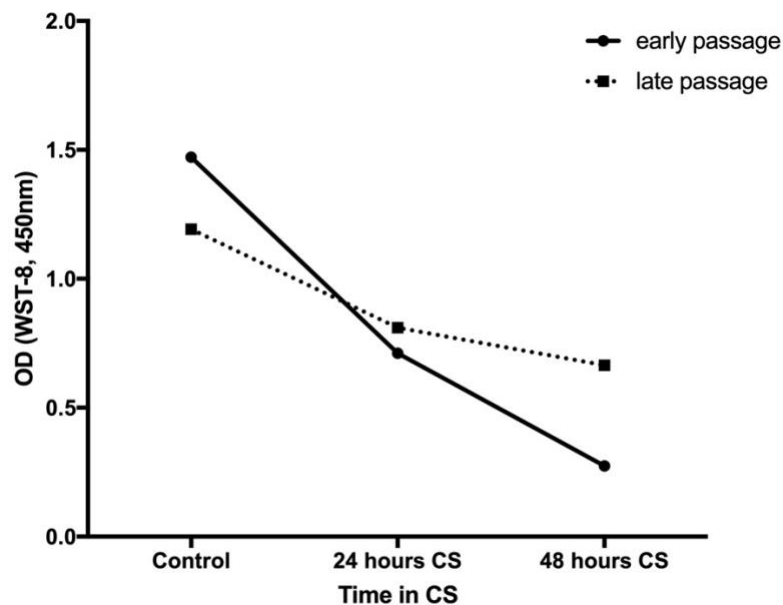
Figure 3.3 Cell lines with higher passage number may be more resistant to preservation injury during cold storage

While not statistically significant, the slope of the line between the points on this graph correlates to the rate of preservation injury in HepG2 cells. Cells with a higher passage number are not as susceptible to hypothermic ischemic insult as their early passage counterparts. Control and 24 hours cold storage (CS) (n=3), 48 hours CS (n=2), no statistical analysis performed due to n<3.

3.2.3 Considerations for cell origin

This model was developed to provide a more simplistic method to evaluate the intracellular molecular mechanisms associated with preservation injury, removing the confounding factor of intercellular microenvironment and tissue-level milieu. We have an isolated perfused liver (Section 3.3) and an orthotopic rat liver transplant model (Section 3.4) that provide a more physiologic, complex investigation into these mechanisms. However, they are lower resolution and examine different functional parameters than an *in vitro* model using isolated cell populations. We can use these models to determine how preservation injury affects overall graft function (i.e., measuring bile output, for example), but it is quite challenging to determine which pathway in the hepatocytes or cholangiocytes are responsible for the observed decrease in functional parameter.

Cell origin (primary versus immortalized line) is an important factor to consider in this model, as it dictates all of the aforementioned parameters. Primary cells tend to require a matrix for adherence to the plate, a different type of culture medium, and can withstand far less cold storage time than immortalized cell lines. When adjusting the model for new cell types, considerations for origin suggest the starting point for the optimization process. For example, a primary hepatocyte culture may only require eight (8) hours of cold storage to reach the desired amount of preservation injury (that is, a translatable amount of injury).

Immortalized cell lines are often used when developing new models, even if the endpoint use will be in primary cells, due to their hardiness and proliferation. Benefits of this include reduced animal sacrifice while developing/optimizing a model, easy culture expansion, and

predictable results between replicates. Limitations include the translatability of findings to a primary cell model; cancer cells have altered and upregulated survival signaling, and in a model such as ours (when cellular stress is induced), these cancer cells are likely able to sustain more preservation injury than their primary cell counterparts.

3.3 Isolated perfused liver (IPL)

Cell models of organ preservation and reperfusion are incredibly useful when the research goal is to focus on a single signaling pathway, often from surface receptor intracellularly to multiple downstream effectors. In order to pinpoint how individual proteins and intracellular organelles behave during preservation, an *in vitro* cell model exhibits advantages over more complex, heterogeneous models. However, certain parameters cannot be evaluated with an *in vitro* model, such as intact liver function – the nature of a single cell population in culture does is not conducive to gaining a birds-eye view of how the liver thrives in its physiologic environment.

Adult male Sprague-Dawley rats were anesthetized with isoflurane, and the liver was isolated by R. Li according to previously described methods by Lindell et al. (1996) (Fig 3.4). Briefly, a catheter was placed in the portal vein and the bile duct was cannulated to assess bile production as an endpoint measure. The liver was flushed *in situ* with cold (4°C) heparinized UW solution then removed. The isolated liver was flushed again with the cold heparinized UW solution and then stored in either vehicle (DMSO), ABC294640 (Cayman Chemical, Ann Arbor, MI) low or high dose for 24 hours (Lindell et al. 1996; Limkemann et al. 2016).

Reperfusion was performed in an oxygenated recirculating system with warm (37°C) Krebs-Henseleit bicarbonate (KHB) buffer (which contained in mmol/L: NaCl (118), $NaHCO_3$ (10), KCl (4.7), $MgCl_2$ (1.2), glucose (11.1), KH_2PO_4 (1.2), HEPES (20) and $CaCl_2$ at pH of 7.4)

infused with O_2 (95%) and CO_2 (5%) (Compagnon et al. 2002). The flow through the vasculature was controlled at 3ml/min/g liver and the vascular pressure was continuously monitored. Livers were assessed on the perfusion apparatus for 30 minutes, perfusate was collected and bile production was measured. To determine liver viability and function, LDH, AST/ALT and bile production were measured.
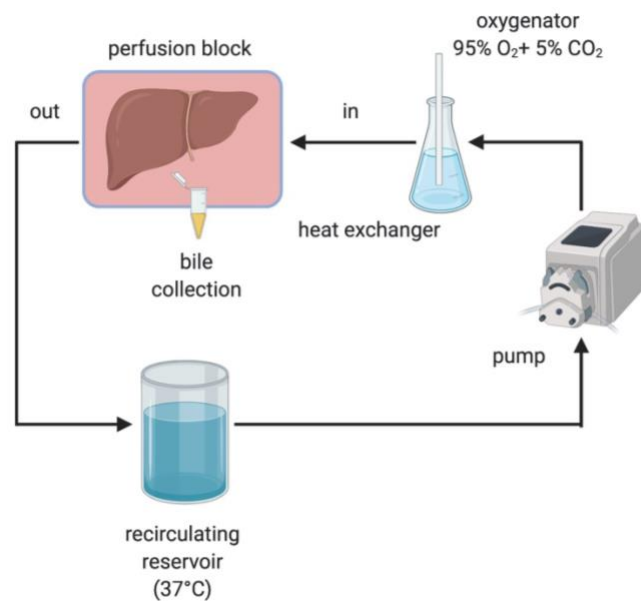
Figure 3.4 Model of isolated perfused liver (IPL)

Rat livers were procured, cold-stored, and then reperfused on this IPL apparatus, where flow was controlled and resistance, LDH release, and bile production were measured to assess liver function. Adapted from (Jimenez-Castro et al. 2013).

3.4 Liver transplant model

The best model for assessing gross liver function is that of a transplantation. Liver procurement and transplantation was performed by S. Lindell according to previously described methods (Sumimoto et al. 1989; Sumimoto, Southard, and Belzer 1993; Lindell et al. 1996). Briefly, livers were isolated from anesthetized male Brown Norway rats and stored in cold (4°C)

UW solution with either vehicle (DMSO) or ABC294640 (10µM or 100µM). After 24 hours of storage at 4°C, the livers were flushed with lactated Ringer's (LR) solution and transplanted into the recipient animals. Transplantation was considered a successful operation if the rats survived until 7 days post-transplant, and all animals were assessed at 4 hours post-op for acute rejection. Outcome measures include LDH and liver enzymes (AST/ALT).

3.5 Western blotting

Evaluation of liver cells for the presence of extracellular LPARs was performed using HepG2 cells (as necessitated by the *in vitro* organ preservation model), SK Hep-1 cells (as a positive control for LPAR expression (REF REF)), and WT mouse hepatocytes. Adherent cells were washed two (2) times with 10mL of 1X PBS, and then 0.25% trypsin-EDTA was applied to dislodge the cells from the plate. It is important to wash adherent cells with PBS because in the case of hepatocytes, they release from the plate when they die. Cells were pelleted by centrifugation of the trypsinized culture suspension at 1000 rpm at 4°C for 5 minutes. The supernatant was removed, and the cell pellet was resuspended in 500µL RIPA buffer with protease inhibitor cocktail (Millipore Sigma). The cell lysate suspension was placed in a microcentrifuge tube and centrifuged at max speed at room temperature for 5 minutes to separate out the DNA and remaining cell debris. The Pierce™ BCA Protein Assay Kit (Thermo Fisher Scientific) was used to quantitate protein concentration in each sample, using a bovine serum albumin (BSA) standard curve. The supernatant was removed (containing the cell lysate), placed in a fresh microcentrifuge tube and Laemmli buffer (with 0.5% reducing agent – B-mercaptoethanol) was added to a final protein concentration of 50µg protein per 20µL buffer. Prepared lysate was boiled in water for 10 minutes and then stored at -20°C.

All western blotting reagents were prepared fresh. 50μg (in 20μL) of each prepared lysate was loaded into a precast polyacrylamide gel (NuPAGE™ 10% Bis-Tris Mini Protein Gel by Invitrogen™, Thermo Fisher Scientific, Inc), and electrophoresis was conducted in MOPS running buffer at 50V for 30 minutes, and then 150V for 30 additional minutes or until the solvent line was at an appropriate distance on the gel. 10μL of Kaleidoscope protein ladder was used in lane one (1) and lane ten (10) on each gel (Bio-Rad). Gels were carefully removed from the plastic housing and transferred to a precut PVDF membrane. Tris-glycine transfer buffer was prepared and the gel:membrane sandwich was placed in the transfer box. Buffer was added and the entire transfer box was placed on ice with a stir bar to keep the cold buffer circulating during transfer. Transfer of proteins from the gel to the membrane was conducted at 100V for 60 minutes. The blot was washed with tap water and incubated with blocking buffer for 30 minutes prior to application of primary antibody overnight (1:500 for SK2). The next day, blots were drained and rinsed with tap water, then incubated with blocking buffer containing the secondary antibody (1:1000) for 60 minutes. All blots were visualized on a Bio-Rad ChemiDoc imager with SuperSignal West Pico PLUS chemiluminescence substrate (Thermo Fisher Scientific, Inc). Band intensity was assessed using Image J (National Institutes of Health) and graphed as relative level (compared to loading control, GAPDH).

3.6 Polymerase chain reaction (PCR)

3.6.1 Primer design and validation

At the time of this investigation, there was limited information available regarding LPA receptor (LPAR) expression in hepatocytes. Various cancer cell lines were known to express LPARs, and published sequences of primers for LPAR1-6 were examined first (Sokolov et al.

2013). The workflow for primer design and validation is shown in Figure 3.4. Primer sequences

can be found in Appendix Tables 10.2.1 (human) and 10.2.2 (rodent). Primer pairs were designed

to include a forward and a reverse primer, each 18-25 nucleotides (NTs) in length, with a GC

content of approximately 50% and complementary melting temperatures. For traditional PCR, the

desired amplicon length was under 450 NTs, while real-time (RT) PCR necessitated a shorter

amplicon (less than 150 NTs).

Primer Sequence
- Search the literature for validated LPAR qPCR primer sequences
- If unknown (e.g. LPAR6), design forward and reverse primers *in silico* using Primer-BLAST (Primer3, NCBI)

Evaluate Sequence
- Primer-BLAST (and integrated global alignment algorithm) checks primer sequence against genome of selected organism
- Initial considerations: mismatching, melting temperature, balanced G/C content, and self-complementarity
- Secondary considerations: primer dimers, secondary structure formation (hairpins)

Validate Primers
- Conduct RT-PCR on cDNA from sample known to express target protein (serial primer dilutions)
- RT-PCR with no template to assess for primer dimer formation / primer contamination

Figure 3.5 Primer design/validation scheme

After verifying the published primer sequences against our biological materials, the need to design

new primers became apparent (only 3 primer pairs from the literature were able to be validated). For those

targets requiring redesign, Primer-BLAST was utilized (Ye et al. 2012). The open-access software allows

the user to input the sequence of the gene of interest and target species, then specify parameters for the

cDNA primer pair (i.e., primer length, GC%, melting temperature, intron/exon spanning, and amplicon

length). Primer-BLAST returns ten (10) primer pair options and based on the aforementioned properties as

well as potential off-target binding, the most suitable primer pairs were then evaluated for hairpin and primer dimer formation (OligoEvaluator[TM], Sigma-Aldrich). Once theoretically validated *in silico*, the primers were ordered, received, appropriately diluted with nuclease-free water (100μM), and finally validated *in vitro*. Serial dilutions on positive (cDNA from sample known to express the target gene) and negative (no template) controls were conducted to determine the optimal primer concentration and rule out any off-target binding (in the form of products of unexpected amplicon length or multiple product bands/peaks) or self-complementary of the primer pairs.

3.6.2 RNA isolation, purification, and quantitation

All RNA isolation and PCR protocols required nuclease-free pipette tips, tubes, and water. The surfaces were cleaned well with 70% ethanol (EtOH) before, during, and after RNA handling. The laboratory bench was designated exclusively for RNA handling. A Thermo Scientific[TM] Nanodrop[TM] ONE pedestal microvolume spectrophotometer assessed RNA sample purity. Absorbance ratios of 260nm/280nm and 260nm/230nm were utilized to establish purity of the RNA sample and identify contaminants. The most common contaminant was guanidine, a common result of the RNA isolation protocol. Pure RNA has an A260/A280 ratio of ~2.0, and an A260/A230 ratio of 2.0-2.2. RNA concentration following either the RNeasy Mini Kit or Trizol® methods of isolation and purification was between 100 – 2,000ng/μL.

Qiagen RNA isolation kit

For the initial RNA isolation procedures, the RNeasy Mini Kit (Qiagen, Germantown, MD) was utilized according to manufacturer's instructions. Briefly, 1×10^7 cells were pelleted and lysed with RLT buffer from the kit. 70% EtOH was added, the sample was transferred to the RNeasy Mini spin column, and the column centrifuged for 15 seconds at $\geq$ 10,000 rpm. RNA binds to the column, while any waste products pass through into the collection tube during the centrifuge cycle.

After several column wash steps, the RNA is eluted from the column membrane with 30μL RNase-free water. Residual DNA contamination was removed by DNase treatment protocol (Qiagen RNase-free DNase Set). Purified RNA was analyzed on the NanoDrop ONE for purity and concentration. Consistently low A260/A280 ratios necessitated a different RNA purification method.

TRIzol® RNA extraction and purification

TRIzol® reagent (Invitrogen[TM]; Thermo Fisher Scientific, Inc.) was utilized according to manufacturer instructions. Briefly, 0.3mL TRIzol® was added to washed adherent cells in culture flasks and the mixture was gently pipetted to completely lyse the cells. The suspension was centrifuged at 4°C, at maximum speed for 15 minutes, resulting in a separation of the lower phenol-chloroform organic layer and upper aqueous layer (containing the RNA). RNA is precipitated from the aqueous phase with isopropanol, and then washed with 75% EtOH. The RNA pellet is then carefully vacuum-dried and solubilized in RNase-free water before purity and yield analysis on the NanoDrop ONE. RNA quality and yield resulting from the TRIzol® protocol was generally superior to that of the Qiagen RNeasy Mini Kit, prompting this method transition.

3.6.3 cDNA synthesis

Purified, quantitated RNA samples were converted into complementary DNA (cDNA) for compatibility with subsequent qRT-PCR. A commercially available reverse transcriptase (RT) cDNA synthesis kit (iScript cDNA Synthesis Kit, Bio-Rad) was employed on RNA samples, producing a presumed 1:1 cDNA product. cDNA synthesis was performed separately than the PCR reaction for use on the CFX Connect, while a one-step RT-PCR was performed on the agarose gel samples. The reaction vials were prepared according to manufacturer's instructions, with 1mg of RNA per reaction, and placed in the thermocycler (manufacturer's instructions for RT (20 minutes

at 46°C) were employed). Samples were then held at 4°C and placed on ice (or frozen at -20°C if endpoint PCR was delayed).

3.6.4 Traditional PCR

Initially, traditional PCR was conducted using the thermocycler and a one-step RT-PCR reagent. The purpose of these amplifications was to simply identify the presence of LPAR RNA, qualitatively. While RT-PCR was in progress according to manufacturer's instructions (SuperScript III™ with *Taq* high-fidelity DNA polymerase, by Invitrogen™, Thermo Fisher Scientific), a 1.8% agarose gel was prepared by boiling TBE buffer with agarose powder until dissolved, cooling to handling temperature, adding ethidium bromide (EtBr) and carefully pouring into a gel mold. A comb was inserted to create sample-loading well, and the gel was allowed to rest at room temperature until set. Samples were loaded into the wells, with a molecular weight marker ladder in the first well (New England Biolabs, Inc). 0.5X TBE buffer was added to the electrophoresis apparatus (Mini-Sub Cell GT Horizontal Electrophoresis System with PowerPac Basic Power Supply, Bio-Rad) to cover the gel and fill the reservoirs on each end, then run for 35-45 minutes at 100V. Finally, the gel was visualized on the Chemi-Doc imaging system (Bio-Rad).

3.6.5 Real-Time PCR

After purchase of a CFX Connect Real-Time PCR Detection System (Bio-Rad), all LPAR gene expression studies were shifted to this instrument. Primers were redesigned to fit the specifications of the instrument (see section 3.6.1 for details). We opted to conduct the reverse transcription step separately and in the thermocycler prior to PCR. cDNA samples were transferred to a 96-well PCR plate and iTaq Universal SYBR Green Supermix (Bio-Rad), forward and reverse primer pairs for the gene of interest (Table 10.XXX) were added to each well. The plate was sealed, centrifuged for 5 minutes on a plate-spinner, and then analyzed in the CFX Connect according to

manufacturer's instructions. CFX Maestro software collects, compiles, and analyzes the resulting data, including amplification cycle and melting curve.

3.7 Sphingosine kinase-2 siRNA application

Commercially available sphingosine kinase-2 (SK2) silencing RNA (siRNA) from Dharmacon (SMARTpool version, containing four (4) unique siRNAs in the mixture for increased potency and specificity, Horizon™) was applied to HepG2 cells in culture using Lipofectamine RNAiMAX for transfection (Thermo Fisher Scientific, Inc). Briefly, Opti-MEM™ Reduced Serum Medium (Gibco) was warmed to 37°C, the siRNA/RNAiMAX solution was prepared according to the manufacturer's instructions (for either 96-well or 6-well plates, depending on the endpoint; viability or protein isolation, respectively), and applied to the HepG2 cells for 48 hours. An RNAiMAX vehicle blank was established to control for any reagent cytotoxicity. After 48 hours of siRNA incubation, the cells were gently washed, fresh culture medium was applied, and cells were analyzed.

3.8 Lipidomics

3.8.1 Mass spectrometry

For the mass spectrometry results presented in this dissertation, all sample preparation and instrumental analysis was performed by the VCU Lipidomics & Metabolomics Core Laboratory. Instrumentation and methods utilized for this sphingolipid analysis includes the QTrap series 5000 Quadropole Linear Ion Trap mass spectrometer (AB Sciex) and extraction protocols previously described (Merrill et al. 2005; Shaner et al. 2009). However, other LPL samples were prepared by the author for mass spectrometric analysis for an unrelated project, according to the methods described below.

Cell culture medium was aspirated from 6-well culture plates, and frozen at -80°C until extraction. Lipid components for analysis were isolated using the Bligh-Dyer method (Bligh and Dyer 1959). Briefly, samples (with the appropriate internal standards depending on the target of the analysis) were added to pure water, methanol (MeOH) and chloroform ($CHCl_3$) in a ratio of 2:1:1.5 and vortexed to mix. Following centrifugation at maximum speed at 4°C, the organic $CHCl_3$ layer was removed, transferred to new autosampler vials, and the $CHCl_3$ was evaporated under vacuum. Samples were resuspended in MeOH and stored at -80°C until mass spectrometry analysis.

3.8.2 FITC-labeled sphingosine-1-phosphate and BSA precipitation

Fluorescently labeled S1P was purchased from Echelon Biosciences, Inc. (S1P fluorescein). An assay was designed to determine how much S1P was bound and sequestered by the FAF-BSA used as a lipid delivery carrier in cold storage experiments. In separate 1.5mL Eppendorf tubes, the amount of FITC-S1P and buffer was kept constant while the concentration of BSA was increased in 10-fold increments (0 – 10%). After 90 minutes of covered incubation on the benchtop, a protein precipitation (BSA) was attempted with 4M ammonium sulfate. The sample was centrifuged, and the supernatant plated in triplicate on a 96-well plate. The amount of fluorescence was measured on an ELX800 plate reader.

3.9 Primary hepatocyte isolation

Primary murine hepatocytes were isolated according to well-established and validated methods (Bissell and Guzelian 1980; Hylemon et al. 1985; Heuman et al. 1991). Briefly, sphingosine kinase-2 null ($SK2^{-/-}$) mice obtained from Dr. R. Proia from the National Institute of Diabetes and Digestive and Kidney Diseases (NIDDK) and their C57BL6 NJ wild-type control

counterparts were anesthetized, and the portal vein was cannulated. Collagenase (type I or type IV) was pumped through the cannula to digest the liver tissue, and centrifugation was utilized to separate the hepatocytes from other cell populations. Isolated hepatocytes were then either pelleted and resuspended in William's medium for plating on collagen-coated polystyrene plates or MiR05 buffer for evaluation of mitochondrial activity.

3.10 High-resolution respirometry analysis of mitochondrial activity

High-resolution respirometry (HRR) was applied to cell and tissue preparations using the Oxygraph-2k (O2k, Oroboros Instruments, Innsbruck, Austria) (Figure 3.6).
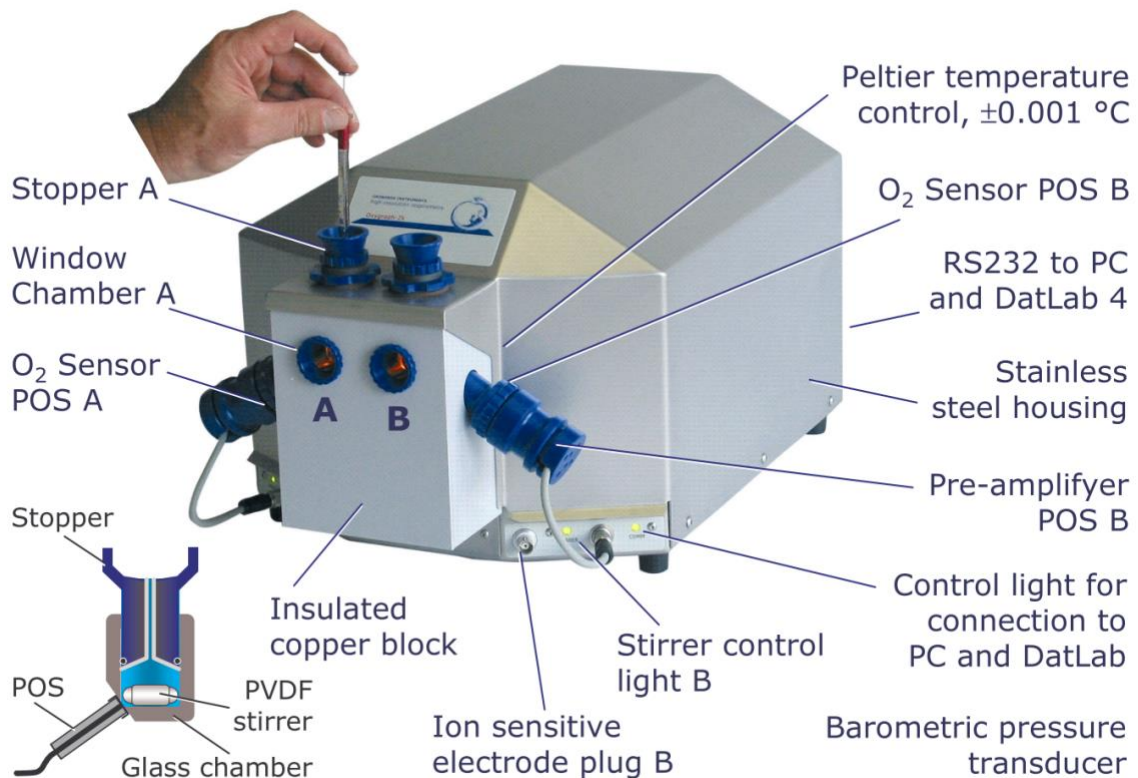
Figure 3.6 The O2k and all of its components (Gnaiger 2008)

3.10.1 Overview of the Oxygraph-2k (O2k)

Briefly, the O2k uses a closed system to measure the amount of oxygen consumed by the sample in the chamber. A Clark electrode (gold cathode and silver/silver chloride anode separated by an electrolyte reservoir, filled with 1M KCl) is separated from the chamber solution by an oxygen-permeable Teflon membrane that is impermeable to ions. As O_2 diffuses across this Teflon membrane, it is reduced by the cathode (creating water and hydroxide), which then results in silver oxidation. A current is produced that is proportional to the partial pressure of O_2 (p_{O2}) in the solution (Gnaiger 2008). The O2k employs a substrate/inhibitor (SUIT) titration protocol to manipulate the individual complexes of the ETC to determine in detail how the experimental conditions impact the ETC complexes in the sample.

The O2k is controlled via computer running DatLab software (version 7.0). The main measures provided are oxygen concentration in the chamber (blue tracing), and oxygen flux (red tracing). Oxygen flux is the change in oxygen consumption and is therefore proportional to the slope of the oxygen concentration tracing (blue). Figure 3.7 shows the standard output of the O2k.
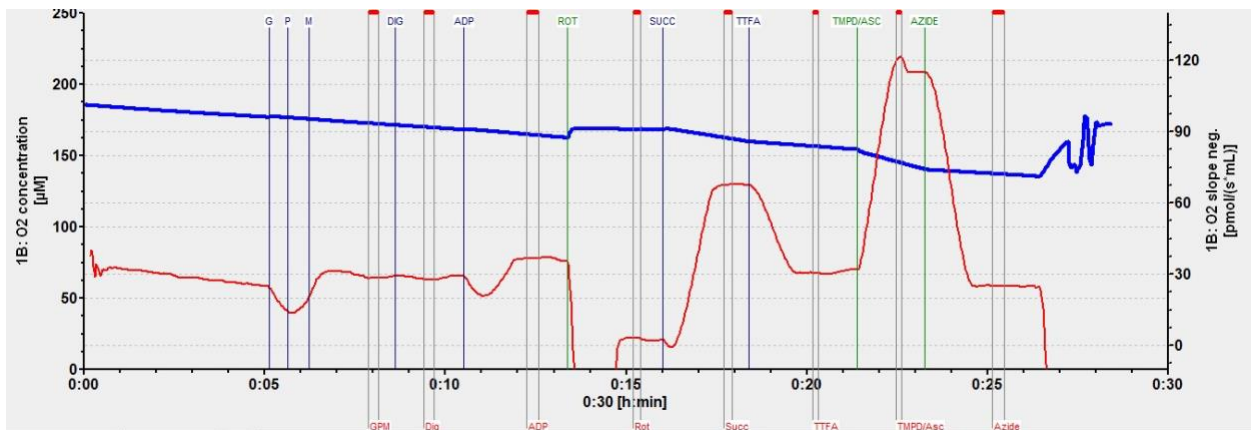
Figure 3.7 Sample output from O2k HRR experiment

Blue line denotes oxygen concentration in the chamber suspension, red line indicates the oxygen consumption or flux (proportional to the slope of the oxygen concentration). When a reagent is injected into the chamber, a mark is created (e.g., G for glutamate, P for pyruvate, and M for

malate, etc.). The plateau after each reagent is marked (red labels below the x-axis), and the average of those values is exported for respiration analysis.

Biological samples are suspended in one of a few types of buffer (see section 3.10.2 below), but all sample suspensions are added to a chamber containing the standard experimental buffer, MiR05. The oxygen solubility factor of MiR05 is 0.92 and describes how the buffer's salt concentration affects oxygen solubility compared to pure water (which is important for calculating oxygen consumption). MiR05 was designed with organ preservation in mind, providing components that protect the mitochondria during analysis in the O2k (Gnaiger et al. 2000; Gnaiger 2008).

3.10.2 Biological sample preparation

Cell preparations (primary hepatocytes and immortalized cell lines) were pelleted and resuspended in MiR05 prior to injection into the O2k chambers. Liver and cardiac tissue homogenates were prepared using a Tenbrook glass homogenizer in cold (4°C) K medium (10mM Tris-HCl, 80mM KCl, 3mM $MgCl_2$, 5mM KH_2PO_4, 0.5mM EDTA, and 0.5 mg/mL fatty acid free bovine serum albumin). A small biopsy from the organ was weighed, placed in the appropriate amount of K medium and 50uL of this homogenate was placed in the chambers. A final amount of 2 – 12 mg of tissue per mL were used and the amount of tissue in the chamber was titrated to instrument sensitivity and basal activity of the tissue sample (similar to the methods described above for cells). For example, a tissue homogenate from a cold-stored organ would be less metabolically active than a homogenate from control tissue. All data were normalized to cell count or tissue weight per mL chamber volume.

3.10.3 Experimental Protocol

All SUIT protocols were adapted from the manufacturer's website to address the needs of each individual experiment (https://wiki.oroboros.at). After overnight storage in 70% ethanol, each chamber and stopper underwent a stringent washing protocol (three (3) distilled water, three (3) 70% ethanol, and finally three (3) distilled water) prior to addition of miR05 buffer. The polarographic oxygen sensor (POS) requires an air calibration each day prior to use, followed by a period of buffer equilibration. Additional POS service was performed (such as zero calibration) after each membrane change or monthly, as needed. Once a stable oxygen flux signal is obtained during the equilibration period, the sample is added to the chamber. A stable rate of oxygen consumption by the sample without depleting the oxygen too quickly is desired (if the sample is too concentrated the rate of oxygen consumption may be too rapid for appropriate experimental measurements to be obtained). If the basal sample respiration was too high, a portion of the sample was removed, documented, and replaced with buffer.

All substrates and inhibitors are displayed in Table 3.1, and the experimental protocol is displayed in Figure 3.8. Most protocols are initiated by adding complex I substrates, often abbreviated as "GPM" (as these three reagents are injected with the same syringe). In whole cell or tissue homogenate suspensions, digitonin must be added to permeabilize the cell membranes (isolated mitochondria do not require digitonin) to allow the reagents access to the intracellular space. Adenosine diphosphate (ADP) is then injected and when complex I is functioning, a spike in oxygen consumption is observed as complex V phosphorylates ADP to ATP. Following a peak in oxygen consumption, rotenone is injected to inhibit complex I. Between each complex, basal respiration is allowed to stabilize before adding new substrates. Succinate is injected as fuel for complex II, and TTFA (thenoyltrifluoroacetone) inhibits complex II after a peak is observed. After

complex II, a choice was made to either investigate complex III or IV. It is not possible to modulate both in the same chamber, as the reagents for complex III interact with those for complex IV and uncontrolled autooxidation is observed (see Fig 10.4.1 in the appendix). For complex III, duroquinone is the substrate and antimycin A is the inhibitor. Finally, for complex IV, ascorbic acid is first added as an antioxidant for the substrate, TMPD (*N*,*N*,*N′*,*N′*-Tetramethyl-*p*-phenylenediamine), and sodium azide inhibits complex IV. Those reagents which are not soluble in water are dissolved in pure EtOH or DMSO and controlled for by injecting a vehicle blank prior to use of the reagent in the chamber.

Compound	Volume added (uL)	Role	Complex	Stock Concentration	Final Concentration
Glutamate	10	Substrate	cI (indirect)	2M	10uM
Pyruvate	5	Substrate	cI (indirect)	2M	5mM
Malate	5	Substrate	cI (indirect)	0.8M	2mM
Digitonin	2	Permeabilizer	N/A	10mg/mL	10ug/mL
ADP	10	Substrate	cV (ATPase)	0.2M	1mM
K145	7.7	SK2 inhibitor	N/A	1mg/mL	10uM
ABC294640	4.5	Inhibitor	cI	1mg/120uL	50uM
Rotenone	10	Inhibitor	cI	0.1mM	0.05uM
Succinate	20	Substrate	cII	1M	10mM
TTFA	8	Inhibitor	cII	20mM	80uM
Duroquinone	10.3	Substrate	cIII	120mM	0.6mM
Antimycin A	5	Inhibitor	cIII	0.4mM	1uM
Ascorbic acid	5	Antioxidant	N/A	0.8M	2mM
TMPD	5	Substrate	cIV	200mM	0.5mM
Azide	50	Inhibitor	cIV	4M	100mM

Table 3.1 Reagents for high-resolution respirometry analysis (O2k)
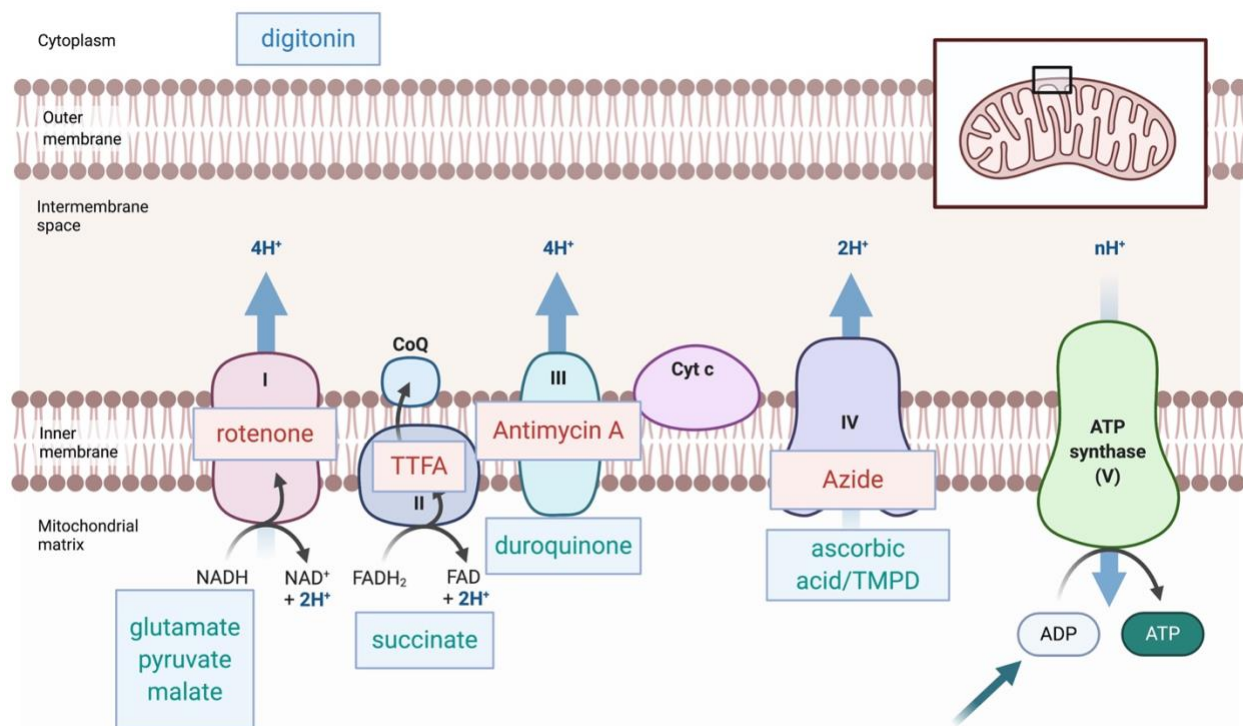
Figure 3.8 HRR SUIT protocol for O2k
Complex I substrates (glutamate, pyruvate, malate) are added, then the plasma membrane is permeabilized with digitonin. ADP is added, and after respiratory peak, rotenone inhibits complex I. Complex II substrate succinate is added, then TTFA inhibits. Duroquinone is the complex III substrate, and antimycin A inhibits. Finally, ascorbic acid and TMPD are complex IV substrates, and sodium azide inhibits.

Appropriate maintenance of the Hamilton syringes is paramount to successful O2k data collection. Other than GPM (which are all drawn up and injected with the same syringe), each reagent is delivered using its own syringe. The syringes used for water-soluble reagents are washed three (3) times with distilled water after each use, while those syringes containing ethanol or DMSO-soluble reagents are only washed three (3) times with 100% ethanol at the end of the day due to the artifact produced by injection of additional ethanol.

3.10.4 Considerations for unique effects on O_2 flux by reagents

Not every reagent that is to be injected into the chamber produces an equivalently shaped change in oxygen consumption (O_2 flux) (see Fig 3.7 at the 13-minute mark for rotenone). For example, since rotenone is soluble only in EtOH, there is a sharp, drastic decrease in O_2 flux upon injection into the chamber that is considered an artifact due to its EtOH origins. Only after the flux recovers and plateaus do we consider the data suitable for analysis. Likewise, DMSO produces a shallower (than EtOH) but long "dip" in flux, with a recovery to baseline flux after about one (1) minute (fondly known as the "DMSO dip") (Fig 3.9).
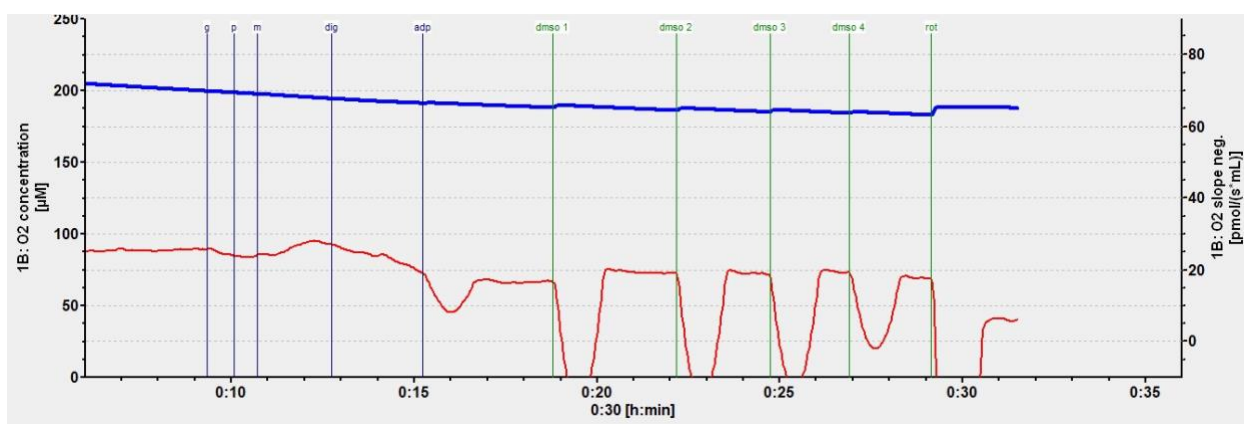
Figure 3.9 DMSO-induced oxygen flux artifact

In preparation for a dose-response experiment using ABC294640 (which is solubilized in DMSO), we conducted a vehicle dose-response with DMSO to ensure that DMSO alone does not have a significant effect on oxygen consumption (red tracing). While the act of injecting the substance leads to an expected dip in oxygen flux, that signal rebounds to near-baseline levels and stabilizes within about one (1) minute. The final mark shows the injection of rotenone, and a subsequent reduction in oxygen flux, indicating inhibition of complex I.

3.11 Statistical analysis

GraphPad PRISM version 7.0 for Windows and Mac was used to conduct these analyses. All data are expressed as mean $\pm$ the standard error of the mean (SEM) unless otherwise noted.

Cell viability data was collected as least in triplicate on each plate, and compiled according to previously defined parameters (Lord et al. 2020). Outliers were identified and removed from the raw *in vitro* cell viability data to account for expected technical inconsistencies using the Tukey test for outliers. Cell viability data was normalized to the vehicle control (either BSA or EtOH, depending on the experiment). Differences between greater than three (3) groups were compared using a one- or two-way ANOVA (Tukey's or Bonferroni's test for multiple comparisons). When only two (2) groups were present, an unpaired student's t-test was conducted. Statistical significance was defined as a p-value of less than 0.05.

Chapter 4: Sublamellar cytoskeletal linker proteins and their upstream regulators in preservation injury

4.1 Abstract

Not only is the actin network disrupted during organ preservation, but cytoskeletal linker proteins are inactivated as well (Molitoris and Finn 2001; Mangino et al. 2008; Tian et al. 2009; 2012). Ezrin, radixin, and moesin family members (ERM proteins) function to anchor intracellular actin to the plasma membrane, stabilizing the cytoskeleton and supporting the morphology (REF REF). ERM activation is partially controlled by Rho kinase (ROK or ROCK) and Rho (small GTPase) (Ponuwei 2016). Using pharmacologic inhibitors for Rho and ROK, we showed that these proteins are important in maintaining cell viability in an *in vitro* model of organ preservation. These data support previous research showing that ERM proteins are deactivated as a result of preservation injury, as these two regulators activate ERMs.

4.2 Background

In epithelial cells, such as hepatocytes and renal tubule cells, a particular architecture is required for cell function. The orientation of various transporters on either the basolateral or apical membrane is critical, and the cytoskeleton is responsible for anchoring those elements to the correct portion of the cell's membrane. ERM proteins are activated in part by phosphorylation, conferring their open conformation and allowing these C-shaped proteins to bind with the intracellular actin network on one end, and the plasma membrane on the other. In addition to rho kinase (ROK), ERM proteins can be phosphorylated by a plethora of other kinases including protein kinase C, Nck interacting kinase, G-protein receptor coupled kinase 2, as well as non-receptor tyrosine kinases (Ponuwei 2016).

Rho kinase (ROK) activity is controlled by members of the Rho family of small G-proteins (Amano, Nakayama, and Kaibuchi 2010). The most well-studied members of the Rho family include RhoA, Cdc42, and Rac1 (and each controls different processes involved in cytoskeletal rearrangement). Rho proteins are a subfamily of the Ras superfamily of small G-proteins, and are primarily GTPases that hydrolyze GTP into GDP, and harness the resulting energy to act as a molecular switch (Smithers and Overduin 2016).

4.3 Results

4.3.1 Inhibition of Rho and ROK during cold storage worsens preservation injury in HepG2 cells

Moesin configuration is an important factor in maintaining HepG2 cell viability during cold storage, as evidenced by mutational studied performed in our laboratory (Tian et al. 2014). Since ROK is known to regulate ERM protein activity, and RhoA controls ROK activation, we used pharmacologic inhibitors to determine if these two proteins play a role in the preservation

injury phenotype. Exoenzyme C3 transferase from *Clostridium botulinum* (Cytoskeleton, Inc., Denver, CO) inhibits RhoA, while a commercially available compound, Y-27632, inhibits ROK. HepG2 cells were treated with either exoenzyme C3 transferase, Y-27632, or a combination of the two compounds and then placed in cold storage for 12 or 24 hours. Figure 4.1 shows that when either of these proteins is inhibited, alone or in combination with the other, the degree of preservation injury is increased compared to vehicle controls at 12 hours of cold storage. As if often the case, no observable differences were seen at 24 hours of cold storage due to the high degree of preservation injury seen.
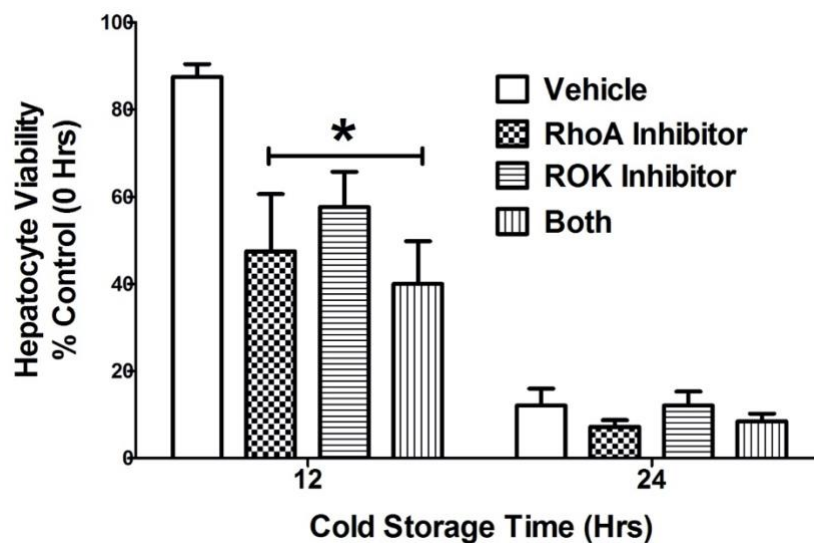
Figure 4.1 Inhibition of RhoA and ROK worsen preservation injury in HepG2 cells

HepG2 cells were plated in 96-well plates. Exoenzyme C3 transferase from c. botulinum (RhoA inhibitor, 0.5μg/mL) and Y-27632 (ROK inhibitor, 10μM) were added to cell culture medium, and the HepG2 cells were treated for two (2) hours prior to induction of hypothermic ischemia. Following cold storage (twelve (12) and twenty-four (24) hours, respectively), the plates were reperfused in the incubator for 1 hour and then cell viability was measured (WST-8 assay). Two-way ANOVA showed significant differences between the vehicle and all other groups at 12 hours of cold storage (n=3, *p<0.05).

4.4 Conclusions

Inhibiting RhoA and ROK during hypothermic ischemia significantly worsens the preservation injury phenotype in HepG2 cells. One limitation is that the exoenzyme C3 transferase from *c. botulinum* is not a specific Rho inhibitor, but rather binds to all three isoforms. This implies that at least one of the affected Rho kinases is important in supporting hepatocytes during hypothermic ischemia, but only when combined with the ROK inhibitor data can we conclude that it might be RhoA that is the most important. Combined with our laboratory's existing data suggesting the defensive role of activated ERM proteins, these results support the hypothesis that downstream effectors of LPL receptors may confer protection against preservation injury.

Chapter 5: Lysophosphatidic acid in preservation injury

5.1 Abstract

Lysophosphatidic acid (LPA) is a pleiotropic, biologically active lipid signaling mediator produced by activated platelets, with demonstrated roles in blood pressure, cell growth and motility, and smooth muscle contraction as well as upregulation in cancer (Ishii et al. 2004). LPA signaling through six (6) G-protein coupled receptors (GPCRs) on the plasma membrane, with a myriad of intracellular actions. Of interest here is the relationship between RhoA, Rho kinase (ROK), and LPA signaling. First, the LPA receptor (*LPAR*) expression profile on hepatocytes was investigated. We found that hepatocytes expressed *LPAR1-6* mRNA. We hypothesized that adding exogenous LPA to cells in culture during cold storage would improve cell viability, thus reducing degree of preservation injury. HepG2 cells were exposed to hypothermic ischemia with increasing concentrations of LPA (carried in aqueous solution by 0.1% FAF-BSA), reperfused for one hour in the incubator, and then cell viability was assessed. We found that LPA does not dose-

dependently improve HepG2 viability following cold storage. However, this may be due to inadequate LPA delivery by BSA in cold storage. Even at standard lipid-carrying concentrations, BSA decreases cell viability following cold storage. These results necessitate the development of an effective lipid delivery system for hypothermic ischemia.

5.2 Background

5.2.1 LPA receptor expression in hepatocytes

At the time these studies were proposed and initiated, the literature was not clear on whether primary hepatocytes expressed LPARs at all, and if so, which ones were biologically relevant? These investigations were carried out both in a traditional PCR method as well as real-time PCR to quantitate mRNA expression.

GAPDH was utilized as a loading control for rodent cDNA samples (mouse and rat). Unfortunately, due to the difference in cycle number of *GAPDH* amplification in our two human cell lines, a new loading control was required. HepG2 cells were often the standard for *in vitro* organ preservation. However, there was discrepancy over whether HepG2 cells expressed LPARs in the quantity required to test the hypothesis of LPAR-mediated protection against preservation injury. In order to validate the primers, a cell type with known *LPAR* expression was required. SK Hep-1 served as a positive control. A literature review indicated the following genes exhibited potential as appropriate candidate loading controls: *B2M*, *HMBS*, and *SDHA*. Primer pairs were designed using Primer-BLAST and validated (see Appendix, Tables 10.2.2 and 10.2.3, for primer sequences). The primer pair for *B2M* yielded the best results and this gene was employed as the loading control for the human cell line studies.

5.3 Results

5.3.1 Primary mouse hepatocytes express LPA receptors

At the time of study initiation, the literature was sparse regarding whether primary hepatocytes expressed LPA receptors (LPARs) in quantities sufficient to elicit a response to exogenously applied LPA during cold storage. qRT-PCR was conducted on cDNA from isolated mouse hepatocyte purified RNA, with forward and reverse primers for each of the six (6) LPARs. Analysis demonstrated that primary hepatocytes do express mRNA for *LPAR1-6* (Figure 5.1). Previous work confirms the presence of LPARs in HepG2 cells, despite the incomplete profile in Fig 5.1 (Sokolov et al. 2013; Zuckerman et al. 2015).
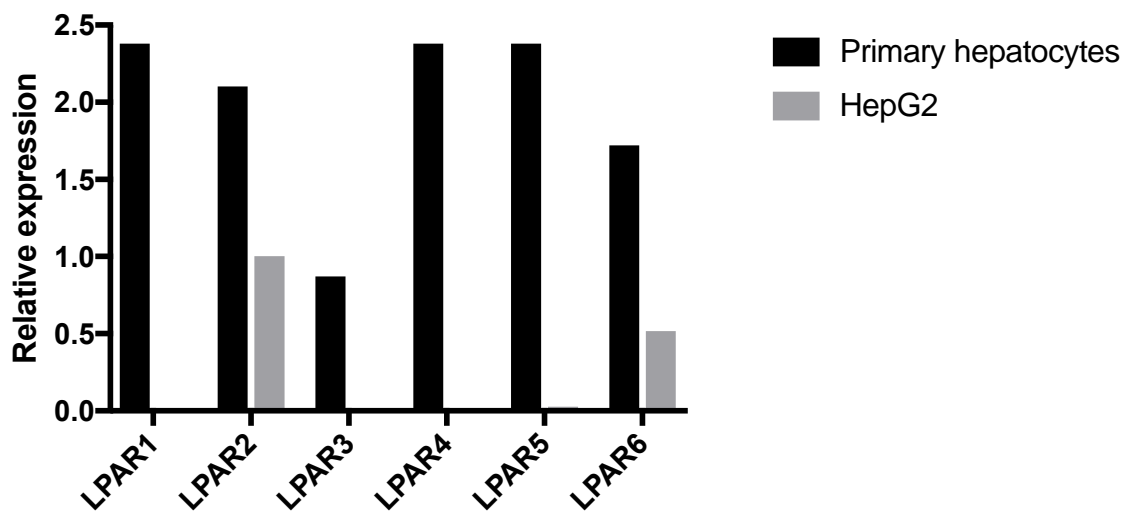
Figure 5.1 Primary mouse hepatocytes express LPA receptors 1-6

Isolated mouse hepatocyte LPAR expression normalized to GAPDH; HepG2 LPAR expression data incomplete, only LPAR2, 5, and 6 were examined in this study prior to abandonment due to new publication; n=1(no statistical analysis performed).

5.3.2 LPA does not attenuate preservation injury phenotype

Once the presence of LPA receptors was confirmed, HepG2 cells were treated with increasing concentrations of LPA with 0.1% fatty acid free bovine serum albumin (FAF-BSA)

and cold stored for 12 and 24 hours. We hypothesized that LPA would dose-dependently improve cell viability in the cold-stored cells relative to controls. The results, shown in Figure 5.2, indicate that LPA *does not* impact cell viability compared to vehicle (0.1% FAF-BSA) controls.
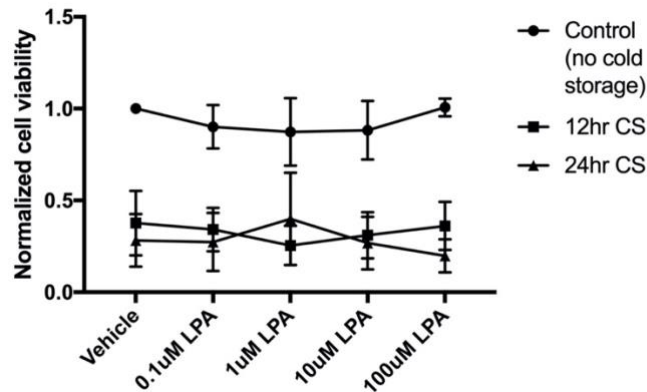
Figure 5.2 Exogenous LPA does not protect HepG2 cells against preservation injury

HepG2 cells were treated with escalating doses of LPA (0.1, 1, 10, and 100uM), and then subjected to cold storage for 12 and 24 hours. The vehicle was 0.1% fatty acid free-bovine serum albumin (FAF-BSA). Data were normalized to the vehicle control cell (no cold storage) viability. Control (n = 17), 12hr CS (n = 10), 24hr CS (n = 8). Two-way ANOVA showed no significant differences between increasing LPA concentrations within each experimental condition (i.e., within the control group, no differences between vehicle and any dose of LPA, etc.), p>0.05.

5.3.3 Bovine serum albumin (BSA) exhibits cytotoxicity

We noticed that it seemed even the vehicle controls in the exogenously applied LPA during cold storage studies exhibited lower viability than the medium alone (Fig 5.3), indicating that any effect LPA might have to protect hepatocytes against preservation injury is likely being masked by the vehicle (0.1% FAF-BSA). Using BSA to carry lipids in aqueous conditions is standard practice, but these studies are most often conducted in physiologic conditions (oxygenated, 37°C). With the introduction of hypothermic ischemia in our *in vitro* cold storage

model of organ preservation, we found that under physiologic conditions, only 10% BSA significantly decreased cell viability (Fig 5.4). However, cold stored HepG2 cells were significantly affected by only 0.1% BSA, the concentration needed to carry LPA in our studies (Figure 5.3).
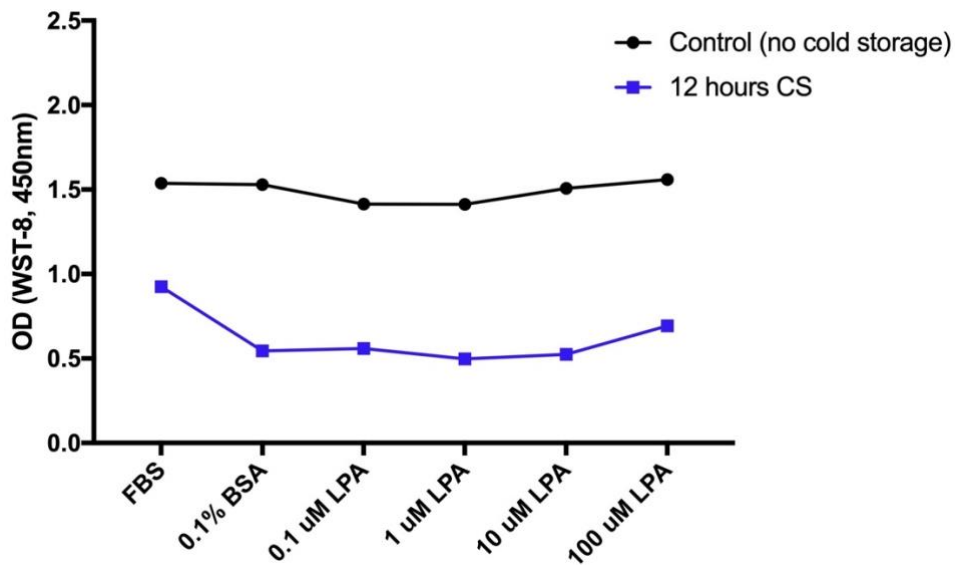
Figure 5.3 0.1% FAF-BSA decreases viability in hepatocytes in cold storage, regardless of LPA concentration

In control cells (incubator storage, 37°C, 5% CO_2), viability was approximately stable regardless of the experimental conditions applied. However, in cold-stored (CS) cells, addition of FAF-BSA led to a decrease in cell viability, that could not be rescued by increasing concentration of LPA, n=2 (no statistical analysis performed).

In order to determine if the level of BSA fatty acid saturation impacted cytotoxicity, we conducted a dose-response with both fatty acid free (FAF) BSA and fatty acid saturated (FAS) BSA. Both forms of BSA were purchased from Sigma-Aldrich, and prepared fresh for each application. We hypothesized that if BSA was exerting negative effects on HepG2 cells (Fig 5.3) by sequestering the available pro-survival signaling molecules (such as LPA and S1P) and

making them unavailable for bind to extracellular LPARs, then the application of FAS-BSA

should confer an <u>increase</u> in cell viability. These FAS-BSA complexes have not been stripped of

their endogenous fatty acid molecules, and therefore do not have extensive binding capacity for

additional fatty acids in the culture medium (Opti-MEM reduced serum medium, Gibco). We

found that the type of BSA applied to HepG2 cells in culture did not differentially affect cell

viability (WST-8) (Figure 5.4).
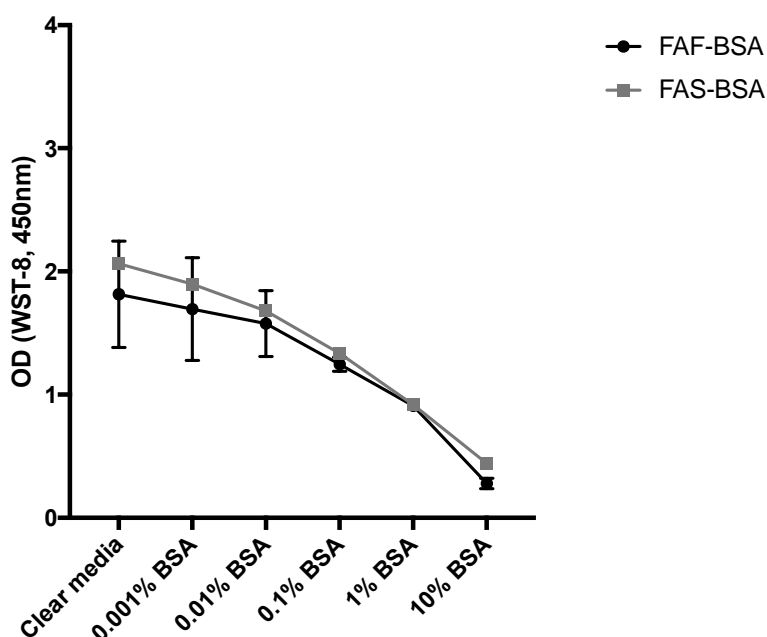
Figure 5.4 Fatty acid saturation of BSA does not impact cytotoxicity

FAF-BSA (n = 3), FAS-BSA (n = 2, no statistical analysis performed), no significant differences between increasing concentrations of FAF-BSA, p>0.05. Error bars are shown for FAF-BSA.

5.3.4 BSA-mediated cytotoxicity is exaggerated in cold storage

Figure 5.3 illustrates how twelve (12) hours of cold storage increases HepG2 cell

susceptibility to BSA cytotoxicity. Increasing the time in cold storage further to twenty-four (24)

hours worsens BSA's negative effect on cell viability (Figure 5.5). 0.1% FAF-BSA doesn't seem

to impact HepG2 viability under control conditions, but nearly decimates viability after 24 hours

of cold storage.
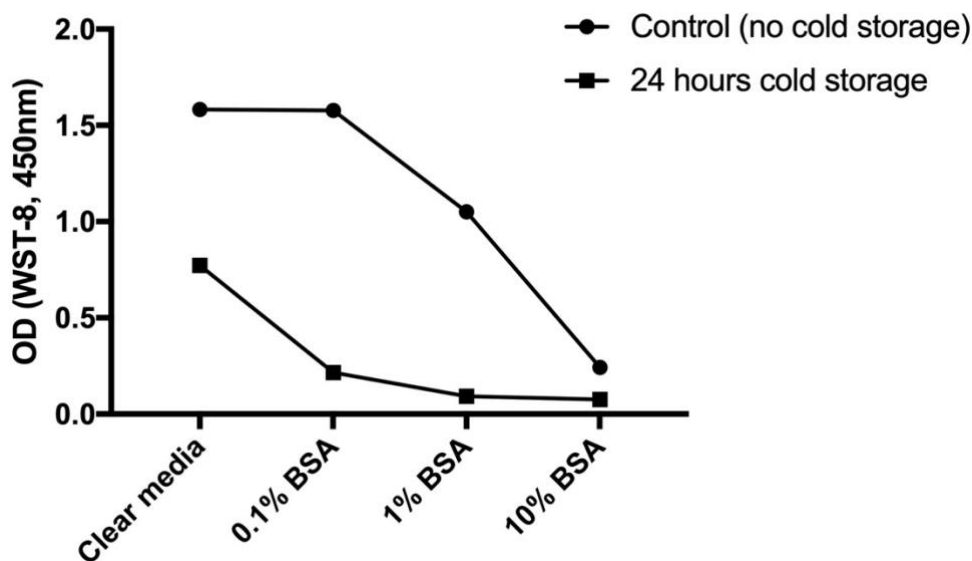
Figure 5.5 Cold storage exacerbates BSA cytotoxicity

Control HepG2 cells (no cold storage) were unaffected by 0.1% BSA, while HepG2 cells cold stored for 24 hours are significantly less viable with 0.1% BSA treatment (n=2, no statistical analysis performed).

5.3.5 Human and bovine serum albumin exert similar effects on cells

Upon the observation that BSA dose-dependently decreased cell viability with and

without cold storage, it was hypothesized that this negative effect may be due to a cross-species

interaction between the bovine albumin and the human cell lines. As such, human serum albumin

(HSA) was dose-dependently applied to immortalized cell lines (HepG2 and SK Hep-1) and

WST-8 conversion correlating the viability was measured. Human and bovine serum albumin

have very similar effects on both HepG2 and SK Hep-1 cells in a dose-dependent manner. With

the exception of 1% albumin in the SK Hep-1 cells (and this same concentration, though not

statistically significant, is trending in that direction in the HepG2 cells), there is no significant

difference between albumin from human or bovine subjects. If any difference did exist, we suspected bovine albumin may be more cytotoxic than albumin from humans. In fact, the opposite was true with 1% HSA decreasing viability compared to 1% BSA in SK Hep-1 cells.
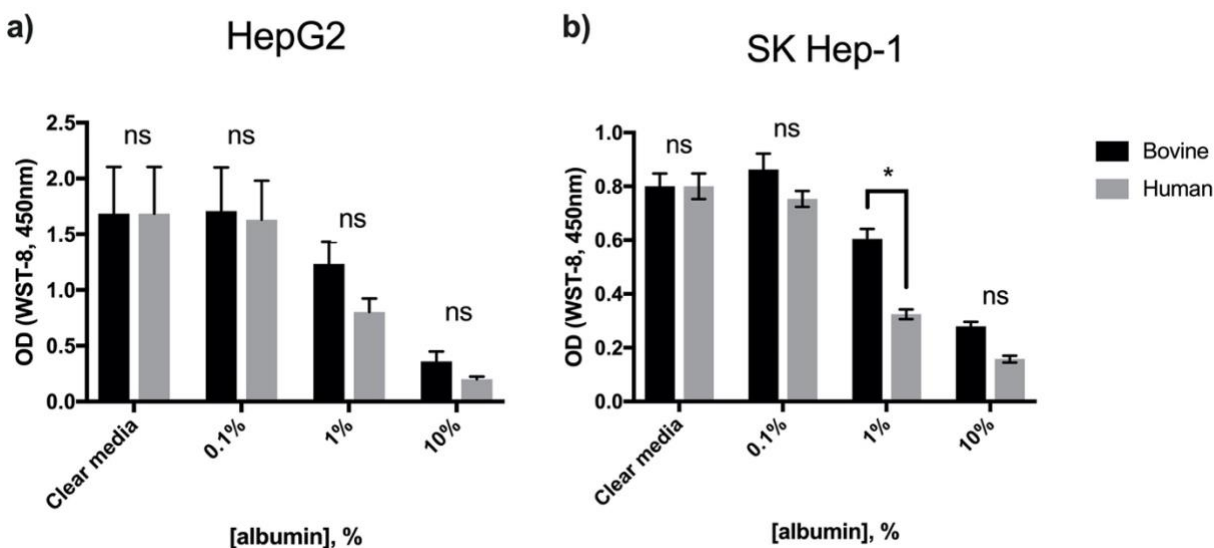
Figure 5.6 Human and bovine serum albumin exhibit similar dose-dependent effects on cells

*a) HepG2 (n = 4) and b) SK Hep-1 (n = 6) cells. With the exception of 1% albumin in the SK Hep-1 cells, there were no significant differences between bovine and human serum albumin. Generally, it seems that human albumin may be trending towards exhibiting more cytotoxicity than bovine albumin at higher concentrations (1% and above). Two-way ANOVA compared all groups within each cell type (bovine and human, as well as increasing albumin concentration), *$p<0.05$.*

5.4 Conclusions

Based on these results, exogenous LPA does not appear to protect hepatocytes against preservation injury, despite the presence of LPARs. This may be an artificial result due to the failure of BSA as a lipid delivery system in cold storage. BSA treatment, regardless of the concentration of LPA, decreases cell viability in cold-stored HepG2 and SK Hep-1 cells. Extent of BSA fatty acid saturation and species of albumin origin did not play a role in the increased

preservation injury observed in cold stored cells with even low concentrations of albumin. Confirmatory western blotting for LPARs (following PCR) was not completed due to publication of these data during this investigation by another group.

Chapter 6: Sphingolipids in preservation injury

6.1 Abstract

For the same reasons that LPA seems an attractive target for investigating the molecular mechanisms of preservation injury in hepatocytes, S1P signaling may play similar and distinct roles in protecting against this injury. S1P receptors control some of the same downstream effectors as LPA (such as Rho), but due to the inside-out signaling mechanism of S1P, intracellularly-produced S1P has biologically distinct roles. Targeting the S1P synthetic pathway, a selective sphingosine kinase-2 (SK2) inhibitor (ABC294640) was used to decrease intracellular S1P production and the phenotype was observed in cold-stored hepatocytes. We saw a decrease in the S1P:ceramide ratio, hepatocyte viability, survival of rodent liver transplant recipients, and functional parameters in an isolated perfused liver (IPL) model. Treatment with ABC294640 during cold storage, presumably through inhibition of its target enzyme, SK2, worsens preservation injury in the liver.

6.2 Background

6.2.1 Sphingolipid synthesis and the "rheostat"

Sphingolipid synthesis is detailed in section 2.3 and figure 2.2. Briefly, sphingosine can be converted into one of two species: S1P (via sphingosine kinases, SK1 and SK2) or ceramide (via ceramide synthase). These species can be back converted to sphingosine by ceramidase or S1P phosphatase. Cell fate can be determined by the sphingolipid rheostat: the balance between pro-

survival S1P and pro-death ceramide at any given time in the cell. Evidence supports the use of this rheostat, as S1P regulates proliferation, angiogenesis, and survival while ceramide is a tumor suppressor and promotes apoptotic and autophagic cell death as well as growth arrest (Newton et al. 2015; Cuvillier et al. 1996).

6.2.2 Fate of S1P in the cell

Once S1P is produced intracellularly, it has three possible fates. First, it can be degraded by S1P lyase. Second, phosphatases can convert it back to sphingosine. And third, it can be pumped out of the cell via a surface transporter called SPNS2 (Santos and Lynch 2015). However, before the first two fates described above, S1P can bind to intracellular targets and elicit a response prior to degradation. It is these intracellular targets of S1P that are of interest in these studies due to evidence showing that SK2-derived S1P is important in the assembly of complex IV of the mitochondria and nuclear gene transcription (Strub et al. 2011).

6.3 Results

6.3.1 BSA binds FITC-labeled S1P in aqueous solution

Armed with the knowledge that BSA seems to be cytotoxic during cold storage, we wanted to test the hypothesis that this effect is due to BSA's tendency to sequester lipid growth factors in aqueous solution. In 1.5mL Eppendorf tubes, 50µL FITC-S1P (in MeOH) and 500µL buffer was added with increasing concentrations of BSA in different tubes (0 – 10% in 10-fold increments). After a covered incubation on the benchtop, we attempted to precipitate the BSA out of solution with concentrated ammonium sulfate. The vials were centrifuged at maximum speed for 5 minutes, and then the supernatant was plated in triplicate on 96-well plates and the fluorescence read on the plate reader. The fluorescent units (FU) are reported in Figure 6.1, and

with the exception of the control and 0.01% BSA conditions, the results are as expected: the

higher the BSA concentration, the more S1P seems to have precipitated out with the protein

resulting in a lower fluorescent signal in the supernatant. Unfortunately, the BSA precipitation

was incomplete and we hypothesized that nonspecific binding of FITC-S1P to the sides of the

Eppendorfs with 0% and 0.01% BSA led to the significantly reduced fluorescence in those

samples (a known complication).
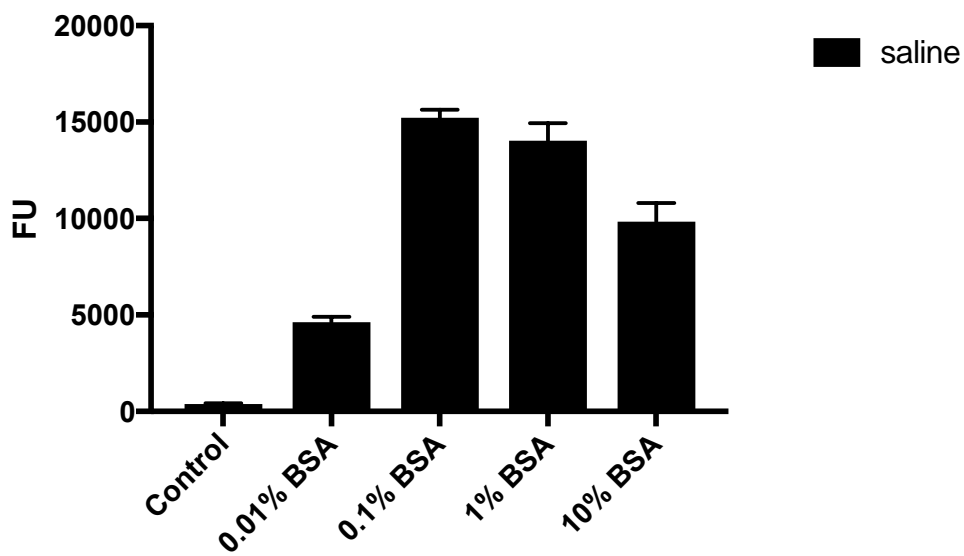
Figure 6.1 BSA dose-dependently sequesters S1P in saline

FAF-BSA was added to a solution containing FITC-S1P, incubated for 90 minutes, and then precipitated with 4M ammonium sulfate. n=1 (no statistical testing performed; error bars represent the standard error of the triplicates on the 96-well plate).

6.3.2 Sphingolipid rheostat response to hypothermic ischemia

It seems intuitive that since the sphingolipid rheostat correlates to cell status, and

hypothermic ischemia causes cellular stress, that this rheostat would be altered in an organ

preservation model. HepG2 cells were plated in 6-well plates, treated with 0.1% FAF-BSA (the

vehicle control for impending lipid application studies), and either placed in the incubator or cold

storage for 12 hours overnight. Following one (1) hour of reperfusion on the cold-stored plate, the supernatant from both plates was collected and frozen. The samples were delivered to the VCU Mass Spectrometry Laboratory for sphingolipid analysis. Results were reported to the author in an Excel spreadsheet, normalized to pmol/mL (data can be found in appendix, Table 10.3.1). While there is likely more information to glean from the extensive data provided, it is important to note that the S1P:Cer ratio is trending in a direction that indicates sphingolipid production may be altered by hypothermic ischemia.
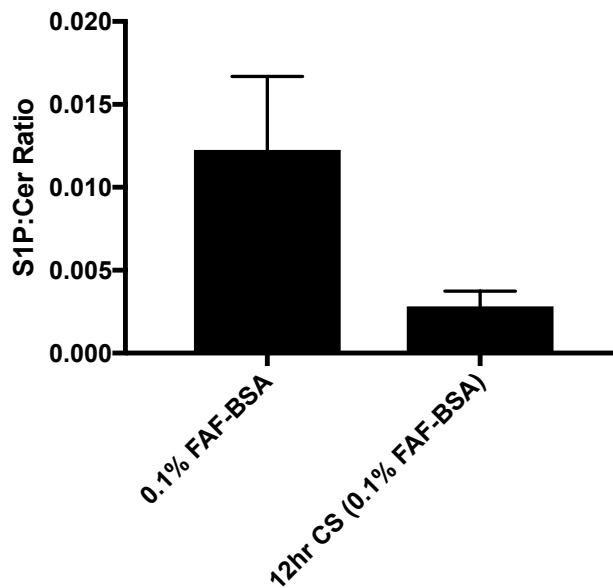
Figure 6.2 S1P:ceramide ratio is decreased in the supernatant from cold-stored HepG2 cells

The ratio of S1P:ceramide indicates how healthy a cell population is at the time of sampling, with a higher ratio suggesting healthier cells. As expected, subjecting cells to hypothermic ischemia is a stressful event, corresponding to a lower S1P:ceramide ratio. n=1 for each group (one experiment conducted, and one vial of sample provided for mass spectrometry analysis for each group), no statistical analysis performed, error bars represent standard error of duplicate (0.1% FAF-BSA control) and triplicate (12 hours CS) measures from the same sample.

6.3.3 Sphingosine-1-phosphate is bound by BSA in aqueous solution

We utilized the lipidomics data from Table 10.3.1 to assess how much S1P is bound up by BSA in aqueous cell culture medium. The negative control, serum-free DMEM, as well as both 0.1% FAF-BSA only (incubator control and 12 hours cold storage) did not exhibit significantly different S1P levels in the precipitate compared to the supernatant, though the results are trending in that direction. The positive control, FBS, did exhibit 3.5 times higher S1P levels in the precipitate compared to the supernatant, confirming that FAF-BSA does sequester S1P and this complex can be precipitated out of solution (Figure 6.3).
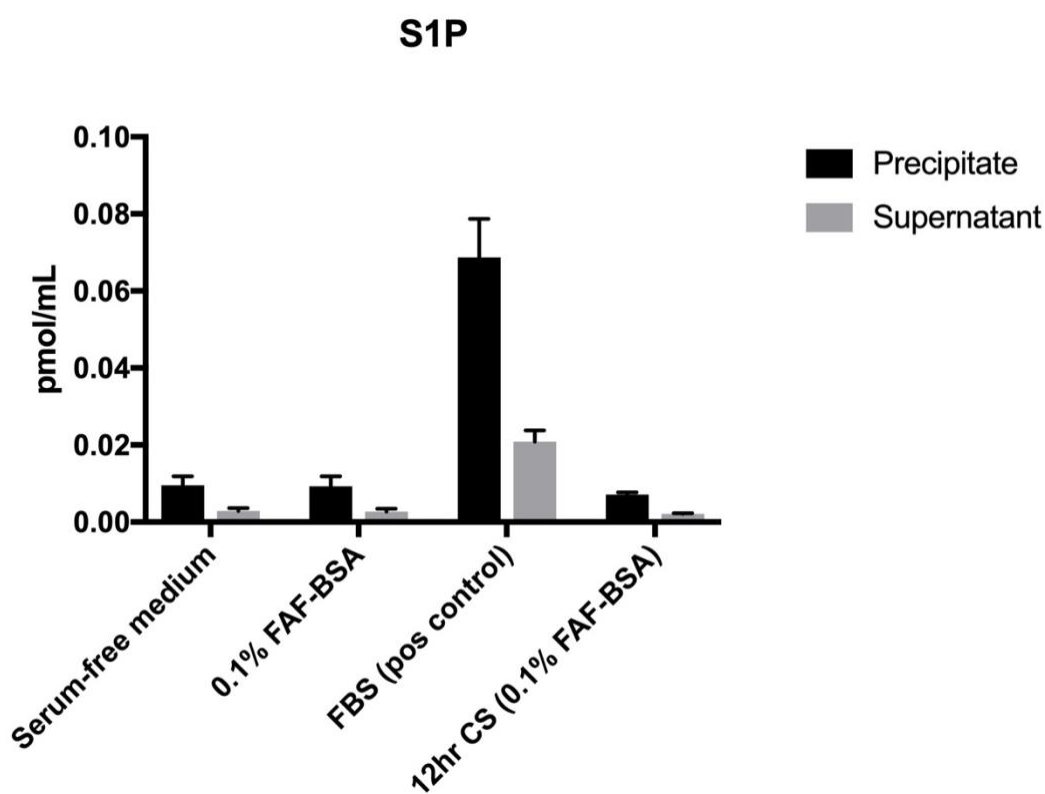
Figure 6.3 BSA binds S1P in aqueous solution

FBS was added to culture medium as a positive control, and the precipitated BSA contained significantly more S1P than the supernatant, supporting FAF-BSA's affinity for S1P in these studies. n=1 for each group (one experiment conducted, and one vial of sample provided for mass spectrometry analysis for each group), no statistical analysis performed, error bars

represent standard error of duplicate (serum-free medium, 0.1% FAF-BSA, and FBS pos control) and triplicate (12 hours CS) measures from the same sample.

6.3.4 Sphingosine kinase-2 in preservation injury

As discussed in section 5.4, BSA is not an adequate carrier protein for lipid mediators in aqueous solution during cold storage, for reasons yet to be determined. As a result, we wanted to continue studying LPL signaling in the meantime and decided to tackle SK2, the enzyme proposed to be responsible for producing most of the intracellularly acting S1P, via pharmacologic means. ABC294640, a selective SK2 inhibitor, was used to treat donor livers during cold storage for 24 hours prior to transplantation. All animals that received a successful transplant (n=5) survived until sacrifice (seven days post-transplant). However, those animals transplanted with a liver which was cold stored in ABC294640 (20 or 100µM) did not survive the first day (Figure 6.4a). At four (4) hours post-transplant, bloodwork was conducted to assess the health of the liver and kidneys. High liver enzyme (ALT) and creatinine (CRE) coupled with low albumin (ALB) are indicative of liver disease/failure and inflammation (Figure 6.4b). The animals receiving ABC294640 did markedly worse than those receiving a transplant cold stored in UW + DMSO. Results in an *in vitro* cell model of organ preservation echoed those of the transplant model (Figure 6.4c).
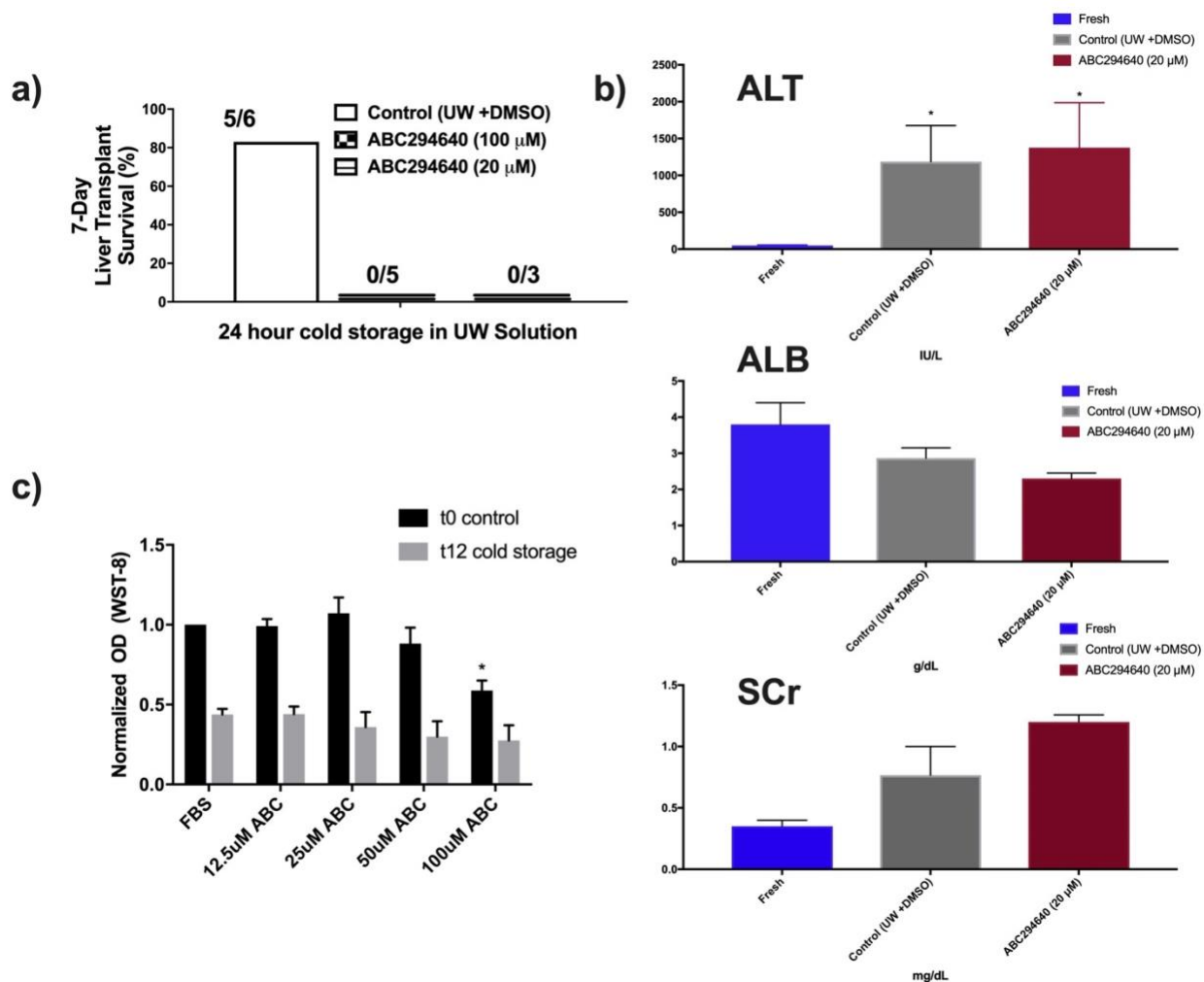
Figure 6.4 ABC294640 treatment during cold storage leads to failed liver transplants

a) All animals successfully transplanted (one experienced a technical complication during the surgery) with a control liver (stored in UW solution + vehicle, n=5) survived until seven days post-transplant. None of the animals receiving an ABC294640-treated liver survived (UW solution + ABC294640, low (n=3) or high (n=5) dose). b) Rats receiving liver transplants (depicted in panel (a)) had labs drawn (blood for ALT and urine for ALB/SCr) at four (4) hours post-transplant to assess liver and kidney function (n=3). Alanine aminotransferase (ALT) is elevated in both cold-stored groups compared to fresh controls (*p<0.05). However, ABC294640 treatment did not seem to impact ALT compared to UW + DMSO vehicle (p>0.05). ALB is decreased in both cold-stored groups compared to fresh controls, though not statistically significant (p>0.05). Likewise, SCr is increased in both cold-stored groups compared to fresh controls (p>0.05). c) HepG2 cells (n=5) were treated with escalating doses of ABC294640, and either left in the incubator (control) or cold-stored for twelve (12) hours. Cell viability was then measured (WST-8) following one (1) hour of reperfusion. Two-way ANOVA with Bonferroni's

70

multiple comparisons test showed that all cold-stored samples were significantly less viable than incubator controls, regardless of ABC294640 dose (p<0.05). Important, though, is the observation that 100µM ABC294640 significantly decreases cell viability compared to FBS and lower doses of ABC294640 within the incubator control group (p<0.05).

A lower resolution, but more efficient method of evaluating liver graft function is an *ex vivo* perfusion model (isolated, perfused liver, or IPL). R. Li conducted IPL studies on livers cold-stored in UW solution with ABC294640 and found that the drug dose-dependently decrease bile production and increased LDH release following preservation for 24 hours compared to vehicle controls (Figure 6.5a, b). Though not significant, the biological ramifications of a cessation of bile production at higher concentrations of ABC294640 correlates with the increased LDH release and failed transplants of a dysfunctional liver (in Figure 6.4). While these functional parameters were impacted by the dose of ABC294640, flow and resistance parameters were not significantly different between the groups, indicating that these livers were perfusing on the IPL apparatus (Figure 6.5c). Small changes in flow with opposite changes in resistance indicate those livers receiving 105 and 131µM ABC294640 have tighter vasculature, matching the functional profile of a more damaged liver.
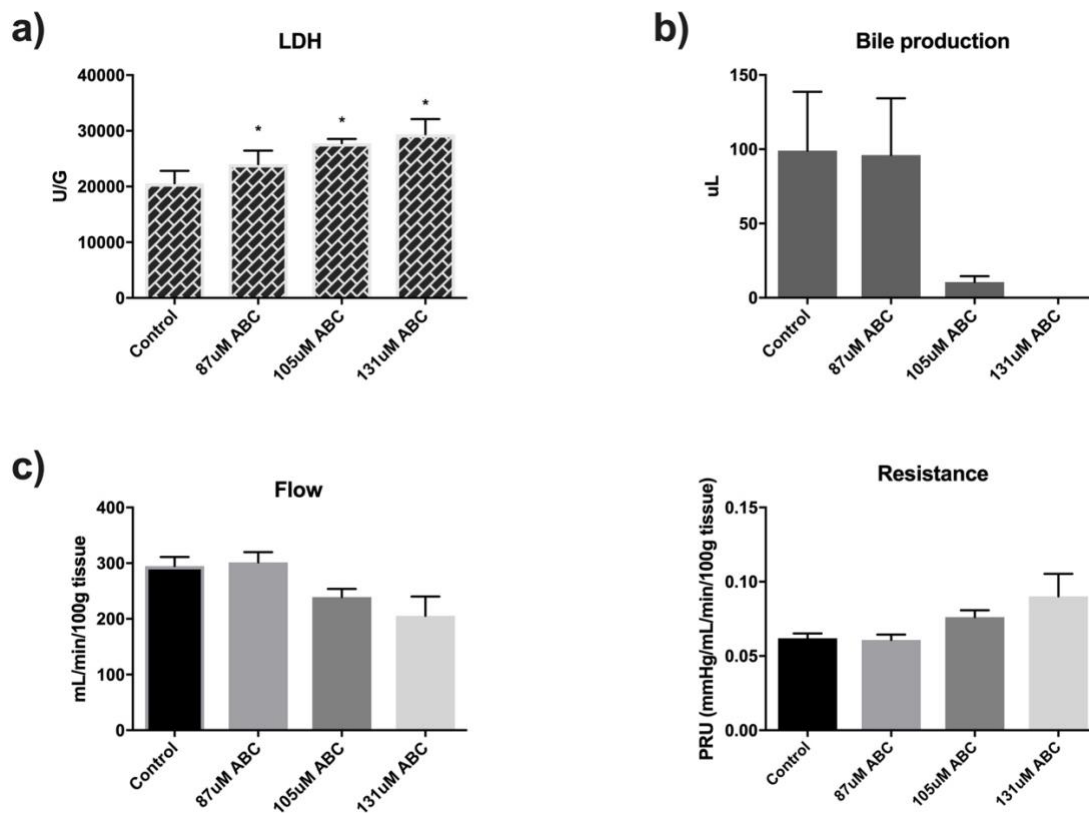
Figure 6.5 Isolated perfused liver (IPL) showed detrimental effects of ABC294640 treatment during cold storage

Rat livers exhibited signs of preservation injury following twenty-four (24) hours of cold storage with escalating concentrations of ABC294640 on IPL apparatus. Control (n=6), 87μM (n=6), 105μM (n=4), 131μM (n=3), two-way ANOVA with Bonferroni's multiple comparisons test performed, statistically significant when *p<0.05. a) LDH release, a marker of tissue damage, is increased in those livers treated with ABC294640, at any concentration, compared to control. b) Bile production is decreased, and ultimately ceases, with increasing doses of ABC294640 compared to control (not significant). c) Flow and resistance are not markedly altered by ABC294640 treatment compared with control livers.

6.3.5 Warm ischemia worsens preservation injury phenotype

Preparing this *in vitro* organ preservation model to study DCD in the future, we introduced one (1) hour of warm ischemia (WI) prior to 24 hours of cold storage and compared these cells to those receiving cold storage alone (as well as fresh incubator controls). Cells were treated with

ABC294640 (100µM) prior to cold storage. The HepG2 cells receiving WI for one (1) hour were significantly less viable than their fresh or CS alone counterparts (Figure 6.6). However, there was no difference between the groups that all received ABC294640 treatment; all were less viable than their vehicle counterparts, regardless of storage conditions.
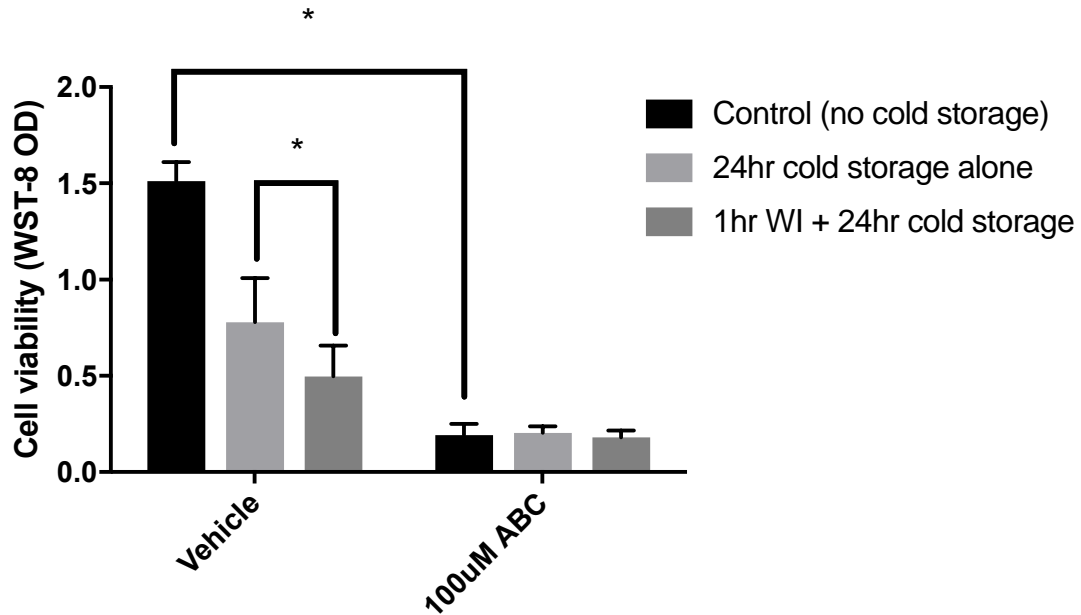
Figure 6.6 Warm ischemia worsens preservation injury phenotype in HepG2 cells

ABC294640 treatment (100µM) decreased cell viability, regardless of the conditions imposed on HepG2 cells. There was no difference between control, 24hr CS, and 1hr WI+24hr CS groups that received ABC194640. Among those groups receiving vehicle (DMSO), there was a significant decrease in cell viability between incubator controls and 24hr CS groups. Adding warm ischemia (WI) only decreased viability further. Two-way ANOVA with Bonferroni's multiple comparisons test performed to compare all groups (n=3 in each group, statistically significant when *p<0.05).

6.3.6 SK2 siRNA

Silencing SK2 in HepG2 cells would provide another confirmation of any effects of SK2 in preservation injury. Genetic knockout (KO) mice were available in limited quantities, and due to the sensitivity of primary cells, they are not conducive to cold storage method optimization.

As such, we purchased a pooled siRNA from Dharmacon (recommended by a collaborator) and

tasked C. Chmielewski with this portion of the project, overseen by the author. Despite many

attempts with the siRNA, we did not see sufficient knockdown of SK2 compared to the

RNAiMAX lipofectamine controls (Figure 6.7a). Functionally, HepG2 cells treated with siRNA

for 24 hours were cold stored for an additional 12 hours, and viability was measured (Figure

6.7b). We hypothesized that knocking down SK2 with siRNA would result in a decrease in cell

viability, showing that SK2 activity may regulate a process that is disrupted by hypothermic

ischemia. There was no difference between the lipofectamine controls and cells treated with the

SK2 siRNA.
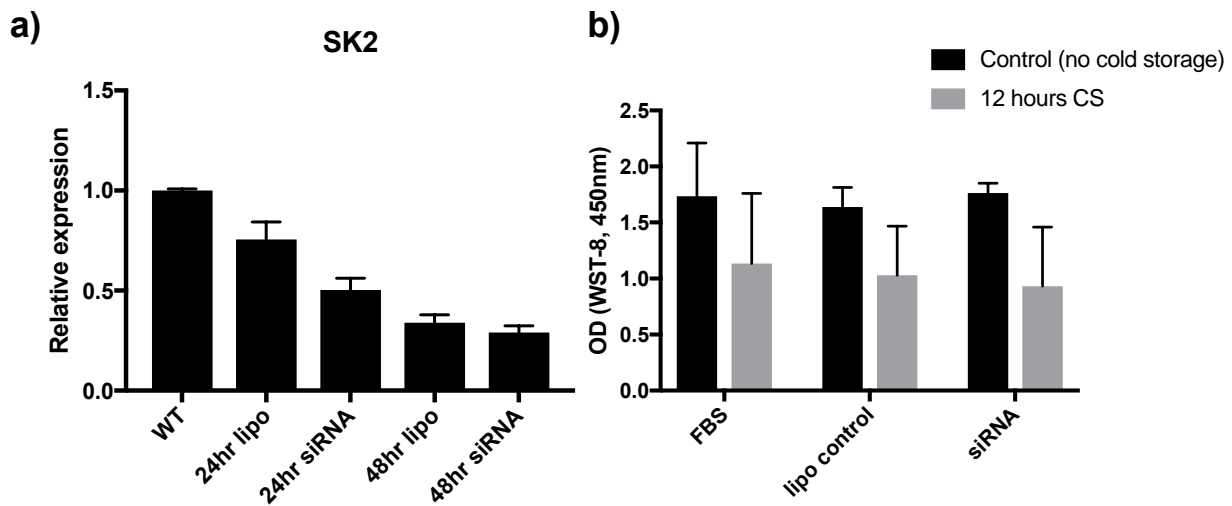
Figure 6.7 Application of SK2 siRNA to HepG2 cells

a) Western blotting showed no significant reduction in SK2 protein levels compared to lipofectamine (lipo) controls, at 24 or 48 hours (n=2, error bars represent variation of the mean between triplicates per blot). Expression relative to GAPDH loading control. b) Following 12 hours of cold storage, HepG2 cells treated with SK2 siRNA for 24 hours were equally as viable as controls as measured by WST-8 assay (n=2, error bars represent variation of the mean between triplicates per plate).

6.3.7 ABC294640 treatment decreases complex I activity in the electron transport chain

Since ABC294640 treatment of HepG2 cells results in decreased viability following cold storage, we wanted to examine if mitochondrial activity was causatively involved in this decrease. We showed that HepG2 cells exhibit decreased respiration following 24 hours of cold storage (no drug treatment), an expected result (Figure 6.8). Complex I respiration is calculated by subtracting oxygen flux following rotenone injection from the flux following ADP injection. Complex II respiration is calculated by subtracting flux after TTFA from flux after succinate injection. Complex IV respiration is calculated by subtracting flux after azide from flux after TMPD injection.
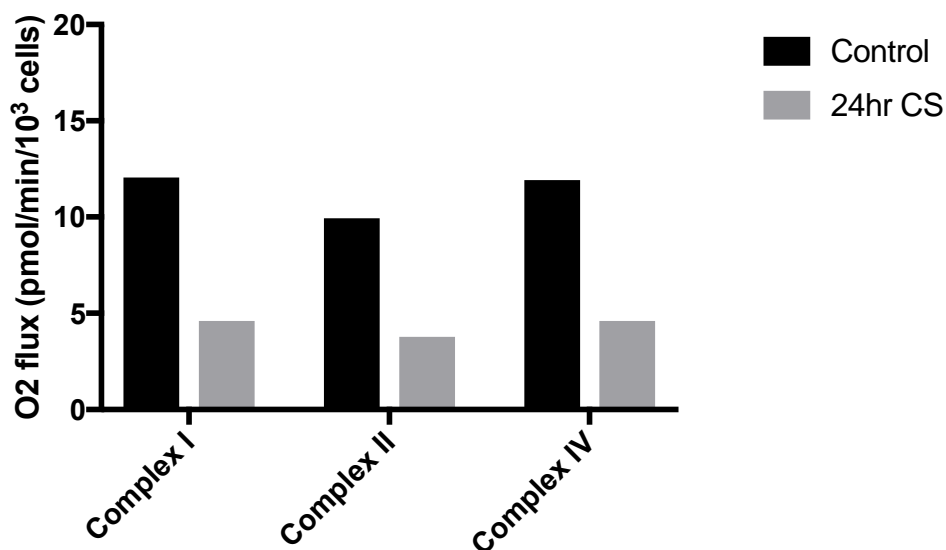
Figure 6.8 HepG2 cellular respiration is decreased following 24hr of cold storage (CS)

HepG2 cells were pelleted and divided evenly between chambers A and B on the O2k following 24 hours in the incubator (control) or in cold storage (CS). All respiratory activity normalized to cell count per chamber. No statistical analysis performed, n=1.

To first assess how HepG2 cell mitochondria respond at baseline (i.e., no cold storage), we treated a T75 flask of HepG2 cells with either 50µM ABC294640 or DMSO vehicle control and replaced them in the incubator for 12 hours. Each flask was analyzed separately in the O2k

in duplicate. While this 12-hour ABC294640 treatment had a global effect on mitochondrial

respiration, the most striking decrease was in complex I respiration (Figure 6.9).
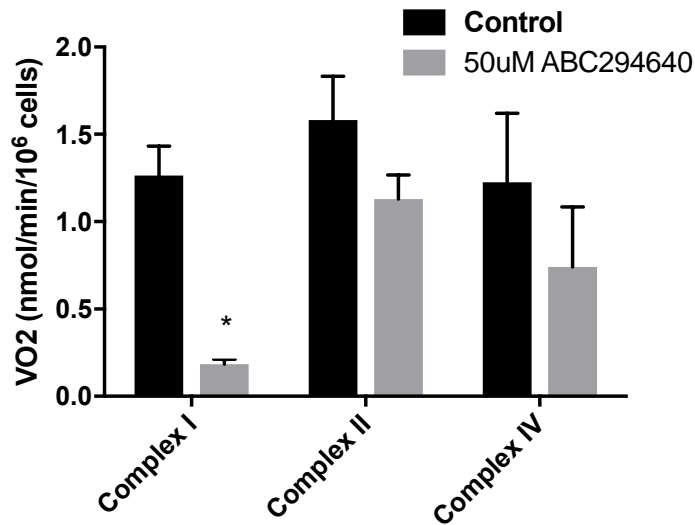
Figure 6.9 ABC294640 treatment decreases ETC activity in HepG2 cells

After 12 hours of ABC294640 treatment, HepG2 cells exhibited a significant defect in complex I respiration. Complex I activity was significantly decreased compared to complexes II and IV following ABC294640 treatment. One-way ANOVA with Bonferroni's multiple comparison test performed, comparing the control group with the ABC294640-treated group at all complexes, n=3, *p<0.05.

6.4 Conclusions

Sphingolipid metabolism is dysregulated by hypothermic ischemia, as evidenced by the

slight shift in the sphingolipid rheostat during cold storage. In terms of experimental design,

FAF-BSA does sequester S1P in aqueous solution, and extrapolating from the LPA studies, this

further supports the notion that FAF-BSA is not an optimal or effective carrier for LPLs during

hypothermic ischemia. Inhibiting SK2 with ABC294640 during cold storage leads to a dose-

dependent decrease in cell viability. Furthermore, ABC294640 treatment results in a defect in

ETC complex I respiration in HepG2 cells (without cold storage). The mechanism of this

complex I defect is discussed in Chapter 7. Further studies are needed to verify the siRNA

knockdown of SK2 and any functional effects that may have on hepatocyte viability during cold storage.

Chapter 7: Novel mechanism of ABC294640

7.1 Abstract

ABC294640, a selective SK2 inhibitor, is utilized clinically and experimentally in the laboratory to modulate S1P synthesis. Modulating this pathway is of great interest due to its vast involvement in many pathophysiologies, including liver cancer, lung cancer, and inflammatory diseases. Determining the underlying mechanism of ABC294640's devastating impact on livers during preservation, for both transplantation into rodents and *ex vivo* IPL, is very important to consider for a drug currently in clinical trials. As the mitochondria are a) a downstream target of LPL signaling, b) dysregulated during organ preservation, and c) SK2 is an important source of S1P in the mitochondria that is important for complex IV assembly, it was prudent to investigate the if the mitochondria were affected by treatment with this SK2 inhibitor using high-resolution respirometry (HRR). We found that 12 hours of ABC294640 treatment significantly reduced complex I respiration compared to vehicle controls. Furthermore, this effect is independent of ABC294640's primary mechanism of action (SK2 inhibition). Injection of ABC294640 directly into the HRR chambers rapidly inhibits complex I, but not complexes II-IV. SK2 null hepatocytes exhibited the same complex I inhibition as a result of ABC294640 injection into the HRR chambers as their wild-type counterparts. This indicates a novel mechanism of action of ABC294640, which must be considered due to the drug's current clinical trial applications.

7.2 The discovery and utility of ABC294640, a selective sphingosine kinase-2 inhibitor

Targeting sphingosine kinases 1 and 2 (SK1 and SK2, respectively) emerged in the early 2000s as a desirable avenue for drug development, primarily due to the combined roles of sphingolipid signaling in cancer and a lack of selective SK2 inhibitors (many also inhibited other protein kinases) (K. French et al. 2010). ABC294640, the structure of which is shown in figure 7.1, was first identified in a screen for compounds containing an aryladamantane scaffold, due to its good oral bioavailability (K. J. French et al. 2006; K. French et al. 2010; K. J. French et al. 2003; Xun et al. 2015). The IC_{50} of this compound is around 40µM, and it is selective for the SK2 isoform up to 100µM, making it a seemingly perfect compound for drugging SK2 *in vivo* (Gao et al. 2012). ABC294640 competes with sphingosine for the active site on SK2, with a K_i of around 10µM (K. French et al. 2010).

IC$_{50}$= 40uM

Selective for SK2 >>> SK1 (up to 100uM)
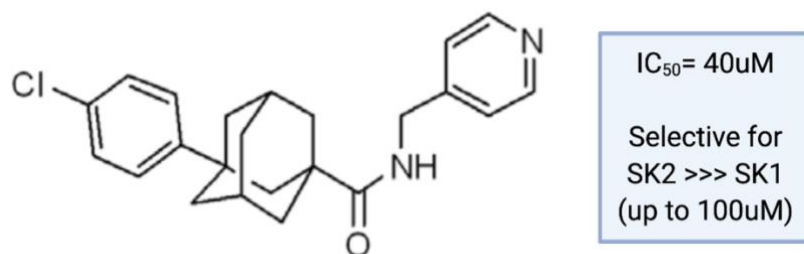
Figure 7.1 Structure and selectivity of ABC294640, a sphingosine kinase-2 inhibitor

ABC294640 was first studied in a murine model of inflammatory bowel disease, but its utility was realized and studies expanded to include other diseases with inflammatory origins, as well as several types of cancer (Britten et al. 2017; Maines et al. 2008; Lewis, Voelkel-Johnson, and Smith 2018). Low toxicity combined with efficient oral delivery of the drug makes it attractive

for clinical use, and it is currently being investigated in several phase II-III clinical trials for solid tumors, as well as COVID-19-associated pneumonia (NIH 2020).

7.3 Results

7.3.1 ABC294640 dose-dependently inhibits complex I respiration in multiple cell types

To evaluate the mechanism of ABC294640's toxicity in hepatocytes (Chapter 6), high-resolution respirometry (HRR) on the Oroboros Oxygraph-2k (O2k) was performed. Upon ABC294640 injection into the O2k chambers with either HepG2 or SK Hep-1 cells, there was an immediate reduction in oxygen consumption (or flux), which was not further reduced by rotenone (Figure 7.2a). The concentration of ABC294640 chosen for subsequent HRR studies, 50µM, was selected due to a) its neutral effect in control cells, b) its cytotoxicity in cold stored cells, and c) it is the lowest effective concentration required to inhibit complex I to the same degree as rotenone (Figure 7.2b). A dose-response of DMSO vehicle was conducted as well, with no significant changes in oxygen flux. At the 31-minute mark in Figure 7.2c, labeled "ABC" in green, the immediate decrease in oxygen flux after injection of ABC294640 can be observed.
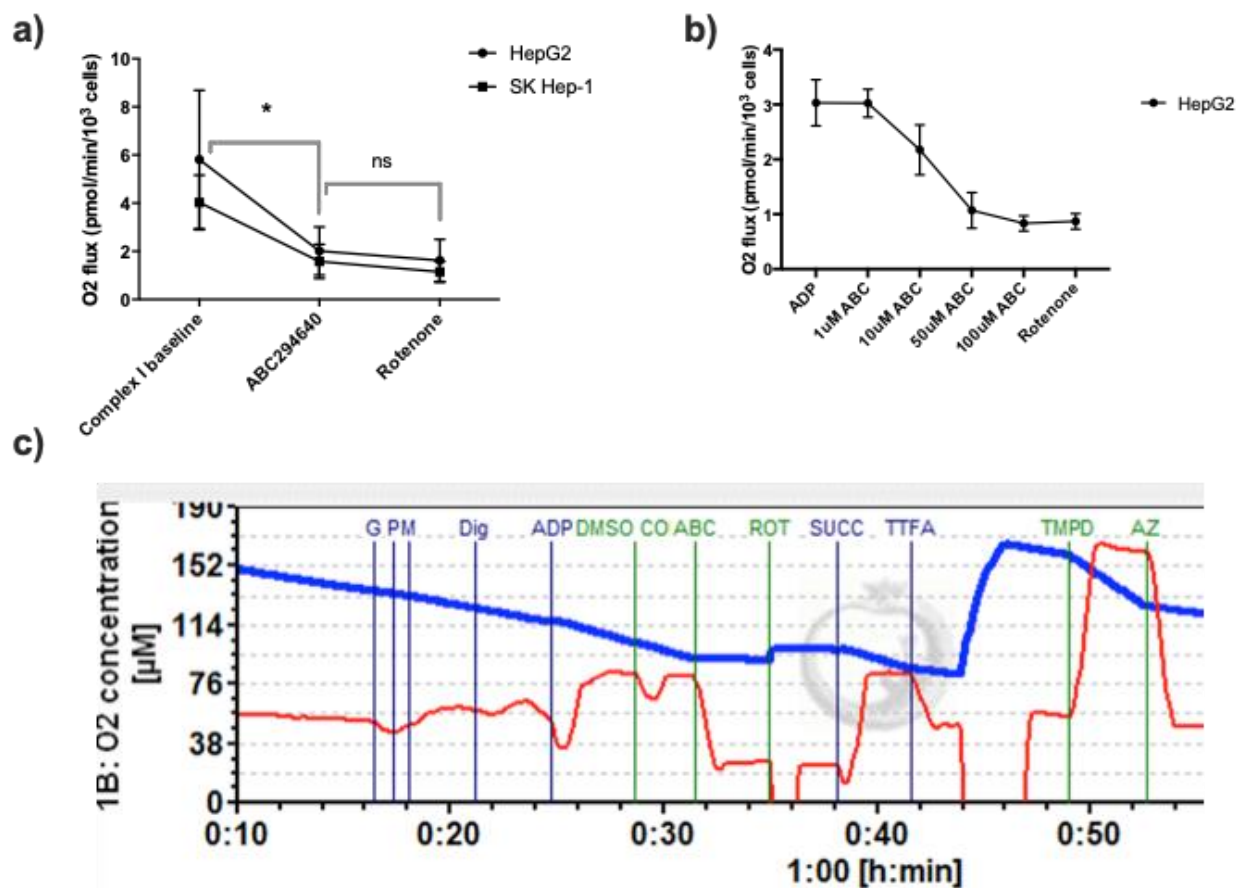
Figure 7.2 ABC294640 directly inhibits complex I of the ETC

a) HepG2 (n=3) and SK Hep-1 (n=4) cells are responsive to ABC294640 as a direct complex I inhibitor. Two-way ANOVA with Bonferroni's multiple comparisons test showed that complex I baseline flux is significantly higher than that of ABC294640 (in both cell types), while the flux following ABC294640 treatment is not different compared to rotenone (in both cell types), *p<0.05; b) Complex I inhibition is dose-dependent, with no obvious difference between 50µM, 100µM, and rotenone (n=2, no statistical analysis performed); c) O2k output tracing, showing the DMSO artifact and rapid inhibition of complex I by ABC294640. Of note, at the 42 minute mark, the chamber was opened to allow dissolved oxygen to replenish prior to complex IV substrate addition. The flux (red) drops off, while the oxygen concentration (blue) increases, restabilizing after the chamber is closed.

7.3.2 ABC294640 does NOT inhibit activity at complexes II-IV

When examining complex I in the O2k, it is possible that oxygen consumption occurring

in downstream ETC complexes (II-IV) may manifest at complex I. As the experiment moves down

the ETC, and the inhibitor for each complex is added, the activity of individual complexes can be separated. We investigated if ABC294640 was exerting its inhibitory effect on complexes II-IV, to confirm that the decrease in oxygen flux at complex I was in fact due to ABC294640 directly inhibiting complex I, and not a downstream ETC complex. Injecting ABC294640 into the O2k chambers does not significantly decrease oxygen consumption after complex II, III, or IV substrates (Figure 7.3). Furthermore, addition of the complex-specific inhibitors after ABC294640 injection elicited the expected response: a decrease in oxygen flux.
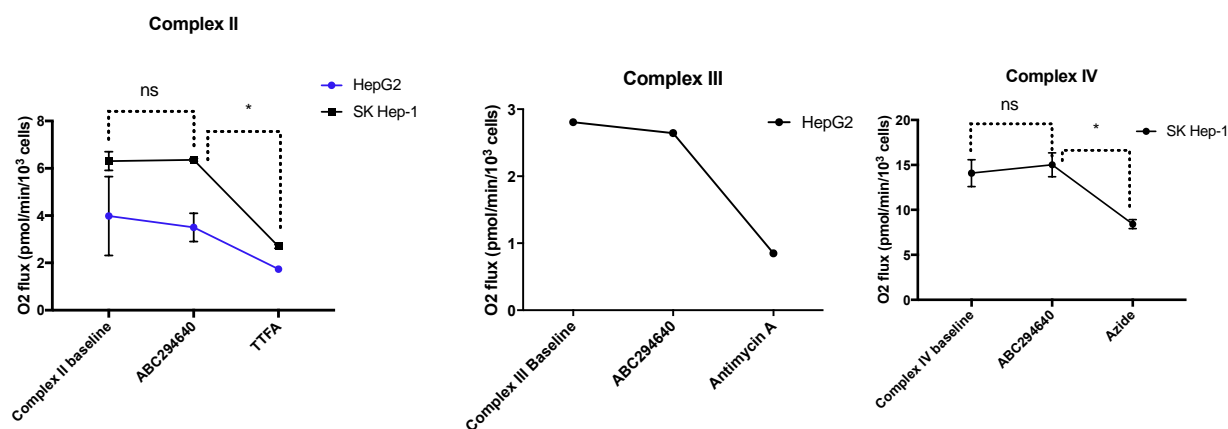
Figure 7.3 ABC294640 does NOT inhibit complexes II, III, or IV

Complex II: HepG2 (n=3), SK Hep-1 (n=3), one-way ANOVA with Bonferroni's multiple comparisons test compared flux following injection of each chemical within each cell type, there was no difference between complex II baseline (following succinate injection) and ABC294640, and there was a significant difference between the flux following ABC294640 and that following TTFA. Complex III: HepG2 (n=1, no statistical tests conducted), trending such that flux following complex III substrate injection is not different from that following ABC294640 injection, while antimycin A produces a decrease in flux. Complex IV: SK Hep-1 (n=3), ABC29464 injection does not decrease flux following injection of complex IV substrates, while there is a significant decrease in flux following azide injection. *p<0.05 is considered statistically significant for all above datasets/analyses.

7.3.3 K145 does NOT inhibit complex I respiration

K145, a structurally distinct SK2 inhibitor with an IC_{50} of 4.3µM, was injected into the O2k chambers (final concentration 5µM) after addition of ADP and the effect on oxygen consumption was observed (DMSO vehicle control was included and showed no significant effect on O_2 flux outside of the known "vehicle dip"). Figure 7.4 shows how HepG2, SK Hep-1, and MDCK cells respond to K145 injection into the O2k chambers. Due to K145's structural uniqueness compared to ABC294640 and rotenone, we believe this evidence strengthens the argument that ABC294640 is acting on complex I through an SK2-independent mechanism.

a)

K145 structure

b)

c)
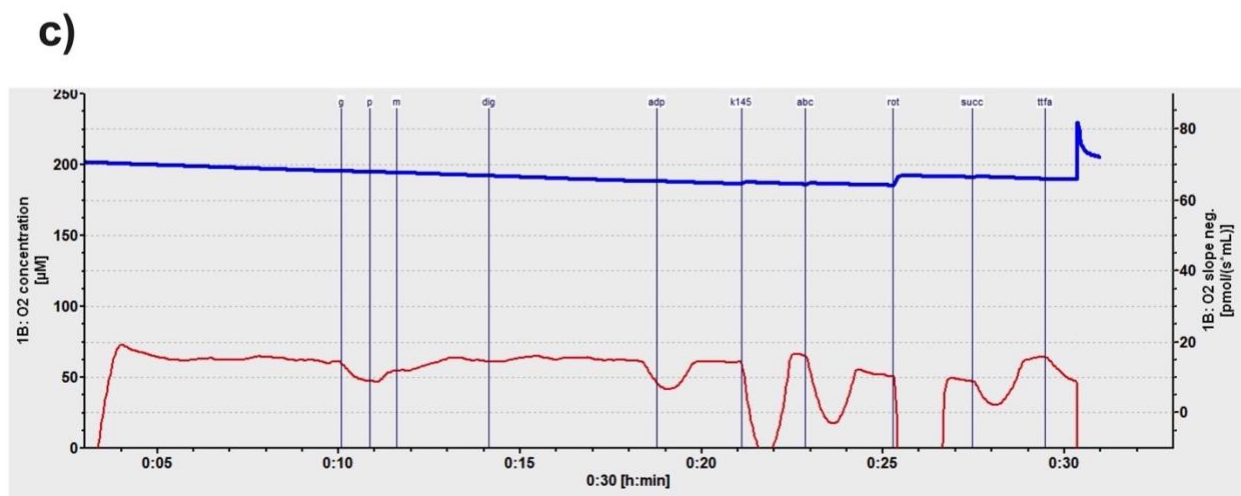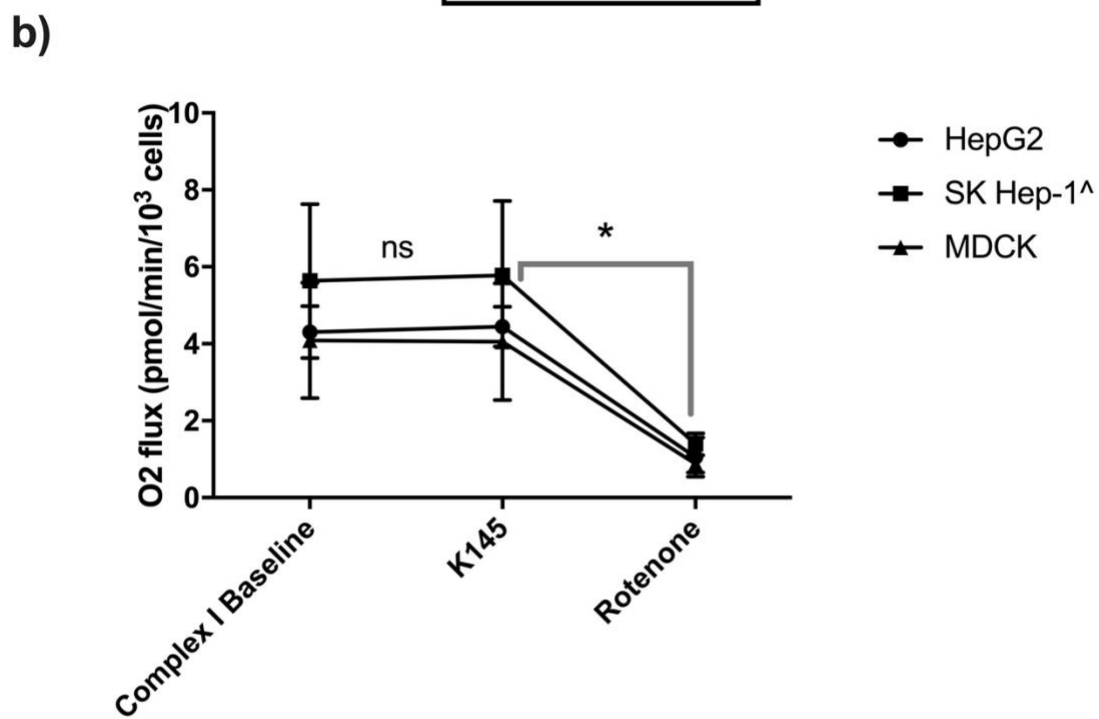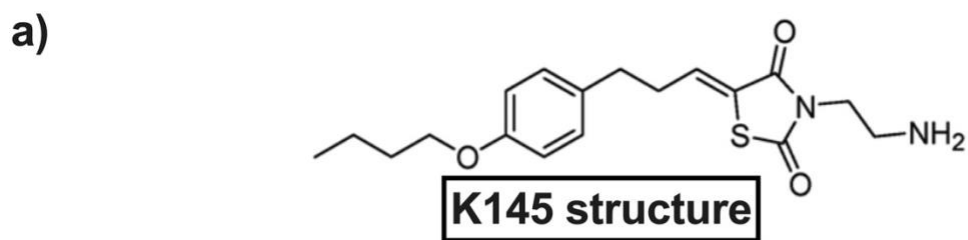
Figure 7.4 K145 does not inhibit complex I respiration

After oxygen signal stabilization, addition of complex I substrates and ADP, the "complex I baseline" was obtained. K145 was injected in place of ABC294640 after addition of ADP to determine the effect of K145 on complex I activity. No significant decrease in flux was observed following K145 injection. Two-way ANOVA with Bonferroni's multiple comparisons test compared flux following chemical injection within each of the three cell types, n=3 in each group, *p-value < 0.05 is considered statistically significant.
^ The only sample with a statistically significant difference between K145 and rotenone were SK Hep-1 cells. The other two cell types, however, exhibit a response trending in that direction.

7.3.4 Novel mechanism of ABC294640 action is <u>independent</u> of SK2 activity

To complement the pharmacologic data on ABC294640, genetically-modified biologic materials were used to confirm that this drug was working independent of SK2, the primary target of ABC294640 and enzyme responsible for producing intracellular S1P. We first attempted silencing/knockdown of SK2 (protocol described previously) with pooled siRNA from Dharmacon and conducted HRR analysis in tandem with western blotting for protein levels (see Figure 6.7 for SK2 protein expression and impact on cell viability). We did not see a significant decrease in SK2 protein levels following siRNA treatment compared to lipofectamine controls (Fig 6.7a), and the HRR data showed no difference between SK2 siRNA and lipofectamine (Fig 7.5a). Likewise, with primary hepatocytes isolated from SK2 KO mice and their WT counterparts responded similarly to ABC294640 injection into the O2k chambers with a significant reduction in complex I activity, not further reducible by rotenone (Fig 7.5b).
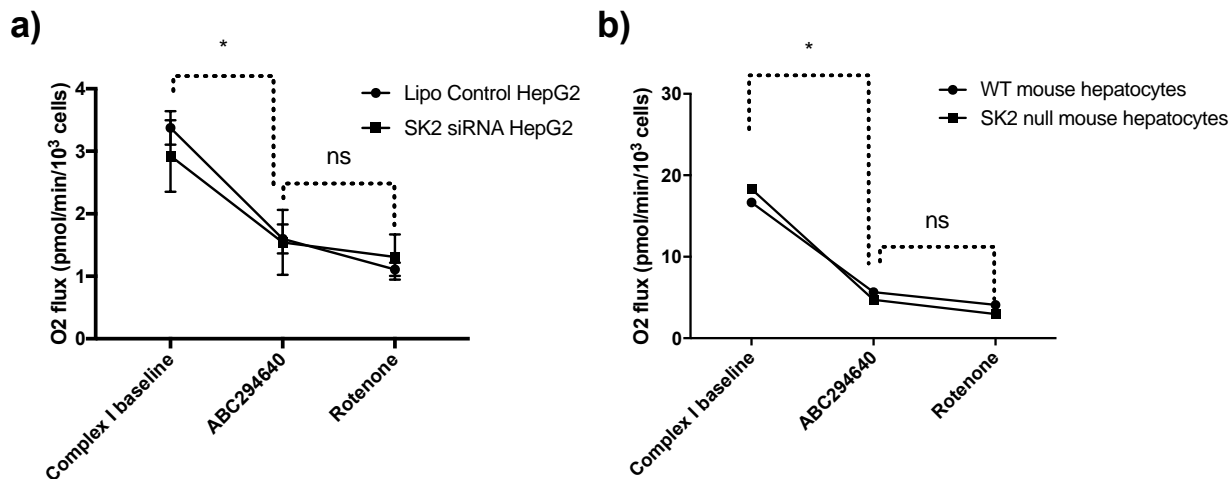
Figure 7.5 Genetic manipulation of SK2 did not impact ABC294640's complex I inhibition

*a) Functional results of SK2 siRNA and lipofectamine controls in HRR analysis (no significant protein level reduction, n=4); b) Germline SK2 knockout mouse hepatocytes respond to ABC294640-mediated complex I inhibition in the same manner as WT littermates (n=3); Two-way ANOVA with Bonferroni's multiple comparisons test examined flux following injection of each chemical, within each cell type and between cell types, *p<0.05 is considered statistically significant.*

7.4 Conclusions

The mechanism of ABC294640's devastating effects on livers for transplant is likely in part due to the drug's direct chemically-mediated inhibition of complex I of the ETC. When HepG2 cells were treated with ABC294640 overnight, they exhibited a significant complex I defect compared to vehicle controls. Upon further investigation, ABC294640 was found to directly inhibit complex I oxygen consumption without impacting complexes II, III, or IV. K145, a structurally distinct SK2 inhibitor had no effect on complex I activity, indicating that the mechanism of action may be independent of SK2. Finally, hepatocytes lacking SK2 were responsive to ABC294640-mediated complex I inhibition, confirming that SK2 is not involved in modulating this response. These data uncover a novel mechanism of action for ABC294640.

Chapter 8: Discussion

8.1 Methodological development and optimization

It may seem obvious that biological systems behave differently under hypothermic ischemia compared to physiologic conditions. Why do we study protein behavior and signaling under these conditions, if they are not in line with traditional mammalian physiology? Organ preservation remains an essential component of transplantation, and advances in this field will open the doors required for many more Americans (and people of the world) to receive their life-saving organ transplant. Hypothermic ischemia is the reality of organ preservation, despite advances in mid- and normothermic oxygenated perfusion. Even if the latter advances gain more traction, hypothermic ischemic static cold storage will *always* be the default if problems arise.

Our research group developed an *in vitro* model for organ preservation, involving airtight Tupperware, tissue culture plates (6-, 24-, and 96-well), a nitrogen purge, and storage on slushy ice (2-4°C) for the desired amount of time. After cold storage and one (1) hour of reperfusion in the incubator, the endpoint is assessed (cell viability, protein/RNA expression, lipidomics analysis, etc.). However, novel to these studies is the application of lipid mediators (such as LPA) to the cell culture medium during cold storage. LPA (and S1P, for the sake of future experiments) is a lipid and is therefore hydrophobic and requires a carrier system for delivery to aqueous solutions. Typically, bovine serum albumin (BSA) is used to carry lipid mediators into aqueous *in vitro* studies, at a concentration of 0.1-0.5% (Cerutis et al. 2014). As mentioned previously, the behavior of the entire biological system changes in the cold and this is starkly evident when attempting to apply LPA to cells in culture prior to induction of hypothermic ischemic cold storage.

It is also important to ensure that ischemia is induced on the entire 96-well plate. We initially conducted a nitrogen purge for 5 minutes in the inner container, and 5 minutes in the outer container. However, after careful inspection, we found that the outermost wells, regardless of experimental condition, were significantly more viable than those towards the interior of the plate. This was resolved by increasing the nitrogen purge to 10 minutes for each container. We also performed temperature monitoring in the cold storage boxes, due to results indicating that the extent of preservation injury was not appropriate for the applied time frame of hypothermic ischemia.

Overall limitations for these studies are further complicated by a low sample size. During method development, each replicate is different (as is necessary to optimize the methods), so the resulting sample size is small. Another global limitation is translatability of HepG2 mechanistic data to primary hepatocytes and thus physiologic preservation injury. However, the goal is not to translate immortalized cancer cell line results to the clinic; rather, it is to optimize methods until they are suitable for application to primary hepatocytes. As will be covered in the discussion, a new method of delivering LPLs in cold storage will be required to continue these studies.

8.2 RhoA and ROK in preservation injury

Moesin, the dominant ERM protein in the liver, is inactivated by hypothermic ischemia. Mutation of moesin to either an ON or OFF configuration confers protection or worsening of the preservation injury phenotype, respectively (Tian et al. 2014). When moesin is phosphorylated at the threonine-558 position, it becomes activated and open, allowing the linker element to bind the actin cytoskeleton to the plasma membrane, stabilizing cell morphology. The activation of ERM proteins is controlled, in part, by Rho kinase (ROK), and ROK activity is modulated by RhoA. Inhibiting ROK and RhoA during preservation increases preservation injury in HepG2

cells, suggesting these two proteins play a role in protecting the cells during hypothermic ischemia. Lysophospholipids (LPLs) are bioactive lipid growth factors that circulate in the blood stream, are upstream of the RhoA/ROK/ERM axis and are washed away during organ preservation. Thus, the motivation for the studies in this dissertation began with these early studies on downstream effectors.

It is important to remember that ROK is not the only kinase shown to phosphorylate ERM proteins *in vivo*. Protein kinase C (PKC), Nck interacting kinase, G-protein receptor coupled kinase 2, as well as non-receptor tyrosine kinases are also responsible for controlling ERM activation via phosphorylation. Likewise, proteins responsible for inactivation via dephosphorylation include protein phosphatase 1α (PP1α) and myosin light chain phosphatase; targeting phosphatases to upregulate ERM protein activation is another mechanism that warrants further investigation (Ponuwei 2016).

8.2 Lysophosphatidic acid (LPA) in preservation injury

8.2.1 LPA is not protective against preservation injury

Despite many attempts to troubleshoot testing the hypothesis that LPA signaling is protective against preservation injury, we found that there is no significant reduction in HepG2 cell preservation injury associated with the application of exogenous LPA. Escalating doses of LPA (0.1 – 1000μM) did not significantly improve the phenotype following cold storage, although at the highest concentration of LPA (1000μM), the response is trending in a positive direction. However, at these high concentrations, solubility becomes a challenge, and they are above physiologic serum levels in humans.

While serum and plasma concentrations of LPA are 1-10μM and less than 2nM, respectively, we are proposing an adjuvant to an existing preservation solution as the end-goal of this research (Panetti 2002). The required concentration of adjuvant, in this case LPA, to elicit a protective response in UW solution would not need to correlate to physiologic conditions. UW solution, by nature, is not physiologic – if physiologic conditions were sufficient to prevent preservation injury, the field of organ preservation would be much farther along. LPA and other growth factor signaling pathways (in addition to those included in these studies) such as VEGF/EGF provide exciting therapeutic exploration opportunities in many pathophysiologies, including cancer, inflammatory diseases, and even organ preservation/transplantation.

There is debate amongst statisticians and other scientific professionals about the validity and reproducibility of data that has been subjected to outlier removal. According to a survey conducted by Gress et al. in 2018, scientists with medical school faculty appointments who held a PhD were nearly twice as likely to exclude outliers than their MD/DO counterparts, regardless of the availability of a statistician. There are several acceptable methods for removing outliers, including the Tukey method and Grubb's test (ESD method). Editing data by removing outliers may introduce type I error, where researchers may find a statistically significant difference where one actually does not exist (Gress, Denvir, and Shapiro 2018).

Another point to consider, however, is the known plethora of inconsistencies with *in vitro* experiments, especially those conducted in 96-well plates in multiplicate. When designing an experiment in this setting, it is standard practice to apply conditions to cells plated in <u>at least</u> triplicate (to account for any plating or other errors that may result). These multiplicates are then assessed for any technical outliers (such as plating errors, drug application errors, plate edge effects, etc.) using one of the aforementioned outlier tests. Once the technical outliers are removed,

the mean is calculated for the remaining multiplicate wells and this value is reported as an "n" of one (1). Since the cells contained within the single plate were from a single population, albeit an immortalized one in many of these studies, and the conditions were applied all at once, it is correct to count the entire plate as one (1) replicate of the experiment (Lord et al. 2020). Upon evaluation of all of the cell viability data collected for these studies, we decided to remove outliers from the raw data using the Tukey outlier test (which relies on the interquartile range, or IQR, to set the boundaries for inclusion). Often times, it is obvious with the naked eye at the completion of an experiment which wells were incorrectly plated (such as a large clump of cells in one well, which is a problem with "sticky" or overly adherent cell lines), over- or underconfluent, incorrectly pipetted, or otherwise technically inept. Our practice was to mark these wells at the conclusion of the experiment, and these blind assessments were confirmed by the Tukey outlier test.

As optimization of these studies progressed, it was observed that any experimental conditions containing bovine serum albumin (BSA) led to cells which a) were less viable than the clear medium controls, and b) were equally viable, regardless of additional reagents such as LPA in the solution. To determine if this was the cause for the lack of response to LPA in cold-stored HepG2 cells, we investigated the role of BSA in this process.

8.2.2 LPA receptors in preservation injury

LPA receptor expression is variable between different tissue types, and has been shown to be altered following injury to the liver in the form of a partial hepatectomy (Simo et al. 2014). As we progressed through these studies, another group published on the presence of LPA receptors in primary hepatocytes, so we postponed this investigation (Bae et al. 2017). However, it is important to note that based on the data from Simo et al. (2014), an increase in circulating LPA and specific LPARs as a result of hepatic injury is also a possibility in the case of preservation injury. It remains

90

to be determined how the hypothermic aspect of preservation may alter LPAR expression, but if these receptors are upregulated and washout eliminates circulating LPA, then we may have a druggable target. It is a challenge to conduct cold storage experiments on primary hepatocytes; these cells require a matrix for adherence and exhibit low overall optical density values upon WST-8 assay for viability; detecting changes as a result of LPA administration may not be possible. It is also possible that the BSA carrier protein required had a disproportionate effect on the primary cells, resulting in an even lower overall optical density. Future studies would be required to optimize the method for lipid delivery during cold storage to primary cells.

8.3 Albumin exhibits cytotoxicity *in vitro*, which worsens following cold storage

After careful consideration of the results reported in Chapter 5, perhaps BSA is masking any protective effects of LPA treatment. Independent of the presence of LPA, we found that even at low concentrations (0.1%), BSA is cytotoxic to cells in culture following a period of cold storage (while the cytotoxic threshold was increased to 10% BSA in incubator-kept cells). In line with the idea that lipid growth factors may protect against preservation injury, we examined how fatty acid saturation affected cytotoxicity of BSA during cold storage. Fatty acid saturated and fatty acid free BSA were equally as harmful to HepG2 cells during hypothermic ischemia. Initially, we also hypothesized that the species origin of BSA may be the cause of the detrimental effects. However, upon replication with human serum albumin (HSA), the species of origin did not change the outcome. Albumin is used clinically in organ transplantation to maintain blood volume post transplantation, so these data should be considered if any albumin is being added during preservation (Amouzandeh et al. 2018). A different lipid delivery method would be needed to continue these studies.

8.4 Sphingolipid signaling may be involved in preservation injury

The balance between pro-survival and pro-apoptotic sphingolipids is a determining factor in cell fate. Organ preservation conditions shift this balance from pro-survival to pro-death, correlating to a decrease in S1P:Ceramide ratio. Preliminary data showed that treating livers with ABC294640, a selective sphingosine kinase-2 (SK2) inhibitor, during preservation led to fatal graft failure in recipients post-transplant and increased damage to isolated perfused livers. This trend continued in the *in vitro* organ preservation model, resulting in a dose-dependent decrease in HepG2 cell viability following cold storage. These data suggest that SK2 is important in maintaining hepatocytes during liver preservation. However, further examine was needed to determine the mechanism of such a significant liver injury.

8.5 ABC294640 is an ETC complex I inhibitor

8.5.1 Comparison of ABC294640 and rotenone

We found that ABC294640 possesses a secondary, novel mechanism of action as an ETC complex I inhibitor (in addition to inhibiting its primary target, SK2). ABC294640, developed due to the increasing demand for specific sphingosine pathway pharmacologics, has been shown effective against many types of cancer *in vitro*, *in vivo*, and is now in human clinical trials for cancers as well as the treatment of COVID19-associated pneumonia (NIH 2020). Its widespread clinical utility coupled with its numerous laboratory uses makes ABC294640 a powerful and popular compound (Lewis, Voelkel-Johnson, and Smith 2018). And until recently, it was thought to only possess one mechanism of action: inhibiting SK2 by binding competitively with sphingosine at the enzyme's active site (K. French et al. 2010). We showed that ABC294640 directly inhibits complex I of the ETC, independent of SK2. This effect on complex I oxygen flux

is similar to that of rotenone, the most well-studied complex I inhibitor. If this compound is to be continued in the clinic, determining the mechanism of this action is crucial to understanding how ABC294640 behaves in different pathophysiologies.

The site of action of rotenone in complex I was discovered in 1968 through mutational studies. Rotenone binds to the non-heme iron the NADH dehydrogenase enzyme, blocking electron transfer through the iron centers of complex I. However, this does not seem to be the only site of rotenone binding to complex I, making it difficult to identify if any single interaction is the most important for rotenone's mechanism of action (Palmer et al. 1968). There are multiple inhibitors of complex I, including piericidin A, mucidin, and capsaicin, which exhibit diverse actions at complex I (Sharma, Lu, and Bai 2009). A structural comparison between ABC294640 and these compounds may provide insight into the mechanism of action.

8.5.2 Selectivity of ABC294640 on the basis of ETC complex structure

At the beginning of an O2k HRR experiment, when complex I substrates and ADP are added to the chamber, it is possible that any defects seen in complex I activity are artifacts from a downstream ETC complex. In order for the oxygen to be consumed, those electrons must be transferred all the way down through complexes II, III, and IV before arriving at their final destination. If there is a defect in complex II, it is possible that it will show up when modulating complex I as well as complex II. As such, we needed to ensure that ABC294640 was not acting at a downstream ETC complex and manifesting that inhibition in the respiration capacity of complex I. By injecting ABC294640 directly into the chamber in place of TTFA (complex II), antimycin A (complex III), and sodium azide (complex IV), we showed that ABC294640 only acts on complex I of the ETC.

If this novel mechanism is truly a chemical interaction independent of ABC294640's target protein, SK2, then a structurally distinct SK2 inhibitor producing no response in the O2k would confirm this suspicion. K145 was created at Virginia Commonwealth University in the Department of Medicinal Chemistry, is a selective SK2 inhibitor (IC_{50} of 4.3μM), and has a unique chemical structure compared to ABC294640 (and rotenone) (Liu et al. 2013). Since K145 is soluble in DMSO (like ABC294640), we confirmed with a vehicle only injection that DMSO had no appreciable effect on oxygen consumption. K145 was then injected into the chambers in place of rotenone (to a final concentration of 5μM) and no significant changes in oxygen consumption were observed, further confirming our hypothesis that ABC294640 was acting on complex I independent of SK2.

8.5.3 SK2 null (SK2$^{-/-}$) mouse hepatocytes are equally as responsive to ABC294640-mediated inhibition of complex I as their WT counterparts

Pharmacologic methods attempting to manipulate SK2 (via K145 injection) are only one half of this puzzle. The ultimate proof of concept is genetic manipulation of the gene controlling the protein of interest. Based on the pharmacologic data discussed above, we hypothesized that SK2 was not involved in this response of complex I to ABC294640 treatment. To test this, we isolated hepatocytes from SK2 knockout mice (and their WT litter mates) and placed them in the O2k chambers for HRR analysis. When SK2 null cells were subjected to ABC294640 injection in the chamber in place of rotenone, a significant decrease in complex I activity was observed. This result was similar to the response of the WT control cells, confirming that SK2 is not involved in this response of hepatocytes to ABC294640 in the O2k chambers.

8.5.4 Autoxidation of TMPD

Many users of the O2k create unique protocols to satisfy their experimental requirements. Unfortunately, there are over one hundred (100) SUIT protocols published on the manufacturer's website (https://wiki.oroboros.at/index.php/MitoPedia:_SUIT). While this provides a wide variety of options for using the instrument to its fullest potential, these protocols can be cumbersome and may be extraneous for the users' goals. For these studies, we were specifically interested in complexes I – IV and the behavior of each following the injection of ABC294640 to the chamber. Early experiments were conducted following a published protocol from a collaborating laboratory, which focused exclusively on complexes I, II, and IV (Mohsin et al. 2019). As the project progressed, small adjustments were made according to the manufacturer's website, cited publications, and direct correspondence from Oroboros instrumental support.

Due to the scarcity of several biological samples (such as the SK2 null mice used for hepatocyte isolation), it was favored to examine as many complexes in one experiment (i.e. one chamber) as possible. A lack of literature on the subject of cross-reactivity of reagents in the chamber led us to believe that all four (4) complexes could be modulated in a single experiment. We tested this assertion on HepG2 cells due to their abundance and found that complex III and IV reagents were incompatible with each other. That is to say, once duroquinone and antimycin A were in the chamber, the POS couldn't handle the addition of ascorbic acid and TMPD (Fig 10.4.1). While it is known that TMPD is susceptible to autoxidation (and ascorbic acid is added to prevent this during the experiment), this level of oxygen consumption is extreme and the result of an unknown interaction between one of the complex III reagents and TMPD (Munday 1988). This effect was observed with and without cells in the chamber, further confirming that the reagents and not the sample were responsible for autoxidation (Fig 10.4.2).

8.5.5 O2k setup and maintenance complications

The author was involved in setting up the O2k out of the box, with limited guidance from the manufacturer. Some of the early data collected from the instrument had high interchamber variability, likely a result of bubble formation under the Teflon membrane and/or incomplete POS calibration. Once realized, and the membranes replaced, variably between chambers was reduced. Unfortunately, after 3 months in storage due to the COVID-19 pandemic, one of the POS electrodes was unable to be calibrated following a membrane change and POS service. There is one remaining option for the lab in the form of troubleshooting before the POS must be sent back to the manufacturer in Austria, postponing any remaining studies until service is complete.

8.6 Considerations for future expansion of these projects

The global COVID-19 pandemic delivered a devastating blow to the world in March 2020, and graduate students were certainly not spared. Between being out of the lab for over three (3) months, working in healthcare on the front lines (and supporting a spouse who does the same), and worrying about the health of my medically fragile mother and brother, this dissertation completion could not have come at a more stressful time. That said, as a result of the pandemic, many of the studies proposed in this section scheduled for this year were not able be completed, prior to the submission of this dissertation. Therefore, I will propose them as ongoing/future directions for this work, which I believe has opened an exciting door in the world of organ preservation.

8.6.1 Selecting an appropriate SK2 inhibitor

Before moving forward with repeating the cold storage studies in hepatocytes while inhibiting SK2 (as the first round of studies used ABC294640, which as explained in section 8.5, is not an appropriate drug for these experiments), we must identify a suitable pharmacologic agent

for targeting SK2. There are several options available commercially, including K145 and SLR080811, but many more compounds are in the pipeline due to the utility of these inhibitors in cancer treatment and laboratory exploration (Cao et al. 2018). Selective inhibition of SK2 *in vitro* has the ability to increase circulating S1P in an SK1-dependent manner, which is why the development of these compounds is a challenge (Kharel et al. 2012). *In silico* screening is a powerful tool for identifying new potential therapeutics, though the crystal structure of SK2 has not yet been solved. Homology modeling with the known crystal structure of SK1 may provide some insights into potential active sites on the enzyme. More importantly, a selective inhibitor of SK2 would provide a molecular tool for discerning the role of S1P from SK2 intracellularly during organ preservation.

8.6.2 Treatment with exogenous LPLs during cold storage

The ultimate proof-of-concept is in the lipid mediator rescue studies to determine if the overall preservation injury phenotype can be improved by application of exogenous lipids, such as LPA or S1P. If an improvement in cell viability is observed, then using some of the molecular tools described throughout this dissertation to investigate at what level of the signaling cascade this improvement lies. Is it in the more distal proteins, such as Rho? Or, at the proximal end of the pathway, at the level of ERM protein configuration, transcription, or mitochondrial activity? Or perhaps even an intracellular mechanism yet to be characterized? Our lab has previously worked from the inside out, and now we are proposing focusing on cell surface signaling as a potential therapeutic strategy. As discussed in section 8.3, before these rescue protocols can be explored, either a new method of lipid delivery in aqueous cold storage must be developed or water/DMSO-soluble LPL mimetic or agonists must be identified. A limitation of using C3 exoenzyme transferase from *c. botulinum* is that it inhibits all three isoforms of Rho (RhoA, RhoB, and RhoC).

While not the focus of this research, the role of the immune system in transplant recipients is vastly important. Despite advances in immunosuppressant therapy, graft-versus-host disease (GVHD) and allograft rejection are still observed. S1P signaling has been demonstrated to regulate the immune response to small bowel transplant. S1P receptor agonists, such as FTY720 and KRP-203, have efficacy against acute causes of rejection in animal transplant models (Kimura et al. 2003; Shimizu et al. 2005; Fujishiro et al. 2006). W-061, another S1P receptor agonist, binds to all receptors except S1PR2 and prevents immune cell recruitment to the transplanted small bowel (Song et al. 2012). If we can elucidate the role of S1P in preventing physiological consequences of preservation injury (i.e. cytoskeletal stability and mitochondrial function), then targeting S1P signaling would be a dual treatment in organ transplantation: inhibiting donor and recipient immunoreactivity to the graft and preventing physiologic disruption in the organ during preservation.

8.6.3 Other possible downstream effectors contributing to preservation injury phenotype

Following pathways other than that of Rho/ROK, existing data suggests that Erk may play a protective role in ischemia-reperfusion (I-R) injury. The mechanism gets complicated, because in the setting of myocardial infarction and ischemic stroke, mild hypothermia is protective against I-R injury (by maintaining Erk phosphorylation) (Choi et al. 2017). However, organ preservation is a two-fold insult: profound hypothermia coupled with I-R injury. A study in 2005 on rat liver grafts showed that phosphatidylinositol 3-kinase (PI-3K) and Akt signaling is not only disrupted during liver preservation, but contributes to the phenotype (Li et al. 2005). Mutational studies conferring highly activated Akt proved to protect livers against I-R injury (Harada et al. 2004). The common theme: all of these pathways are LPL effectors. However, studies must not be limited to only signaling mediators associated with LPL receptors. It could take decades to figure out

underlying mechanisms, and there could be too many to count; however, the goal of this work is to develop a therapeutic strategy to prevent preservation injury. Understanding the most basic mechanisms, while important, is therefore only half of the puzzle.

8.6.4 Continuing evaluation of ABC294640 and its novel mechanism of action at ETC complex I

Due to the clinical utility of this compound, the exact mechanism of interaction between ABC294640 and complex I of the ETC should be characterized. *In silico* and *in vitro* studies combined would likely give the best outcome. Molecular modeling and ligand docking software (such as Modeller, Chimera, Autodocker, etc.) can be used to predict where ABC294640 and complex I may interact (and if this site is distinct from that of rotenone). All that is needed is a .pdb file of the crystal structure of complex I, the structure of the ligand(s) (ABC294640 and rotenone), and a bit of trial and error with the software to determine the optimal kinetics and dynamics of the simulation.

Once a tentative binding site is proposed, then mutational studies *in vitro* can be conducted, similar to those for rotenone, to confirm the active site of ABC294640 (Palmer et al. 1968). For final confirmation, mitochondrial respiration can be measured in cells containing the mutant complex I that is unresponsive to ABC294640 binding. We would expect to see no significant effect in complex I, II, III, or IV activity in these complex I-mutant cells. It is at this point that considerations can be made about the clinical value of this drug weighed against the newly described risks involving the mitochondria.

8.6.5 The future of organ preservation

It is appropriate to end with how the field is advancing, what works and what does not in terms of improving graft survival, and any gaps that remain and could be good targets for future research. With all of the advances in biomolecular engineering on the horizon, 3-dimensional

bioprinting of organs may become a reality (either using a 3-D printer (Faulkner-Jones et al. 2015), or with a decellularized extracellular matrix from an existing organ (Jing et al. 2018)). Machine perfusion is improving every day, with new *ex vivo* perfusion devices being built and trialed around the country. Manipulating the temperature of preservation is also a consideration, one that comes with some advantages (such as a reduction in those detrimental effects caused by hypothermia) and some marked disadvantages (such as an increased metabolic demand and need for additional oxygenation) (Boteon and Afford 2019). Expanding the organ donor pool to meet the growing needs of the waitlist will be crucial, and that must be done by improving preservation methods with the ultimate goal of rehabilitating organs from uncontrolled DCD donors.

Chapter 9: Bibliography & academic acknowledgements

Alivizatos, Peter A. 2017. "Fiftieth Anniversary of the First Heart Transplant: The Progress of American Medical Research, the Ethical Dilemmas, and Christiaan Barnard." *Baylor University Medical Center Proceedings* 30 (4): 475–77. https://doi.org/10.1080/08998280.2017.11930236.

Amano, Mutsuki, Masanori Nakayama, and Kozo Kaibuchi. 2010. "Rho-Kinase/ROCK: A Key Regulator of the Cytoskeleton and Cell Polarity." *Cytoskeleton*. https://doi.org/10.1002/cm.20472.

Amouzandeh, Mariam, Greg Nowak, Anna Januszkiewicz, Jan Wernerman, Olav Rooyackers, and Ake Norberg. 2018. "Albumin Mass Balance and Kinetics in Liver Transplantation." *Critical Care* 22 (1): 1–10. https://doi.org/10.1186/s13054-018-2053-6.

Anliker, Brigitte, and Jerold Chun. 2004. "Lysophospholipid G Protein-Coupled Receptors." *Journal of Biological Chemistry* 279 (20): 20555–58. https://doi.org/10.1074/jbc.R400013200.

Arpin, Monique, Dafne Chirivino, Alexandra Naba, and Ingrid Zwaenepoel. 2011. "Emerging Role for ERM Proteins in Cell Adhesion and Migration." *Cell Adhesion and Migration*. https://doi.org/10.4161/cam.5.2.15081.

Bae, Geon Ho, Sung Kyun Lee, Hyung Sik Kim, Mingyu Lee, Ha Young Lee, and Yoe-Sik Bae. 2017. "Lysophosphatidic Acid Protects against Acetaminophen-Induced Acute Liver Injury." *Experimental & Molecular Medicine* 49. https://doi.org/10.1038/emm.2017.203.

Barker, Clyde F., and James F. Markmann. 2013. "Historical Overview of Transplantation." *Cold Spring Harbor Perspectives in Medicine* 3 (4): 1–18. https://doi.org/10.1101/cshperspect.a014977.

Belzer, F O, and J H Southard. 1988. "Principles of Solid-Organ Preservation by Cold Storage." *Transplantation* 45 (4): 673–76. https://doi.org/10.1097/00007890-198804000-00001.

Binder, Bernard Y.K., Priscilla A. Williams, Eduardo A. Silva, and J. Kent Leach. 2015. "Lysophosphatidic Acid and Sphingosine-1-Phosphate: A Concise Review of Biological Function and Applications for Tissue Engineering." *Tissue Engineering - Part B: Reviews* 21 (6): 531–42. https://doi.org/10.1089/ten.teb.2015.0107.

Bissell, D. Montgomery, and Philip S. Guzelian. 1980. "Phenotypic Stability of Adult Rat Hepatocytes in Primary Monolayer Culture." *Annals of the New York Academy of Sciences* 349 (1): 85–98. https://doi.org/10.1111/j.1749-6632.1980.tb29518.x.

Bligh, E.G., and W.J. Dyer. 1959. "A RAPID METHOD OF TOTAL LIPID EXTRACTION AND PURIFICATION." *Canadian Journal of Biochemistry and Physiology* 37 (8).

Boettcher, Wolfgang, Frank Merkle, and Heinz Hermann Weitkemper. 2003. "History of Extracorporeal Circulation: The Conceptional and Developmental Period." *Journal of Extra-Corporeal Technology* 35 (3): 172–83.

Boteon, Yuri L, and Simon C Afford. 2019. "Machine Perfusion of the Liver: Which Is the Best Technique to Mitigate Ischaemia-Reperfusion Injury?" *World Journal of Transplantation* 9 (1): 14–20. https://doi.org/10.5500/wjt.v9.i1.14.

Britten, Carolyn D., Elizabeth Garrett-Mayer, Steven H. Chin, Keisuke Shirai, Besim Ogretmen, Tricia A. Bentz, Alan Brisendine, et al. 2017. "A Phase I Study of ABC294640, a First-in-Class Sphingosine Kinase-2 Inhibitor, in Patients with Advanced Solid Tumors." *Clinical Cancer Research* 23 (16): 4642–50. https://doi.org/10.1158/1078-0432.CCR-16-2363.

Cao, Mengda, Chunmei Ji, Yanjun Zhou, Wen Huang, Weiwei Ni, Xunliang Tong, and Ji Fu Wei. 2018. "Sphingosine Kinase Inhibitors: A Patent Review." *International Journal of Molecular Medicine* 41 (5): 2450–60. https://doi.org/10.3892/ijmm.2018.3505.

Ceresa, Carlo D.L., David Nasralla, Constantin C. Coussios, and Peter J. Friend. 2018. "The Case for Normothermic Machine Perfusion in Liver Transplantation." *Liver Transplantation* 24 (2): 269–75. https://doi.org/10.1002/lt.25000.

Cerutis, D Roselyn, Michael D Weston, Afolabi O Ogunleye, Timothy P. McVaney, and Takanari Miyamoto. 2014. "Lysophosphatidic Acid (LPA) 18:1 Transcriptional Regulation of Primary Human Gingival Fibroblasts." *Genomics Data* 2: 375–77. https://doi.org/10.1016/j.gdata.2014.10.014.

Choi, Dae Eun, Jin Young Jeong, Hyunsu Choi, Yoon Kyung Chang, Moon Sang Ahn, Young Rok Ham, Ki Ryang Na, and Kang Wook Lee. 2017. "ERK Phosphorylation Plays an Important Role in the Protection Afforded by Hypothermia against Renal Ischemia-Reperfusion Injury." *Surgery (United States)* 161 (2): 444–52. https://doi.org/10.1016/j.surg.2016.07.028.

Collins, G.M., Maria Bravo-Shugarman, and P.I. Terasaki. 1969. "Kidney Preservation for Transportation: Initial Perfusion and 30 Hours' Ice Storage." *The Lancet* 2: 1219–22. https://gwu.illiad.oclc.org/illiad/pdf/277299.pdf%5Cnpapers2://publication/uuid/FA3E868D-2CDC-4D5B-B2F8-DDC06AE176E7.

Compagnon, Philippe, Hong Bing Wang, James H. Southard, and Martin J. Mangino. 2002. "Ischemic Preconditioning in a Rodent Hepatocyte Model of Liver Hypothermic Preservation Injury." *Cryobiology* 44 (3): 269–78. https://doi.org/10.1016/S0011-2240(02)00033-0.

Cuvillier, Olivier, Grisha Pirianov, Burkhard Kleuser, Philip G Vanek, Omar A. Coso, J. Silvio Gutkind, and Sarah Spiegel. 1996. "Suppression of Ceramide-Mediated Programmed Cell Death by Sphingosine-1-Phosphate." *Nature* 381 (6585): 800–803. https://doi.org/10.1038/381800a0.

Faulkner-Jones, Alan, Catherine Fyfe, Dirk-Jan Cornelissen, John Gardner, Jason King, Aidan Courtney, and Wenmiao Shu. 2015. "Bioprinting of Human Pluripotent Stem Cells and Their Directed Differentiation into Hepatocyte-like Cells for the Generation of Mini-Livers in 3D." *Biofabrication* 7 (4): 044102. https://doi.org/10.1088/1758-5090/7/4/044102.

Fehon, Richard G, Andrea I McClatchey, and Anthony Bretscher. 2010. "Organizing the Cell Cortex: The Role of ERM Proteins." *Nature Reviews Molecular Cell Biology* 11 (9): 674–

674. https://doi.org/10.1038/nrm2955.

French, Kevin J., Randy S. Schrecengost, Brian D. Lee, Yan Zhuang, Staci N. Smith, Justin L. Eberly, Jong K. Yun, and Charles D. Smith. 2003. "Discovery and Evaluation of Inhibitors of Human Sphingosine Kinase." *Cancer Research* 63 (18): 5962–69.

French, Kevin J, John J Upson, Staci N Keller, Yan Zhuang, Jong K Yun, and Charles D Smith. 2006. "Antitumor Activity of Sphingosine Kinase Inhibitors." *Journal of Pharmacology and Experimental Therapeutics* 318 (2): 596–603. https://doi.org/10.1124/jpet.106.101345.

French, KJ, Yan Zhuang, LW Maines, Peng Gao, Wenxue Wang, Vladimir Beljanski, JJ Upson, CL Green, SN Keller, and CD Smith. 2010. "Pharmacology and Antitumor Activity of ABC294640, a Selective Inhibitor of Sphingosine Kinase-2." *The Journal of Pharmacology and Experimental Therapeutics* 333 (1): 129–39. https://doi.org/10.1124/jpet.109.163444.

Fujishiro, Jun, Shinji Kudou, Satomi Iwai, Masafumi Takahashi, Yoji Hakamata, Miki Kinoshita, Satoru Iwanami, et al. 2006. "Use of Sphingosine-1-Phosphate 1 Receptor Agonist, KRP-203, in Combination with a Subtherapeutic Dose of Cyclosporine A for Rat Renal Transplantation." *Transplantation* 82 (6): 804–12. https://doi.org/10.1097/01.tp.0000232687.78242.cd.

Fye, W Bruce. 1995. "Profiles in Cardiology Julien Jean César Legallois" 600: 599–600.

Gandy, K. Alexa Orr, Patrick Roddy, Masayuki Wada, Ashley J. Snider, Mohamad Adada, Yusuf A. Hannun, Daniel Canals, and Lina M. Obeid. 2012. "Sphingosine 1-Phosphate Induces Filopodia Formation through S1PR2 Activation of ERM Proteins." *Biochemical Journal* 449 (3): 661–72. https://doi.org/10.1042/bj20120213.

Gao, Peng, Yuri K. Peterson, Ryan A. Smith, and Charles D. Smith. 2012. "Characterization of Isoenzyme-Selective Inhibitors of Human Sphingosine Kinases." *PLoS ONE* 7 (9). https://doi.org/10.1371/journal.pone.0044543.

Gardell, Shannon E., Adrienne E. Dubin, and Jerold Chun. 2006. "Emerging Medicinal Roles for Lysophospholipid Signaling." *Trends in Molecular Medicine* 12 (2): 65–75. https://doi.org/10.1016/j.molmed.2005.12.001.

Glanemann, Matthias, Jan M Langrehr, J Stange, Ulf Neumann, Utz Settmacher, and Peter Neuhaus. 2003. "Clinical Implications of Hepatic Preservation Injury After Adult Liver Transplantation." *American Journal of Transplantation* 3: 1003–9. papers://16e02c8a-055e-

489e-98cb-cab41915d6df/Paper/p462.

Gnaiger, Erich. 2008. "Polarographic Oxygen Sensors , the Oxygraph , Respirometry To Assess." *Drug-Induced Mitochondrial Dysfunction*, 327–48.

Gnaiger, Erich, Andrej V. Kuznetsov, Stefan Schneeberger, RÜdiger Seiler, Gerald Brandacher, Wolfgang Steurer, and Raimund Margreiter. 2000. "Mitochondria in the Cold." In *Life in the Cold*, edited by G Heldmaier and M Klingenspor, 431–42. Springer Berlin Heidelberg. https://doi.org/10.1007/978-3-662-04162-8_45.

Gress, Todd W., James Denvir, and Joseph I. Shapiro. 2018. "Effect of Removing Outliers on Statistical Inference: Implications to Interpretation of Experimental Data in Medical Research." *Marshall Journal of Medicine* 4 (2). https://doi.org/10.18590/mjm.2018.vol4.iss2.9.

Harada, Nobuko, Etsuro Hatano, Naoki Koizumi, Takashi Nitta, Masanori Yoshida, Naritaka Yamamoto, David A. Brenner, and Yoshio Yamaoka. 2004. "Akt Activation Protects Rat Liver from Ischemia/Reperfusion Injury." *Journal of Surgical Research* 121 (2): 159–70. https://doi.org/10.1016/j.jss.2004.04.016.

Heuman, Douglas M., W. Michael Pandak, Philip B. Hylemon, and Z. Reno Vlahcevic. 1991. "Conjugates of Ursodeoxycholate Protect against Cytotoxicity of More Hydrophobic Bile Salts: In Vitro Studies in Rat Hepatocytes and Human Erythrocytes." *Hepatology* 14 (5): 920–26. https://doi.org/10.1002/hep.1840140527.

Hylemon, P. B., E. C. Gurley, W. M. Kubaska, T. R. Whitehead, P. S. Guzelian, and Z. R. Vlahcevic. 1985. "Suitability of Primary Monolayer Cultures of Adult Rat Hepatocytes for Studies of Cholesterol and Bile Acid Metabolism." *Journal of Biological Chemistry* 260 (2): 1015–19.

Ishii, Isao, Nobuyuki Fukushima, Xiaoqin Ye, and Jerold Chun. 2004. "Lysophospholipid Receptors: Signaling and Biology." *Annual Review of Biochemistry* 73 (1): 321–54. https://doi.org/10.1146/annurev.biochem.73.011303.073731.

Jimenez-Castro, M.B., M. Elias-Miro, A. Casillas-Ramirez, and C. Peralt. 2013. "Experimental Models in Liver Surgery." In *Hepatic Surgery*. InTech. https://doi.org/10.5772/51829.

Jing, Lei, Leeann Yao, Michael Zhao, Li Ping Peng, and Mingyao Liu. 2018. "Organ Preservation: From the Past to the Future." *Acta Pharmacologica Sinica* 39 (5): 845–57.

https://doi.org/10.1038/aps.2017.182.

Kawaguchi, Kotoku, Saori Yoshida, Ryo Hatano, and Shinji Asano. 2017. "Pathophysiological Roles of Ezrin/Radixin/Moesin Proteins." *Biol. Pharm. Bull* 40 (40): 381–90. https://doi.org/10.1248/bpb.b16-01011.

Kharel, Yugesh, Mithun Raje, Ming Gao, Amanda M Gellett, Jose L Tomsig, Kevin R. Lynch, and Webster L. Santos. 2012. "Sphingosine Kinase Type 2 Inhibition Elevates Circulating Sphingosine 1-Phosphate." *Biochemical Journal* 447 (1): 149–57. https://doi.org/10.1042/BJ20120609.SPHINGOSINE.

Kihara, Yasuyuki, Michael Maceyka, Sarah Spiegel, and Jerold Chun. 2014. "Lysophospholipid Receptor Nomenclature Review: IUPHAR Review 8." *British Journal of Pharmacology* 171 (15): 3575–94. https://doi.org/10.1111/bph.12678.

Kimura, Takuya, Toshimichi Hasegawa, Hiroshi Nakai, Tatsuo Azuma, Noriaki Usui, Takashi Sasaki, and Akira Okada. 2003. "FTY720 Reduces T-Cell Recruitment into Murine Intestinal Allograft and Prevents Activation of Graft-Infiltrating Cells." *Transplantation* 75 (9): 1469–74. https://doi.org/10.1097/01.TP.0000058816.13525.92.

Kondo, Takahisa, Kosei Takeuchi, Yoshinori Doi, Shigenobu Yonemura, Shigekazu Nagata, Shoichiro Tsukita, and Sachiko Tsukita. 1997. "ERM (Ezrin/Radixin/Moesin)-Based Molecular Mechanism of Microvillar Breakdown at an Early Stage of Apoptosis." *Journal of Cell Biology* 139 (3): 749–58. https://doi.org/10.1083/jcb.139.3.749.

Lewis, Clayton S., Christina Voelkel-Johnson, and Charles D. Smith. 2018. "Targeting Sphingosine Kinases for the Treatment of Cancer." *Advances in Cancer Research* 140: 295–325. https://doi.org/10.1016/bs.acr.2018.04.015.

Li, Xian Liang, Kwan Man, Kevin T Ng, Chris K Sun, Chung Mau Lo, and Sheung Tat Fan. 2005. "The Influence of Phosphatidylinositol 3-Kinase/Akt Pathway on the Ischemic Injury during Rat Liver Graft Preservation." *American Journal of Transplantation : Official Journal of the American Society of Transplantation and the American Society of Transplant Surgeons* 5 (6): 1264–75. https://doi.org/10.1111/j.1600-6143.2005.00877.x.

Limkemann, Ashley, Susanne L. Lindell, Heather Reichstetter, Valerie Plant, Dan Parrish, Clementina Ramos, Chris Kowalski, Cristiano Quintini, and Martin J. Mangino. 2016. "Donor Gluconate Rescues Livers from Uncontrolled Donation after Cardiac Death."

Surgery (United States) 159 (3): 852–61. https://doi.org/10.1016/j.surg.2015.10.022.

Lin, Mu En, Deron R. Herr, and Jerold Chun. 2010. "Lysophosphatidic Acid (LPA) Receptors: Signaling Properties and Disease Relevance." *Prostaglandins and Other Lipid Mediators* 91 (3–4): 130–38. https://doi.org/10.1016/j.prostaglandins.2009.02.002.

Lindell, S L, T Hansen, M Rankin, R Danielewicz, F O Belzer, and J H Southard. 1996. "Donor Nutritional Status–a Determinant of Liver Preservation Injury." *Transplantation* 61 (2): 239–47.

Liu, Kai, Tai L Guo, Nitai C Hait, Jeremy Allegood, Hardik I Parikh, Wenfang Xu, Glen E Kellogg, Steven Grant, Sarah Spiegel, and Shijun Zhang. 2013. "Biological Characterization of 3-(2-Amino-Ethyl)-5-[3-(4-Butoxyl-Phenyl)-Propylidene]-Thiazolidine-2,4-Dione (K145) as a Selective Sphingosine Kinase-2 Inhibitor and Anticancer Agent." *PLoS ONE* 8 (2). https://doi.org/10.1371/journal.pone.0056471.

Lord, Samuel J, Katrina B Velle, R Dyche Mullins, and Lillian K Fritz-Laylin. 2020. "SuperPlots: Communicating Reproducibility and Variability in Cell Biology." *Journal of Cell Biology*. https://doi.org/10.1083/JCB.202001064.

Macknight, A DC, and A Leaf. 1977. "Regulation of Cellular Volume." *Physiological Reviews* 57 (3): 510–73.

Maines, Lynn W, Leo R Fitzpatrick, Kevin J French, Yan Zhuang, Zuping Xia, Staci N Keller, John J Upson, and Charles D Smith. 2008. "Suppression of Ulcerative Colitis in Mice by Orally Available Inhibitors of Sphingosine Kinase." *Digestive Diseases and Sciences* 53 (4): 997–1012. https://doi.org/10.1007/s10620-007-0133-6.

Mangino, Martin J., Tao Tian, Mary Ametani, Susanne Lindell, and James H. Southard. 2008. "Cytoskeletal Involvement in Hypothermic Renal Preservation Injury." *Transplantation* 85 (3): 427–36. https://doi.org/10.1097/TP.0b013e31815fed17.

Margreiter, R. 1997. "The History of Intestinal Transplantation." *Transplantation Reviews* 11 (1): 9–21. https://doi.org/10.1016/S0955-470X(97)80033-X.

Matsui, Takeshi, Masato Maeda, Yoshinori Doi, Shigenobu Yonemura, Mutsuki Amano, Kozo Kaibuchi, Sachiko Tsukita, and Shoichiro Tsukita. 1998. "Rho-Kinase Phosphorylates COOH-Terminal Threonines of Ezrin/Radixin/Moesin (ERM) Proteins and Regulates Their Head-to-Tail Association." *Journal of Cell Biology* 140 (3): 647–57.

https://doi.org/10.1083/jcb.140.3.647.

McClatchey, Andrea I. 2014. "ERM Proteins at a Glance." *Journal of Cell Science* 127 (15): 3199–3204. https://doi.org/10.1242/jcs.098343.

Merrill, Alfred H., M. Cameron Sullards, Jeremy C. Allegood, Samuel Kelly, and Elaine Wang. 2005. "Sphingolipidomics: High-Throughput, Structure-Specific, and Quantitative Analysis of Sphingolipids by Liquid Chromatography Tandem Mass Spectrometry." *Methods* 36 (2 SPEC. ISS.): 207–24. https://doi.org/10.1016/j.ymeth.2005.01.009.

Milane, Lara, Malav Trivedi, Amit Singh, Meghna Talekar, and Mansoor Amiji. 2015. "Mitochondrial Biology, Targets, and Drug Delivery." *Journal of Controlled Release*. https://doi.org/10.1016/j.jconrel.2015.03.036.

Mohsin, Ahmed A., Qun Chen, Nanhu Quan, Thomas Rousselle, Michael W. Maceyka, Arun Samidurai, Jeremy Thompson, Ying Hu, Ji Li, and Edward J. Lesnefsky. 2019. "Mitochondrial Complex I Inhibition by Metformin Limits Reperfusion Injury." *Journal of Pharmacology and Experimental Therapeutics*, May, 282–90. https://doi.org/10.1124/jpet.118.254300.

Molitoris, B A, and W Finn. 2001. *Acute Renal Failure: A Companion to Brenner and Rector's the Kidney*. First. Philadelphia: Saunders.

Molitoris, B A, J Leiser, and M C Wagner. 1997. "Role of the Actin Cytoskeleton in Ischemia-Induced Cell Injury and Repair." *Pediatric Nephrology* 11 (6): 761–67. https://doi.org/10.1007/s004670050385.

Munday, R. 1988. "Generation of Superoxide Radical, Hydrogen Peroxide and Hydroxyl Radical during the Autoxidation of N, N, N', N'-Tetramethyl-p-Pheylenediamine." *Chem.-Biol. Interactions* 65: 133–43.

Nasralla, David, Constantin C Coussios, Hynek Mergental, M. Zeeshan Akhtar, Andrew J Butler, Carlo D L Ceresa, Virginia Chiocchia, et al. 2018. "A Randomized Trial of Normothermic Preservation in Liver Transplantation." *Nature* 557 (7703): 50–56. https://doi.org/10.1038/s41586-018-0047-9.

Newton, Jason, Santiago Lima, Michael Maceyka, and Sarah Spiegel. 2015. "Revisiting the Sphingolipid Rheostat: Evolving Concepts in Cancer Therapy." *Experimental Cell Research* 333 (2): 195–200. https://doi.org/10.1016/j.yexcr.2015.02.025.

Nielsen, Ole Haagen, Yuan Li, Bengt Johansson-Lindbom, and Mehmet Coskun. 2017. "Sphingosine-1-Phosphate Signaling in Inflammatory Bowel Disease." *Trends in Molecular Medicine*. https://doi.org/10.1016/j.molmed.2017.02.002.

NIH. 2020. "Clinical Trials Registry." US National Library of Medicine. 2020. www.clinicaltrials.gov.

Oliveira, Paulo J. 2018. *Mitochondrial Biology and Experimental Therapeutics*. *Mitochondrial Biology and Experimental Therapeutics*. https://doi.org/10.1007/978-3-319-73344-9.

Palmer, G, DJ Horgan, H Tisdale, TP Singer, and H Beinert. 1968. "Studies on the Respiratory Chain-Linked Reduced Nicotinamide Adenine Dinucleotide Dehydrogenase." *Journal of Biological Chemistry* 243 (4): 844–47.

Panetti, Tracee Scalise. 2002. "Differential Effects of Sphingosine 1-Phosphate and Lysophosphatidic Acid on Endothelial Cells." *Biochimica et Biophysica Acta* 1582 (1–3): 190-6. https://ac.els-cdn.com/S1388198102001555/1-s2.0-S1388198102001555-main.pdf?_tid=fecc8e08-0144-11e8-ad92-00000aacb35d&acdnat=1516825828_eb2ed6e09b7dd51c7c868a2aaef2d3d5.

Patterson, G. A., J. D. Cooper, J. H. Dark, and M. T. Jones. 1988. "Experimental and Clinical Double Lung Transplantation." *Journal of Thoracic and Cardiovascular Surgery* 95 (1): 70–74. https://doi.org/10.1016/s0022-5223(19)35388-7.

Petrowsky, Henrik, and Pierre Alain Clavien. 2015. "Principles of Liver Preservation." In *Transplantation of the Liver: Third Edition*, edited by Ronald W Busuttil and Göran B G Klintmalm, Third, 582–99. Philadelphia: Elsevier Saunders. https://doi.org/10.1016/B978-1-4557-0268-8.00044-0.

Ponuwei, Godwin A. 2016. "A Glimpse of the ERM Proteins." *Journal of Biomedical Science* 23: 35. https://doi.org/10.1186/s12929-016-0246-3.

Raman, Renuka, Clyde Savio Pinto, and Mahendra Sonawane. 2018. "Polarized Organization of the Cytoskeleton: Regulation by Cell Polarity Proteins." *Journal of Molecular Biology* 430 (19): 3565–84. https://doi.org/10.1016/j.jmb.2018.06.028.

Reffelmann, Thorsten, and Robert A Kloner. 2002. "THE 'NO-REFLOW' PHENOMENON: BASIC SCIENCE AND CLINICAL CORRELATES." *Heart* 87: 162–68.

Santos, Webster L., and Kevin R. Lynch. 2015. "Drugging Sphingosine Kinases." *ACS Chemical*

Biology 10 (1): 225–33. https://doi.org/10.1021/cb5008426.

Schlegel, Andrea, Philipp Kron, and Philipp Dutkowski. 2016. "Hypothermic Machine Perfusion in Liver Transplantation." *Current Opinion in Organ Transplantation*. https://doi.org/10.1097/MOT.0000000000000303.

Serracino-Inglott, F, N A Habib, and R T Mathie. 2001. "Hepatic Ischemia-Reperfusion Injury." *American Journal of Surgery* 181 (2): 160–66. https://doi.org/10.1016/S0002-9610(00)00573-0.

Shaner, Rebecca L., Jeremy C. Allegood, Hyejung Park, Elaine Wang, Samuel Kelly, Christopher A. Haynes, M. Cameron Sullards, and Alfred H. Merrill. 2009. "Quantitative Analysis of Sphingolipids for Lipidomics Using Triple Quadrupole and Quadrupole Linear Ion Trap Mass Spectrometers." *Journal of Lipid Research* 50 (8): 1692–1707. https://doi.org/10.1194/jlr.D800051-JLR200.

Sharma, Lokendra, Jianxin Lu, and Yidong Bai. 2009. "Mitochondrial Respiratory Complex I: Structure, Function and Implication in Human Diseases." *Current Medicinal Chemistry* 16 (10): 1266–77. https://doi.org/10.2174/092986709787846578.

Shaw, Reuben J, Michael Henry, Frank Solomon, and Tyler Jacks. 1998. "RhoA-Dependent Phosphorylation and Relocalization of ERM Proteins into Apical Membrane/Actin Protrusions in Fibroblasts." *Molecular Biology of the Cell* 9 (2): 403–19. https://doi.org/10.1091/mbc.9.2.403.

Shimizu, Hisashi, Masafumi Takahashi, Takashi Kaneko, Takashi Murakami, Yoji Hakamata, Shinji Kudou, Tetsuya Kishi, et al. 2005. "KRP-203, a Novel Synthetic Immunosuppressant, Prolongs Graft Survival and Attenuates Chronic Rejection in Rat Skin and Heart Allografts." *Circulation* 111 (2): 222–29. https://doi.org/10.1161/01.CIR.0000152101.41037.AB.

Simo, Kerri A., David J. Niemeyer, Erin M. Hanna, Jacob H. Swet, Kyle J. Thompson, David Sindram, David A. Iannitti, et al. 2014. "Altered Lysophosphatidic Acid (LPA) Receptor Expression during Hepatic Regeneration in a Mouse Model of Partial Hepatectomy." *HPB (Oxford)* 16 (6): 534–42. https://doi.org/10.1111/hpb.12176.

Smithers, Cameron C, and Michael Overduin. 2016. "Structural Mechanisms and Drug Discovery Prospects of Rho GTPases." *Cells* 5 (26): 1–15.

https://doi.org/10.3390/cells5020026.

Sokolov, Eugene, Ashley L Eheim, William a Ahrens, Tracy L Walling, Jacob H Swet, Matthew T McMillan, Kerri a Simo, Kyle J Thompson, David Sindram, and Iain H McKillop. 2013. "Lysophosphatidic Acid Receptor Expression and Function in Human Hepatocellular Carcinoma." *The Journal of Surgical Research* 180 (1): 104–13. https://doi.org/10.1016/j.jss.2012.10.054.

Solinet, Sara, Kazi Mahmud, Shannon F. Stewman, Khaled Ben El Kadhi, Barbara Decelle, Lama Talje, Ao Ma, Benjamin H. Kwok, and Sébastien Carreno. 2013. "The Actin-Binding ERM Protein Moesin Binds to and Stabilizes Microtubules at the Cell Cortex." *Journal of Cell Biology* 202 (2): 251–60. https://doi.org/10.1083/jcb.201304052.

Song, Jinghai, Hiroshi Hagiya, Haruto Kurata, Hirotaka Mizuno, and Toshinori Ito. 2012. "Prevention of GVHD and Graft Rejection by a New S1P Receptor Agonist, W-061, in Rat Small Bowel Transplantation." *Transplant Immunology* 26 (2–3): 163–70. https://doi.org/10.1016/j.trim.2011.12.005.

Southard, J H, and F O Belzer. 1993. "Principles of Organ Preservation: Part I&II." *Surgical Rounds*.

———. 1995. "Organ Preservation." *Annu Rev Med* 46: 235–47.

Southard, J H, T M Van Gulik, M S Ametani, P K Vreugdenhil, S L Lindell, B L Pienarr, and F O Belzer. 1990. "Important Components of the UW Solution." *Transplantation* 49 (2): 251–57.

Starzl, T E., J Fung, R Venkataramman, S Todo, A J. Demetris, and A Jain. 1989. "Fk 506 for Liver, Kidney, and Pancreas Transplantation." *The Lancet* 334 (8670): 1000–1004. https://doi.org/10.1016/S0140-6736(89)91014-3.

Starzl, T E, T L Marchioro, K N Von Kaulla, G Hermann, R S Brittain, and W R Waddell. 1963. "Homotransplantation of the Liver in Humans." *Surg Gynecol Obstet* 117: 659–76. https://doi.org/10.1097/00000658-197808000-00001.

Strub, G M, Michael Maceyka, Nitai C Hait, Sheldon Milstien, and Sarah Spiegel. 2010. "Extracellular and Intracellular Actions of Sphingosine-1-Phosphate." *Advances in Experimental Medicine and Biology* 688: 141–55. https://doi.org/10.1007/978-1-4419-6741-1_10.

Strub, G M, M. Paillard, J. Liang, L. Gomez, J. C. Allegood, N. C. Hait, M. Maceyka, et al. 2011. "Sphingosine-1-Phosphate Produced by Sphingosine Kinase 2 in Mitochondria Interacts with Prohibitin 2 to Regulate Complex IV Assembly and Respiration." *The FASEB Journal* 25 (2): 600–612. https://doi.org/10.1096/fj.10-167502.

Sumimoto, R., J. H. Southard, and F. O. Belzer. 1993. "Livers from Fasted Rats Acquire Resistance to Warm and Cold Ischemia Injury." *Transplantation* 55 (4): 728–32. https://doi.org/10.1097/00007890-199304000-00008.

Sumimoto, R, N V Jamieson, K Wake, and N Kamanda. 1989. "24-Hr Rat Liver Preservation Using UW Solution and Some Simplified Variants." *Transplantation* 48 (1): 1–5.

Takabe, Kazuaki, Steven W Paugh, Sheldon Milstien, and Sarah Spiegel. 2008. "'Inside-Out' Signaling of Sphingosine-1-Phosphate: Therapeutic Targets." *Pharmacological Reviews* 60 (2): 181–95. https://doi.org/10.1124/pr.107.07113.

Tanimizu, Naoki, and Toshihiro Mitaka. 2016. "Morphogenesis of Liver Epithelial Cells." *Hepatology Research* 46 (10): 964–76. https://doi.org/10.1111/hepr.12654.

Taylor, Michael J. 2007. "Biology of Cell Survival in the Cold: The Basis for Biopreservation of Tissues and Organs." In *Advances in Biopreservation*, edited by J G Baust and J M Baust, 15–62. Boca Raton, FL: CRC/Taylor & Francis. papers2://publication/uuid/C1CAE898-61F0-4C04-A799-31F4F2F2F9EA.

Tian, Tao, Susanne L. Lindell, Chris Kowalski, and Martin J. Mangino. 2014. "Moesin Functionality in Hypothermic Liver Preservation Injury." *Cryobiology* 69 (1): 34–40. https://doi.org/10.1016/j.cryobiol.2014.04.017.

Tian, Tao, Susanne L. Lindell, Melody Lam, and Martin J. Mangino. 2012. "Ezrin Functionality and Hypothermic Preservation Injury in LLC-PK1 Cells." *Cryobiology* 65 (1): 60–67. https://doi.org/10.1016/j.cryobiol.2012.04.003.

Tian, Tao, Susanne L Lindell, Scott C Henderson, and Martin J Mangino. 2009. "Protective Effects of Ezrin on Cold Storage Preservation Injury in the Pig Kidney Proximal Tubular Epithelial Cell Line [LLC-PK1]." *Transplantation* 87 (10): 1488–96. https://doi.org/10.1097/TP.0b013e3181a43f18.

Toronto Lung Transplant, Group. 1986. "Unilateral Lung Transplantation for Pulmonary Fibrosis." *The New England Journal of Medicine* 314 (18): 1140–45.

Vaughan, Catherine A., Isabella Pearsal, Shilpa Singh, Brad Windle, Swati P. Deb, Steven R. Grossman, W. Andrew Yeudall, and Sumitra Deb. 2016. "Addiction of Lung Cancer Cells to GOF P53 Is Promoted by Up-Regulation of Epidermal Growth Factor Receptor through Multiple Contacts with P53 Transactivation Domain and Promoter." *Oncotarget* 7 (11): 12426–46. https://doi.org/10.18632/oncotarget.6998.

Venuta, Federico, and Dirk Van Raemdonck. 2017. "History of Lung Transplantation." *Journal of Thoracic Disease* 9 (12): 5458–71. https://doi.org/10.21037/jtd.2017.11.84.

Watson, Christopher J.E., Vasilis Kosmoliaptsis, Lucy V. Randle, Alexander E. Gimson, Rebecca Brais, John R. Klinck, Mazin Hamed, Anastasia Tsyben, and Andrew J. Butler. 2017. "Normothermic Perfusion in the Assessment and Preservation of Declined Livers Prior to Transplantation." *Transplantation* 101 (5): 1. https://doi.org/10.1097/TP.0000000000001661.

Wirth, Christophe, Ulrich Brandt, Carola Hunte, and Volker Zickermann. 2016. "Structure and Function of Mitochondrial Complex I." *Biochimica et Biophysica Acta - Bioenergetics* 1857 (7): 902–14. https://doi.org/10.1016/j.bbabio.2016.02.013.

Wu, Meng Yu, Giou Teng Yiang, Wan Ting Liao, Andy Po Yi Tsai, Yeung Leung Cheng, Pei Wen Cheng, Chia Ying Li, and Chia Jung Li. 2018. "Current Mechanistic Concepts in Ischemia and Reperfusion Injury." *Cellular Physiology and Biochemistry*. https://doi.org/10.1159/000489241.

Xun, Cai, Min Bin Chen, Li Qi, Zhang Tie-Ning, Xue Peng, Li Ning, Chen Zhi-Xiao, and Wang Li-Wei. 2015. "Targeting Sphingosine Kinase 2 (SphK2) by ABC294640 Inhibits Colorectal Cancer Cell Growth in Vitro and in Vivo." *Journal of Experimental and Clinical Cancer Research* 34 (1). https://doi.org/10.1186/s13046-015-0205-y.

Ye, Jian, George Coulouris, Irena Zaretskaya, Ioana Cutcutache, Steve Rozen, and Thomas L. Madden. 2012. "Primer-BLAST: A Tool to Design Target-Specific Primers for Polymerase Chain Reaction." *BMC Bioinformatics* 13: 134. https://doi.org/10.1186/1471-2105-13-134.

Zhao, Ru Zhou, Shuai Jiang, Lin Zhang, and Zhi Bin Yu. 2019. "Mitochondrial Electron Transport Chain, ROS Generation and Uncoupling (Review)." *International Journal of Molecular Medicine* 44 (1): 3–15. https://doi.org/10.3892/ijmm.2019.4188.

Zhao, Yutong, and Viswanathan Natarajan. 2013. "Lysophosphatidic Acid (LPA) and Its

Receptors: Role in Airway Inflammation and Remodeling." *Biochimica et Biophysica Acta - Molecular and Cell Biology of Lipids* 1831 (1): 86–92. https://doi.org/10.1016/j.bbalip.2012.06.014.

Zuckerman, Valentina, Eugene Sokolov, Jacob H. Swet, William A. Ahrens, Victor Showlater, David A. Iannitti, and Iain H. Mckillop. 2015. "Expression and Function of Lysophosphatidic Acid Receptors (LPARs) 1 and 3 in Human Hepatic Cancer Progenitor Cells." *Oncotarget* 7 (3): 2951–67. https://doi.org/10.18632/oncotarget.6696.

Shared Core Service and Academic Acknowledgements

Chapter 10: Appendix

10.1 Abbreviations

ADP	adenosine diphosphate
ALT	alanine aminotransferase
AST	aspartate aminotransferase
ATP	adenosine triphosphate
ATX	autotaxin

Cer	ceramide
CS	cold storage
DBD	donation after brain death
DCD	donation after cardiac death
DHS1P	dihydrosphingosine-1-phosphate
DHSo	dihydrosphingosine
FAF-BSA	fatty acid free-bovine serum albumin
FAS-BSA	fatty acid saturated-bovine serum albumin
GDP	guanosine diphosphate
GPCR	G-protein coupled receptor
GTP	guanosine triphosphate
HexCer	hexosylceramide
HRR	high-resolution respirometry
ICU	intensive care unit
IRI	ischemia-reperfusion injury
K+	potassium (ion)
LPA	lysophosphatidic acid
LPL	lysophospholipids
MP	machine perfusion
Na+	sodium (ion)
NADH	nicotinamide adenine dinucleotide
O2k	Oroboros Oxygraph-2k
OR	operating room
OXPHOS	oxidative phosphorylation
PCR	polymerase chain reaction
POS	polarographic oxygen sensor
rpm	revolutions per minute
S1P	sphingosine-1-phosphate
SCS	static cold storage
SK1	sphingosine kinase-1

SK2		sphingosine kinase-2		
SM		sphingomyelin		
So		sphingosine		
TMPD		N,N,N',N'-Tetramethyl-p-phenylenediamine		
TTFA		thenoyltrifluoroacetone		
WI		warm ischemia		
WT		wild-type		

10.2 Final Primer Sequences

Target	Direction	Sequence	T_m (°C)	Amplicon Length
LPAR1	Forward	GGCTATGTTCGCCAGAGGACTAT	62	135 NT
	Reverse	TCCAGGAGTCCAGCAGATGATAA	61	
LPAR2	Forward	GCTCTGTCGAGCCTGCTTGTCTTC	66	149 NT
	Reverse	ACAGTCTTGACCAGGCTGAGCGTG	67	
LPAR3	Forward	TCCAACCTCATGGCCTTCTT	59	101 NT
	Reverse	GACCCACTCGTATGCGGAGA	61	
LPAR4	Forward	GGGTGACAGAAGATTCATTGACTTCC	62	415 NT*
	Reverse	GGCCAGGAAACGATCCACACTA	62	
LPAR5	Forward	ATGTTAGCCAACAGCTCCTCAACC	63	262 NT
	Reverse	GCCAGTGGTGCAGTGCGTAGTA	65	
LPAR6	Forward	GGTAAGCGTTAACAGCTCCCACT	63	139 NT
	Reverse	TTTGAGGACGCAGATGAAAATGT	59	
GAPDH^	Forward	GTCAACGGATTTGGTCGTATT	56	223 NT
	Reverse	GATCTCGCTCCTGGAAGATGG	60	
B2M	Forward	AGATGAGTATGCCTGCCGTG	60	96 NT
	Reverse	TCAAACCTCCATGATGCTGCT	60	

Table 10.2.1 Human Primers

*All sequences are in a 5' to 3' orientation. *denotes primer that was designed for traditional PCR.*
^primer sequences from (Vaughan et al. 2016).

Target	Direction	Sequence	T_m	Amplicon Length
LPAR1	Forward	GGCTATGTTCGCCAGAGGACTAT	60	118 NT
	Reverse	TCCAGGAGTCCAGCAGATGATAA	60	
LPAR2	Forward	AAACTCCATGAGGAAGGGGC	60	109 NT
	Reverse	GACCTCAGGCCTGGCATATC	60	
LPAR3	Forward	TCTTAGGAGCCTTCGTGGTG	59	93 NT
	Reverse	TCACGTGCTGCACATTACAC	59	
LPAR4	Forward	TTTGTTAAAGGCATGCGGGC	60	111 NT
	Reverse	TCCTTACTGCAAACCGCTCA	60	
LPAR5	Forward	GAAGGTATCTGTGGTCAAGGC	60	84 NT
	Reverse	AGCTCGGTACATCCTTCCCA	60	
GAPDH	Forward	AGTGCCAGCCTCGTCTCATA	60	248 NT
	Reverse	GATGGTGATGGGTTTCCCGT	60	

Table 10.2.2 Rodent Primers

All sequences are in a 5' to 3' orientation.

10.3 Data Tables

	Precipitate				Supernatant			
	Serum-free medium	*0.1% FAF-BSA*	*FBS (pos control)*	*12hr CS (0.1% FAF-BSA)*	*Serum-free medium*	*0.1% FAF-BSA*	*FBS*	*12hr CS (0.1% FAF-BSA)*
Cer	0.86821	0.86821	0.86821	0.86821	0.14785	0.14785	0.14785	0.14785
HexCer	0.24858	0.24858	0.24858	0.24858	0.0528	0.0528	0.0528	0.0528
SM	8.421165	8.421165	8.421165	8.421165	0.7804	0.7804	0.7804	0.7804
So	0.020373	0.020373	0.020373	0.020373	0.004025	0.004025	0.004025	0.004025
DHSo	0.002095	0.002095	0.002095	0.002095	0	0	0	0
S1P	0.009557	0.009557	0.009557	0.009557	0.0029	0.0029	0.0029	0.0029
DHS1P	0.000703	0.000703	0.000703	0.000703	0	0	0	0

*Table 10.3.1 Sphingolipid mass spectrometry output*

Values are in pmol/mL. Relevant abbreviations: ceramide (Cer), monohexosylceramide (HexCer), sphingomyelin (SM), sphingosine-1-phosphate (S1P), dihydrosphingosine-1-phosphate (DHS1P), sphingosine (So), and dihydrosphingosine (DHSo).

10.4 Supplemental Figures
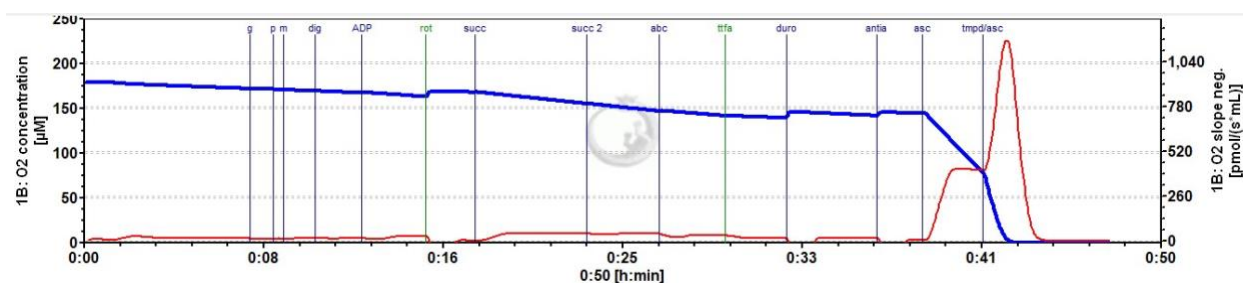
Figure 10.4.1 Interaction between complex III and IV reagents

After addition of complex III substrate (duro) and inhibitor (antia), oxygen flux(red tracing) was stabilized and then we proceeded with complex IV substrates asc (ascorbic acid) and TMPD (tmpd/asc). The blue tracing sharply decreases upon addition of asc, with a further decline to zero upon addition of TMPD (at the 40-minute mark). While TMPD addition leads to a peak in oxygen flux, that peak is limited by the concentration of oxygen in the chamber (the blue tracing bottoms out at zero, around the 42-minute mark). Anecdotally, others who use the O2k have noted the same phenomenon between these reagents; separate experiments must be conducted to acquire complex III and complex IV data.
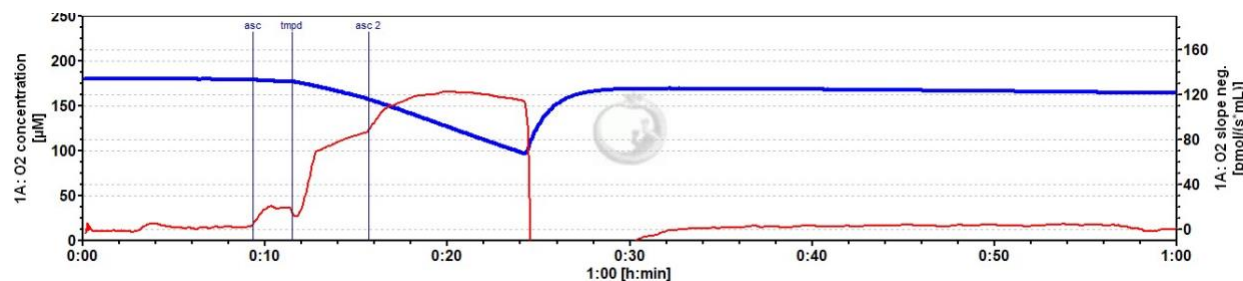
Figure 10.4.2 Cell-free autoxidation of ascorbic acid and TMPD

The addition of TMPD to a cell-free chamber results in an increase in oxygen consumption (red tracing) paired with a decrease in chamber oxygen concentration (blue tracing). This represents the capacity of TMPD to autoxidize. The sharp decline at 22 minutes represents the opening of the chamber stopper.

117

Chapter 11: Vita

Ria Christian Fyffe-Freil was born in Lynchburg, VA and graduated from E.C. Glass High School in 2007. She attended Sweet Briar College, in Amherst County, VA, graduating in 2011 with a bachelor's in chemistry and a mathematics minor. Her undergraduate research focused on the synthesis of a novel 3(2H) furanone derivative with suspected anti-cancer properties, under the guidance of Dr. Abraham Yousef. She worked as an Advanced EMT (AEMT) at UVA Health System for the Pegasus Medical Transport Network (both on an ambulance and in the medical communications/dispatch center) while furthering her education with a post-baccalaureate certificate program in premedical graduate health sciences at Virginia Commonwealth University, a master's degree in addiction science (2015), and finally matriculating into the Ph.D. program in the fall of 2015. With a personal connection to organ donation and transplantation, Ria actively pursued a laboratory in which she could combine her clinical expertise and research interests into a project that would ultimately increase the number of viable organ grafts for transplantation. She will receive her doctoral degree from the department of Physiology and Biophysics (MBG) at Virginia Commonwealth University in 2020.

The following is a brief summary of her accomplishments during her doctoral training at Virginia Commonwealth University:

<u>Publications:</u>

Fyffe-Freil, RC, Kang, HS, & Mangino, MJ. (*in preparation*). Ischemia-reperfusion injury in epithelial cells and the response of intracellular cytoskeletal proteins: review and clinical implications.

Fyffe-Freil, RC, Chmielewski, C, Li, R, Mohsin, A, Lindell, S, Lesnefsky, E, & Mangino, MJ. (*in preparation).* ABC294640, a Selective Sphingosine Kinase-2 Inhibitor, Directly Interferes with Mitochondrial Complex I Respiration.

Wickramaratne, N, Li, R, Tian, T, Khoraki, J, Kang, HS, Chmielewski, C, Liebrecht, L, **Fyffe-Freil, RC,** Lindell, S, & Mangino, MJ. (2020). Cholangiocyte Epithelial to Mesenchymal Transition (EMT) is a Potential Molecular Mechanism Driving Ischemic Cholangiopathy in Liver Transplantation. *PLoS One*, submitted June 2020.

Conferences/Presentations:

Fyffe-Freil, RC, Chmielewski, C, Li, R, Mohsin, A, Lesnefsky, E, & Mangino, MJ. (2020). Novel mechanism of ABC294640 (a selective sphingosine kinase-2 (SK2) inhibitor): Inhibition of mitochondrial complex I activity independent of SK2. *American Chemical Society National Meeting & Exposition*, Virtual Oral presentation.

Fyffe-Freil, RC, Chmielewski, C, Mohsin, A, Lesnefsky, E, & Mangino, MJ. (2019). ABC294640, a Seemingly Selective Sphingosine Kinase-2 Inhibitor, Chemically Attenuates Mitochondrial Complex I Activity. *2019 NHLBI Mitochondrial Biology Symposium*, Bethesda, MD.

Fyffe-Freil, RC, Mohsin, A, Limkemann, A, Lindell, S, Lesnefsky, E, & Mangino, M. (2019). Mechanisms of Hepatocyte Preservation Injury: Sphingosine-1-Phosphate Signaling. *19th Annual American Society of Transplant Surgeons Winter Symposium*, Miami, FL.

Awards, Honors and Graduate Student Engagement:

Dept. of Physiology and Biophysics

 Ramsey Award for Most Outstanding Doctoral Student (2020)

 Certificate of Recognition (2019)

MBG Travel Award (2018)

NIH Clinical and Translational Research Course for the PhD Scientist (2018)

Three Minute Thesis (3MT) Competition, 3rd place (2018)

Graduate School Dean Search Committee (2020)

VCU CareShare Virtual Childcare Services – Founder (2020)

Student Working Groups with the Provost's Office

 Student Health Insurance (2020)

 Student Activity Fee Updates (2019-2020)

MCV Student Leader's Committee (2019-2020)

Graduate Student Association (GSA)

 President (2019-2020)

 Graduate Research Symposium Chair (2018-2019)

Common Book Discussion Leader (2017, 2018, and 2020)